博士論文

論文題目　Neural mechanisms of human bipedal locomotion:
Roles of the cortex and spinal neural circuits

(ヒト二足歩行の神経制御機序～大脳皮質と脊髄神経回路の役割～)

氏名　横山 光

CONTENTS OF THE THESIS

Chapter 6 Study 5

Strengthening of causal connectivity from the cortex to muscles during voluntary gait modification in humans 136

Chapter 7

General discussion 160

List of abbreviations

Abbreviation	Term
AL	adductor longus muscle
AM	adductor magnus muscle
AMICA	adaptive mixture independent component analysis
ANOVA	analysis of variance
ASR	Artifact Subspace Reconstruction
BF	biceps femoris muscle
BMI	brain machine interface
CNS	central nervous system
CPG	central pattern generator
CiD	circumferential ipsilateral descending interneurons
CoA	center of activity
CuN	cuneiform nuclei
DBS	deep brain stimulation
DTF	directed transfer function
EMG	electromyography
ERP	event-related potential
ERSP	event-related spectral pertubation
ES	erector spinae muscle
FES	functional electrical stimulation
ffDTF	full frequency directed transfer function
GM	gluteus maximus muscle

Abbreviation	Term
GRF	ground reaction force
Gmed	gluteus medius muscle
ICA	independent component analysis
ILIO	iliopsoas muscle
INs	interneurons
LG	lateral head of gastrocnemius muscle
MCoD	multipolar commissural descending interneurons
MEP	motor evoked potential
MG	medial head of gastrocnemius muscle
MLR	mesencephalic locomotor region
MN	motor neuron
MVAR	multivariate autoregressive
NIRS	near infrared spectroscopy
NMF	nonnegative matrix factorization
PD	parkinson's disease
PET	positron emission tomography
PCA	principal component analysis
PPC	posterior parietal cortex
PPN	pedunculopontine
PL	peroneus longus muscle
PTN	pyramidal tract neuron
RA	rectus abdominis muscle
RF	rectus femoris muscle
SART	Sartorius muscle

Abbreviation	Term
SCI	spinal cord injury
SE	standard error
SOL	soleus muscle
SPECT	single photon emission computed tomography
ST	semitendinosus muscle
TA	tibialis anterior muscle
TFL	tensor fasciae latae muscle
TMS	transcranial magnetic stimulation
UBG	unit burst generator
VAF	variance accounted for
VL	vastus lateralis muscle
VM	vastus medialis muscle

Chapter 1

Introduction

Neural mechanisms of locomotion in humans and non-human vertebrates have been studied from more than a century ago (Sherrington, 1910; Shik et al., 1966; Andersson et al., 2012). So far, the studies have revealed that control of locomotor muscle activity is achieved by complicated interactions in central nervous system (Shik et al., 1966; Sinnamon, 1993; Orlovsky et al., 1999; Goulding, 2009; Arber, 2012; Kiehn, 2016). Based on a large number of experimental studies on animal models, it has been established that the spinal cord has critical roles for the generation of basic locomotor muscle activity patterns (Grillner, 1981; Kiehn, 2016). In addition, unlike quadruped animals, recent studies have suggested that the cortex is also largely involved in human bipedal locomotion (Wagner et al., 2012; Danner et al., 2015; Enders and Nigg, 2016).

In the present Chapter 1, I review a series of studies from past to present regarding the neural mechanisms underlying control of locomotion in vertebrates. Then, based on the review, I will raise research questions to be answered in this thesis, and present the purpose of this thesis.

1. 1. Three processes for control of locomotion

Takakusaki and Okumura (2008) proposed that locomotor behavior is controlled through the following three processes: “initiation”, “regulation” and “execution” processes.

First, the “initiation” process works as a trigger of locomotion. The trigger drive is derived from voluntary commands from the cerebral cortex and emotional commands from the limbic systems and the hypothalamus (Takakusaki, 2008).

Second, the “regulation process” contributes to achievement of adaptive locomotion. The cerebellum and the basal ganglia are involved in the process. The cerebellum receives locomotor commands as an efferent copy from the cortex and feedback sensory information as a result of locomotor movement. The cerebellum compares the two signals, calculates an error, and modulates the locomotor movement based on the error (Orlovsky, 1972a, b; Udo et al.,

1979). On the other hand, the basal ganglia modulates the locomotor movement based on the volitional reference from the cerebral cortex, emotional information from the limbic system and reward information from the dopamine neurons in the midbrain (Schultz, 1998; Takakusaki et al., 2006).

Finally, the "execution process" is a center of rhythm and pattern generation for locomotor behavior. The process is deeply associated with the brainstem and the spinal cord. The signals arriving from the "initiation process" and "regulation process" are integrated and transmitted to the brainstem and the spinal cord. The spinal cord has been regarded as a center of locomotor control, because it can generate coordinated rhythmic patterns of locomotor muscle activity without any descending and afferent inputs (Grillner, 1981; Kiehn, 2016). The brainstem triggers the generation of patterned locomotor muscle activity from the spinal locomotor networks. In addition to these neural systems, in humans, the cortex has been suggested to be involved in the generation of locomotor muscle activity based on significant corticomuscular connectivity between the motor cortex and lower limb muscles during walking (Petersen et al., 2012; Artoni et al., 2017).

Since the brainstem, the spinal cord and the cortex are key neural bases of locomotor muscle control as mentioned above, I will describe the detailed functions of the brain regions for locomotor control in the following sections.

1. 2. Mesencephalic locomotor region in the brainstem

Using decerebrate cats (resected at the precollicular-postmammillary level), Shik et al. (1966) found that electrical stimulation to the cuneiform nucleus at the ventral inferior colliculus could elicit walking behavior. The stimulated region was named "Mesencephalic Locomotor Region (MLR)". Additionally, they also demonstrated that increment of the stimulation intensity could accelerate the speed and induced gait transitions (i.e., walk to trot, and trot to gallop). The results indicated that the MLR has roles for a trigger of gait initiation and regulation of the

locomotion modes.

It has been demonstrated that the MLR comprises the pedunculopontine (PPN) and cuneiform nuclei (CuN) in cat studies (Garcia-Rill, 1986, 1991, 1997). The MLR was also found in primates and the details of PPN and CuN have been explored by recent studies (Goetz et al., 2016; Sébille et al., 2017). In humans, clinical and electrophysiological results from studies using deep brain stimulation (DBS) of the PPN strongly suggest that the PPN works as a MLR also in humans (Jenkinson et al., 2009; Thevathasan et al., 2012).

1. 3. Spinal control of locomotion

1. 3. 1. Spinal central pattern generators (CPGs)

Sherrington (1910) found that the extension of hip flexor muscles could elicit the alternate activity between flexors and extensors in spinalized cats and dogs. Based on the findings, he proposed that alternate locomotion movement is generated by reciprocal spinal reflex between flexors and extensors. However, Graham-Brown (1911) showed that alternate contraction between flexors and extensors occurred even in the absence of sensory input. He proposed a hypothesis that the flexors and extensors are controlled by two systems of neurons ("half-center") mutually inhibiting each other during locomotion. More than half a century later, Grillner (1981) conceptualized the built-in hardwired neural circuit in the spinal cord for locomotion as central pattern generator (CPG) consisting of unit burst generators (UBG) (Fig. 1-1); a module generating rhythmic contraction individually existed in flexors and extensors in each segment and the modules control each other's activities. Recently, Hägglund et al. (2013) demonstrated the existence of UBG-like modular organization in the spinal cord using optogenetic approaches. Firstly, they demonstrated that blue light stimulation to the lumbar spinal cord could induce coordinated locomotor-like rhythmic activity of motoneurons of flexors and extensors in both left and right sides (Fig. 1-2a). Additionally, the light stimulation to focal area demonstrated that rhythmic activity was induced unilaterally or independently in

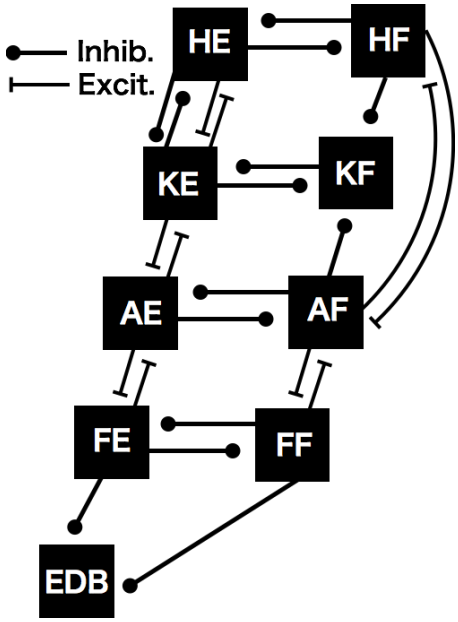

Figure 1-1. Schematic representation of the unit-burst-generator (UBG) model formulated by Grillner (1975, 1981). Each joint muscle group is activated by its own rhythm-generating unit (black squares). Functional synergistic units are connected with each other by mutual excitation, while functional antagonistic units are connected with each other by mutual inhibition. HE: hip extensor, HF: hip flexor, KE: knee extensor, KF: knee flexor, AE: ankle extensor, AF: ankle flexor, FE: foot extensor, FF: foot flexor, EDB: extensor digitorumbrevis (short toe flexor).

(Cited and modified from Grillner 1981)

flexor or extensor networks (Fig. 1-2b).

Regarding organization of the spinal CPG, recent studies using computational modeling proposed a novel organization consisted of two distinct layers: rhythm generation layer (upper layer) and pattern formation networks (lower layer) (McCrea and Rybak, 2008). In the two-level CPG, the rhythm generation layer controls the activation of the pattern formation networks that generate synergistic activation patterns of motoneuron pools for multiple muscles (Fig. 1-3).

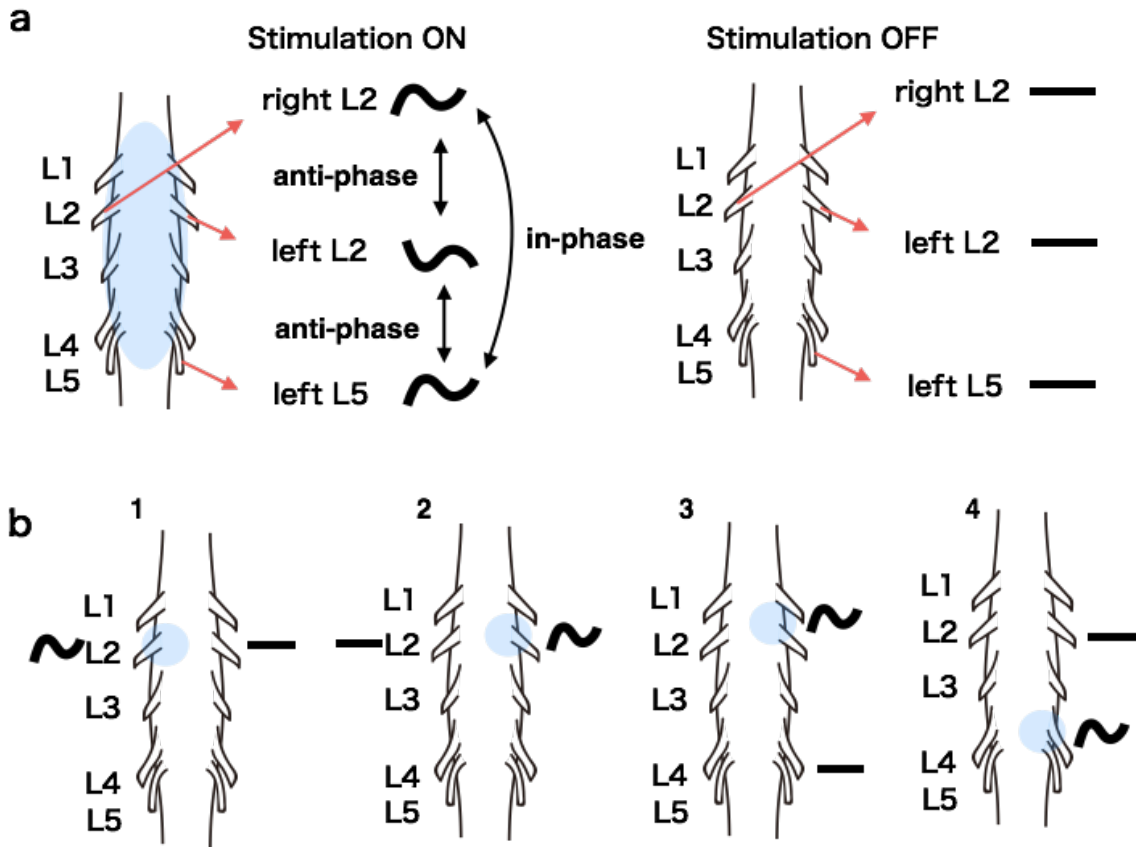

Figure 1-2. Locomotor-like activity induced by an optogenetic method. (a) Blue light stimulation to the ventral surface of the lumbar spinal cord evokes locomotor-like activity. Blue circles denote areas of light stimulation. Waveforms denote active motoneuron pools. Crossbars denote silent motoneuron pools. (b) Stimulation to a unilateral limited area elicits unilateral locomotor-like activity on the same side (1 and 2). Stimulation to a limited area at the rostral or caudal lumbar spinal cord can evoke locomotor-like activity separately in the flexor motoneurons or extensor motoneurons, respectively (3 and 4). Waveforms denote that motoneuron pools are active. Crossbars denote that motoneuron pools are silent. (Cited and modified from Hagglund et al., 2013)

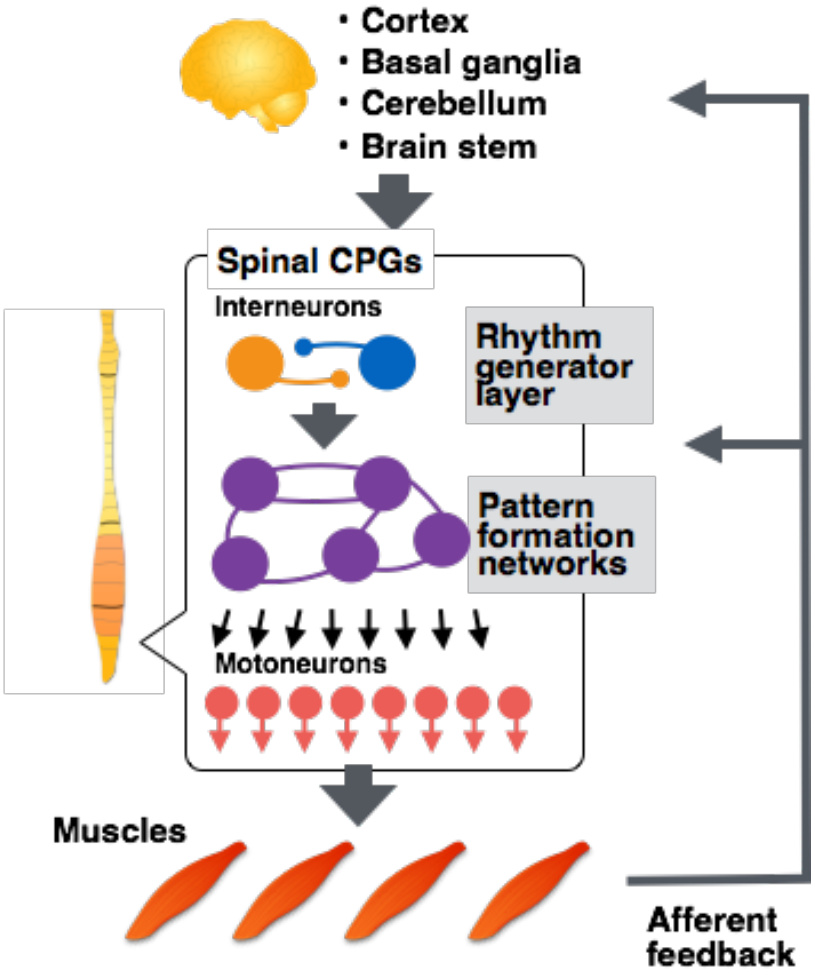

Figure 1-3. Control of locomtor muscle activity through two-layerd CPGs consisting of rhythm generator layer and pattern formation networks in the spinal cord. (Cited and modified from Lacquaniti et al., 2012)

1. 3. 2. Interneurons constituting the spinal central pattern generator

The spinal interneurons have been assumed to constitute the locomotor CPG from early times (Grillner, 1981; Grillner and Wallen, 1985). Nevertheless, the details of the components of spinal CPG remained unclear until recent years. Over the past decade, the roles of individual types of spinal interneurons regarding locomotor control have been revealed thanks to the advent of novel molecular and genetic techniques (Goulding, 2009; Garcia-Campmany et al.,

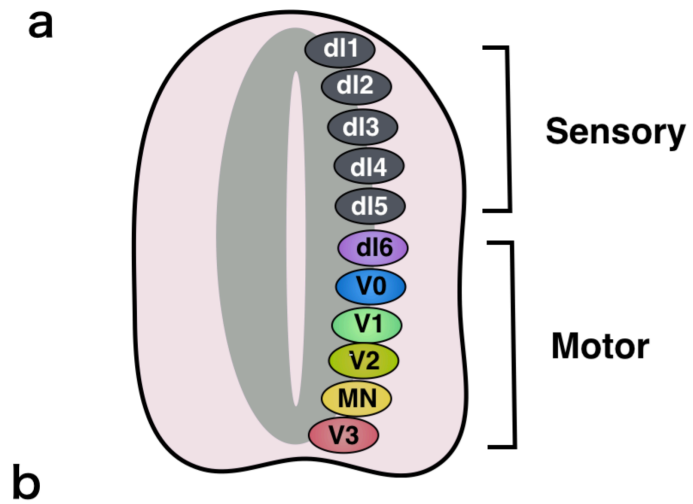

b

Adult cells	Connections	Functions	References
dI6, V0 — Crossed inhibitory INs	Contralateral: V1, MN	Left-right alternation	Goulding et al., (2009); Andersson et al., (2012); Lanuza et al., (2004); Talpalar et al., (2013)
V1 — Renshaw cells, IA inhibitory INs	Ipsilateral: V1, MN	Locomoter cycle speed	Gosgnach et al., (2006); Betley et al., (2009)
V2 — unknown	Ipsilateral: MN, V0	Burst robustness; Locomotor initiation	Kimura et al., (2008); Kyriakatos et al., (2011)
MN — Somatic/visceral motor neurons	Ipsilateral: V1	Muscle contraction	Gosgnach et al., (2006)
V3 — unknown	Contralateral: MN, V1; V2	Symmetrical pattern locomotion; Burst robustness	Zhang et al., (2008); Rabe Bernhardt et al. (2012)

Figure 1-4. Spinal interneurons and motoneurons of embryonic mice. (a) Eleven early types of spinal neuron are represented in the embryonic spinal cord. Upper half of the neuron types are involved in transmission of senseory information (dI1−dI5). Lower half of the neuron types are involved in transmission of motor commands. (b) The mature cell types of embryonic neurons and those connections and functions. MN: motoneuron, IN: interneuron. (Cited and modified from Goulding 2009)

2010; Kiehn, 2016).

Recently, differentiation processes of the spinal neurons involving locomotor control have been revealed in studies using embryonic mice (Goulding, 2009). In the dorsal half of the

neural tube, six progenitors produce embryonic dI1-dI6 interneurons according to the dorsoventral position. The dI1-dI6 interneurons play a role in transmission of sensory information. In the ventral half of the neural tube, the motoneurons and four types of interneurons (V0-V3 interneurons) are generated. These spinal neurons are involved in transmission of motor information (Fig. 1-4a, lower half). Of these spinal interneurons, dI6 and V0-V3 interneurons have crucial roles regarding control of locomotion (Lanuza et al., 2004; Gosgnach et al., 2006; Kimura et al., 2006; Kimura et al., 2008; Zhang et al., 2008; Betley et al., 2009; Goulding, 2009; Kyriakatos et al., 2011; Andersson et al., 2012; Rabe Bernhardt et al., 2012; Talpalar et al., 2013). Therefore, these interneurons are regarded as "core" CPG interneurons (Goulding, 2009). The roles of each type of interneuron are summarized in Figure 1-4b.

1. 3. 3. Speed-dependent recruitments of spinal interneurons and motoneurons

In recent years, the various roles of different types of spinal neurons for locomotion have been revealed. In particular, the roles of spinal interneurons in locomotor speed control is attracting attention (El Manira, 2014). Recently, type-specific recruitment of the spinal interneurons depending on locomotor speed has been frequently reported in zebrafish swimming (McLean et al., 2007; McLean et al., 2008; Zhong et al., 2011; Ausborn et al., 2012; Ampatzis et al., 2013, 2014) and mice walking (Gosgnach et al., 2006; Crone et al., 2009; Zhong et al., 2011; Talpalar et al., 2013).

For example, Talpalar et al. (2013) found that two subtypes of V0 interneurons (commissural interneurons) distinctly contributed to left-right alternation depending on step frequency by using selective elimination of the two subtypes of V0 interneurons. Mice, which was ablated both types of V0 interneurons, lacked the ability to generate normal alternate limb movements. The mice hopped like a rabbit (Fig. 1-5a and Fig. 1-5b second row). Deletion of $V0_V$ interneurons caused deficits in the left-right alternation under fast step frequency (Fig. 1-5b,

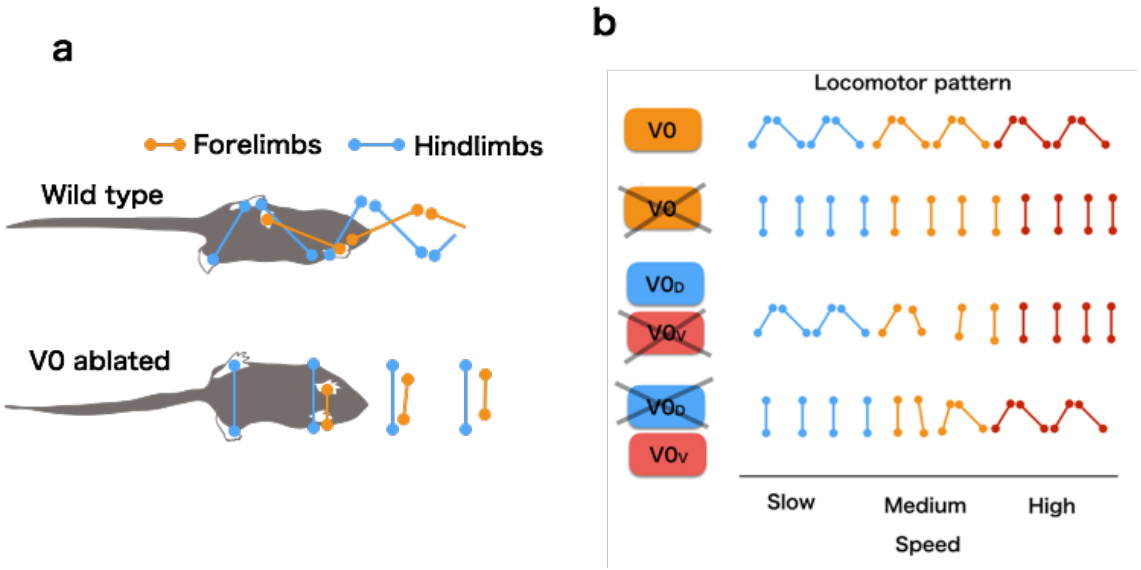

Figure 1-5. Speed dependency of V0 interneurons in left–right alternative locomotion. (a) Schematic of the limb movement of wild type (upper) and V0 ablated mice (lower). (b) Schematic of the limb movement of wild type and mutant mice. Wild type mice (first row) walk alternately and V0-ablated mice (second row) perform hopping across all speeds. $V0_V$ deficient mice have deficits in performing left–right alternation in slow speeds but not in fast speeds. $V0_D$ ablated mice have deficits in left–right cooordination in fast speeds but not in slow speeds. (Cited and modified from Talpalar et al., 2013)

third row). On the other hand, deletion of $V0_D$ interneurons caused deficits in left-right coordination at slow step frequency (Figure 1-5b, fourth row). Thus, this finding indicated that although slow walking and fast walking have been defined as the same locomotor mode, the neural mechanisms underlying slower and faster walking are clearly different in mice.

1. 4. CPGs in human locomotion

Knowledge about human locomotor CPG is limited compared with those in animal models due to the difficulty of access to the spinal neuronal networks. Nevertheless, studies on patients with spinal code injury (SCI) demonstrated several evidences that CPG-like neural networks are phylogenetically preserved in humans (Calancie et al., 1994; Dimitrijevic et al., 1998; Calancie,

2006). Calancie et al. (1994) reported that involuntary step-like movements were observed in a patient with spinal cord injury to the cervical spinal cord. Dimitrijevic et al. (1998) demonstrated more direct evidence using epidural spinal cord stimulation. They demonstrated that stimulation at the L2 spinal segment induced locomotor-like movements in the bilateral legs in patients with complete SCI. Also in healthy peoples, it was demonstrated that involuntary locomotor-like activity could be induced by repetitive spinal electromagnetic stimulation (Gerasimenko et al., 2010).

Recently, it was demonstrated that complex activities of multiple muscles during walking are generated by a small set of locomotor modules, which generate synergistic locomotor muscle activity (Ivanenko et al., 2004; Dominici et al., 2011). The locomotor modules were extracted from multi-muscle electromyographic recordings using decomposition techniques, such as non-negative matrix factorization (NMF) and principal component analysis (PCA). A locomotor module consists of temporal pattern component and muscle weighting component, and it is regarded as a fundamental unit generating functionally relevant patterns of muscle activity (Neptune et al., 2009; Clark et al., 2010). The two different components of human locomotor modules, temporal pattern component and muscle weighting component, are considered to be corresponding to the two distinct layer of the CPG organization, rhythm generation layer and pattern formation networks, respectively (Fig. 1-3). This idea has been supported by a study, which suggested that the modules are encoded in a multi-layered organization of spinal interneuron networks using the module extraction and spinal electrical stimulation to spinalized animals (Hart and Giszter, 2010).

Existence of the locomotor module in the human spinal cord was strongly suggested by a recent study on complete-SCI patients (Danner et al., 2015). This study firstly showed that tonic drive to the lumber spinal cord of complete-SCI patients by epidural electrical stimulation could induce coordinated muscle activities in lower limb muscles. Then they demonstrated that the induced coordinated muscle activity is explained by outputs of a combination of few

locomotor modules extracted by NMF (Danner et al., 2015).

Although it has been strongly suggested existence of the locomotor modules in human spinal cord, the majority of the mechanisms remains unknown. Therefore, it is still unclear whether the neural mechanisms recently revealed in animal models is shared with human locomotor circuits. As for the commonality of the CPG mechanisms among vertebrates, previous studies in various species based on electrophysiological (Quinlan and Kiehn, 2007; Jankowska, 2008), genetic (Lanuza et al., 2004; Satou et al., 2012; Ljunggren et al., 2014), and neurochemical (Reith, 1990; Kehne et al., 1996) approaches demonstrated several common principles in the organization of CPG across species. In particular, the core components of CPG (interneurons related to locomotor control) are largely shared among different species, even between fish and rodents (Goulding, 2009). Dominici et al. (2011) showed the similarity of the temporal characteristics of the locomotor modules among humans and vertebrate animals. Based on the knowledge, there is a high possibility that the CPG mechanisms recently revealed in animals are phylogenetically conserved in human spinal circuits.

1. 5. Cortical involvement in locomotion

Several cat studies have showed that significant involvement of the motor cortex and the corticospinal tract during challenging walking tasks, such as ladder walking and obstacle avoidance (Drew et al., 2008; Drew and Marigold, 2015). Nevertheless, many studies have suggested that cortical activity is not generally required for control of the steady state walking in quadruped animals (Lundberg, 1979; Grillner and Wallen, 1985; Jordan, 1998; Rossignol, 2000).

On the other hand, neuroimaging studies in humans suggest that the cortical regions related to motor control are largely activated even during stereotyped walking. In recent two decades, brain imaging studies during walking demonstrated walking-related activations of several cortical (primary sensory-motor cortex for leg area, supplementary motor area, and

premotor cortex) and subcortical (basal ganglia and cerebellar vermis) structures using single photon emission computed tomography (SPECT) (Fukuyama et al., 1997), positron emission tomography (PET) (Tashiro et al., 2001; La Fougere et al., 2010) and near-infrared spectroscopy (NIRS) (Miyai et al., 2001). More recent studies using functional magnetic resonance imaging (fMRI) with MRI-Compatible treadmill devices have also demonstrated the cortical activity in motor-related regions during locomotor-like stepping task (Dalla Volta et al., 2015; Martínez et al., 2016). However, these neuroimaging techniques have a lack of the time resolution to examine relationships between the cortical activity and locomotor muscle activity dynamically changing within a stride.

Compared with the above mentioned neuroimaging methods, Electroencephalography (EEG), a method for recording electrical activity of the brain, has significantly higher temporal resolution. So far, EEG has rarely been used in dynamic movement task, because the EEG is very sensitive to movement of participants. Recently, however, two new technical developments have made EEG recordings during dynamic movement more feasible (Enders and Nigg, 2016). First, developments of novel artifact removing methods allow us to detect and remove artifact components such as movement, blinking and muscle activity artifacts, from raw EEG signals using independent component analysis (ICA) or principal component analysis (PCA) (Gwin et al., 2010; Mullen et al., 2013). Second, recent small and active EEG electrodes have become more robust to artifacts compared with traditional passive electrodes (Reis et al., 2014).

The above mentioned improvements of EEG measurements have made substantial progress in studies regarding human cortical activity during walking (Gwin et al., 2011; Presacco et al., 2011; Petersen et al., 2012; Presacco et al., 2012; Wagner et al., 2012; Bulea et al., 2015; Enders and Nigg, 2016; Artoni et al., 2017). I summarized the important studies using EEG measurement during walking in table 1-1. These studies examined cortical activity during walking from following three viewpoints: 1) identifying specific brain components (i.e., cortical

regions) that are activated during walking (Gwin et al., 2010, 2011; Wagner et al., 2012; Bulea et al., 2015; Wagner et al., 2016), 2) characterizing the time–frequency oscillation patterns of the observed cortical components with respect to the gait pattern (Gwin et al., 2011; Wagner et al., 2012; Bulea et al., 2015; Wagner et al., 2016), and 3) examining relationships between the identified brain activity and other biomechanical or physiological data (Presacco et al., 2011; Petersen et al., 2012; Artoni et al., 2017). Most commonly, the cortical activity during walking was identified from frontal and sensorimotor areas (Gwin et al., 2011; Wagner et al., 2012; Bulea et al., 2015; Wagner et al., 2016). The identified cortical components had oscillation patterns synchronized to gait cycle events in α (8–12 Hz) and β (12–30 Hz) bands.

Although recent EEG studies on humans revealed the walking-related cortical components, the knowledge of relationships between the identified cortical activity and locomotor muscle activity is still limited. Regarding cortico-muscular connectivity, Petersen et al., (2012) demonstrated significant coherence between EEG signal of Cz electrode (leg sensorimotor area) and EMG signal of tibias anterior muscle during steady-speed walking. The significant coherence was observed in α (8−12 Hz) and β to low γ bands (24−40Hz) prior to heel contact. Additionally, a most recent study demonstrated the causal connectivity from the motor cortex to leg muscles during walking (Artoni et al., 2017). These previous studies strongly suggested cortical involvement in control of muscle during steady state walking in humans. However, the following two points should be explored for further understanding of cortical control of locomotor muscle activity in humans : 1) relationships between the cortical activity and spinal locomotor networks, 2) cortical involvement in voluntary modification of muscle activity during challenging walking.

Table 1-1. Human walking studies utilizing EEG mesurement.

Author (year)	EEG channel No.	Task	EEG analysis	Observed EEG oscillation	Observed Connectivity
Gwin et al. (2010)	248	Walking and jogging	1) Development of a movement artifact removal method based on ICA. 2) ERP of sensorimotor cortex components.		
Gwin et al. (2011)	248	Walking and jogging	ERSP of identified cortical components by ICA.	Fluctuations of neural activity during the gait cycle in α (8-12 Hz), β (12-30 Hz), and high γ (50-150 Hz).	
Petersen et al. (2012)	28	Walking	Corticomuscular coherence between the motor cortex and the tibialis anterior muscle		Corticomuscular coherence between Cz and ankle flexor before heel contact (α [8–12 Hz] and β [24–40 Hz])
Presacco et al. (2011)	60	Walking	Decoding of human walking kinematics from bandpass filtered EEGs (0.1–2 Hz).		
Wagner et al. (2012)	120	Active and passive robot assisted stepping	ERSP of identified cortical components by ICA	Oscillations of motor-related cortical activity during the gait cycle for α (8–12 Hz), β (18–21 Hz), low γ (25–40 Hz). Differences between active and passive walking in sensorimotor areas.	
Mullen et al. (2013)	64	Walking	Development of a movement artifact removal method based on a sliding-window principal componet analysis (PCA).		
Bulea et al. (2015)	64	Speed control of walking	ERSP and power spectram of identified cortical components by ICA.	Oscillations of identified cortical activity during the gait cycle in α (8–13Hz), β (14–30Hz), and low γ (30–50Hz). Enhanced prefrontal synchronizations in fast walking in entire gait cycle.	
Kline et al. (2015)	256	Walking	Isolating gait-related movement artifacts from EEGs by blocking electrophysiological signals using a nonconductive layer (silicone swim cap).	Oscillations of artifact signals were mainly observed in lower than 10Hz.	
Artoni et al. (2017)	64	Walking	Information flow direction between brain (EEG signals) and muscles (EMGs) by using a causality analysis.		Causal unidirectional commands from contralateral motor cortex to leg muscles in the swing phase

ICA: independent component analysis, ERP: event-related potential, and ERSP: event-related spectral pertubation.

1. 6. Purpose and contents of this thesis

The review of the previous studies regarding neural mechanisms of vertebrate locomotion revealed that the spinal cord and the cortex have critical roles in generation of muscle activity in human bipedal locomotion. As for spinal control, the available evidences strongly suggest that humans possess CPG-like neural networks in the spinal cord, which are capable of generating the basic rhythmic activity for walking. In addition, recent neuroimaging studies suggested that the human motor cortex significantly involves in locomotor muscle control even during stereotyped walking, unlike other quadruped animals. Nevertheless, although the neural control of human bipedal locomotion has gradually been become clear, it has not been fully explained yet. Therefore, remaining questions, described below, regarding characteristics of spinal CPGs and cortical control of the spinal cord and muscles are needed to be solved for a better understanding of human locomotor control. The answers to the questions would advance our knowledge of neural control of in particular locomotor muscle activity in humans. Moreover, integrating the new findings for human locomotor control with the previously known animal neural mechanisms would make differences in locomotor control between them clearer, and therefore should provide important insights into the evolution of vertebrate locomotion. Additionally, elucidating cortical control of the spinal circuits and muscles also opens up for novel perspectives on the field of brain–machine interfaces for gait rehabilitation. The above mentioned remaining questions are as follows:

- **Spinal level: The detail characteristics of human spinal locomotor CPG is remain unclear. Are the neural mechanisms, which were revealed in animal models, conserved in human locomotor circuits?**
- **Cortical level: 1) Whether and how does the cortex control activation of the spinal CPG? 2) How does the cortex modify the muscle activity under conditions that require**

voluntary adjustment of walking behavior?

Therefore, the purpose of the thesis is to investigate role of the spinal cord and the cortex in muscle control of human bipedal locomotion by solving the questions. For this purpose, I did five separate studies. In study 1−3 (Chapter 2−4), using several indirect methods to explore the spinal neural networks from EMG signals, I examined whether neural mechanisms in the spinal locomotor networks recently reveled in animal studies are shared with humans. I examined the spinal locomotor networks at three different levels of locomotor CPG components (Fig. 1-3): pattern formation networks (Study 1), rhythm generation layer (Study 3), and motoneuron activity as an output of the CPGs (Study 2). Specifically, the objectives of these studies are to:

(1) Investigate speed- and mode-dependency in the locomotor modules consisting of pattern formation networks in the spinal CPGs (Study1, Chapter 2).

- **Research Question:** Does mode- and/or speed-dependency in the pattern formation networks exist in human locomotor networks, as revealed in mice (Talpalar et al., 2013)?
- **Hypothesis:** Different numbers and types of locomotor modules are extracted during walking and running, and also at different speeds in the same locomotor mode.

(2) Investigate speed dependency in motoneuron (MN) activity during walking. (Study 2, Chapter 3).

- **Research Question:** Are MN activations in the lumber segments of the spinal cord required to achieve a high speed locomotion, as demonstrated in mice (Cazalets and Bertrand, 2000; Talpalar and Kiehn, 2010)?
- **Hypothesis:** MN activity in the lumber segments becomes larger compared with that in

the sacral segments with increasing locomotion speed.

(3) Investigate temporal regulation mechanisms in human locomotor spinal networks. (Study 3, Chapter 4).

- **Research Question:** Does rostrocaudally traveling wave of neural activity, which is considered to be one of mechanisms in temporal layer of CPGs founded in animal models (Cuellar et al., 2009; Saltiel et al., 2015), exist in human spinal networks?
- **Hypothesis:** If the traveling wave of activation exists in the human spinal circuits for recruitment of locomotor modules, the locomotor modules extracted from EMGs are sequentially recruited from rostral to caudal regions in the spinal cord during a step.

Then, in study 4 and 5 (Chapter 5 and 6), I examined cortical involvement in the control of locomotor muscle activity using a brain decoding method and a causal connectivity analysis. Specifically, the objectives of the studies are to:

(4) Investigate how the cortex controls locomotor modules (Study 4, Chapter 5).

- **Research Question:** 1) Does the cortex involve control of spinal locomotor modules? 2) What cortical information (e.g., frequencies and regions) contributes control of the locomotor modules?
- **Hypothesis:** 1) Activations of locomotor modules can be decoded from EEG signals. 2) The decoding are based on cortical information from leg sensorimotor regions in β band, because these are considered to be deeply related to the leg motor control (Engel and Fries, 2010).

(5) **Investigate causal connectivity between the cortex and muscles when voluntarily**

modifying locomotor muscle activity (Study 4, Chapter 5).

- **Research Question**: How does the cortex modify the muscle activity under conditions that require voluntary adjustment of walking behavior?
- **Hypothesis**: The causal connectivity from motor cortex to lower limb muscles is strengthened during a skilled walking task than that during normal walking.

Then, in Chapter 7, I integrate the results at spinal and cortical levels obtained from the five studies and discuss the neural control systems for muscle activity in human bipedal locomotion. Finally, I describe the future directions and the clinical implication of the present findings.

Chapter 2 study 1

Distinct sets of locomotor modules control the speed and modes of human locomotion

This study has been published as:

Yokoyama H., Ogawa T., Kawashima N., Shinya M., Nakazawa K. "Distinct sets of locomotor modules control the speed and modes of human locomotion ". *Scientific Reports* **6**, 36275, 2016.

2. 1. Introduction

In locomotion, both animals and humans use several different locomotor modes to meet the demand for different movement speeds. In animals, for example, larval zebrafish exhibit both "slow swim" and "burst swim" modes by modifying their movement frequencies and kinematics (Budick and O'Malley, 2000). Locomotion modes in horses have more variety, i.e., walk, trot, pace, canter and gallop, on the basis of different patterns of ground contact (Robilliard et al., 2007).

Regarding the neural mechanisms underlying locomotion, experimental studies using animal models in the last few decades have provided explicit evidence for the existence of spinal CPGs, and have revealed that these CPGs consist of spinal interneuron networks that are responsible for generating locomotor rhythms and patterns (Grillner, 1981; Kiehn, 2011). In humans, recent studies on spinal cord-injured (SCI) patients (Calancie et al., 1994; Dimitrijevic et al., 1998; Calancie, 2006; Danner et al., 2015) and on healthy participants (Gerasimenko et al., 2010) have provided indirect evidence of the existence of CPGs.

Among various types of spinal interneurons related to CPGs, recent molecular and genetic techniques have revealed the existence of several subgroups depending on the functional requirement (McLean and Dougherty, 2015). In larval zebrafish, for example, different types of spinal neurons are recruited depending on swimming frequency (as reflections of different locomotion modes) (McLean et al., 2008; Ausborn et al., 2012; Ampatzis et al., 2014). Moreover, in mice, focal lesions in specific subgroups of spinal interneurons impair the natural stepping (walking) patterns in a speed-specific manner, even within the same locomotion mode (Zhong et al., 2011; Talpalar et al., 2013). Thus, these animal studies using newly developed genetic techniques have demonstrated that there are distinct spinal neuronal groups, which are recruited independently in different locomotor modes and even at different speeds in the same locomotor mode. Thus, the question arises if there are similar spinal neuronal groups that are recruited independently during walking and running in humans. This is the primary research question I aim to answer in a series of studies. In previous studies by my laboratory using the well-established locomotor adaptation

paradigm with a split belt treadmill, they demonstrated that locomotor patterns newly acquired in walking rarely transfer to running (Ogawa et al., 2012; Ogawa et al., 2015b, a), suggesting that the neural mechanisms underlying walking and running are not shared, but independent. This result was in line with Vasudevan and Bastian (2010), who showed limited transfer of newly acquired walking patterns across different speeds in the same locomotor adaptation paradigm. These behavioural-based results suggest that similar mode- and/or speed-specific neural mechanisms to those shown in animal studies are shared in humans, which I think are phylogenetically possible. To further explore this possibility in the present study, I applied the EMG signal decomposition technique (NMF) for extracting motor modules (Tresch et al., 1999; Ting and Macpherson, 2005), i.e., spatially fixed locomotor muscle synergies (Fig. 2-1). It has been suggested that the locomotor modules are encoded in spatial pattern formation networks, which activate multiple motor neuron pools, in spinal CPGs (McCrea and Rybak, 2008).

Using decomposition techniques, such as NMF, and principal component analysis (PCA), complex activities of various muscles in human walking have been revealed to be generated by the flexible combination of a small set of modules (Ivanenko et al., 2004; Dominici et al., 2011), i.e., a locomotor module as a functional unit generating functionally relevant patterns of muscle activity (Neptune et al., 2009; Clark et al., 2010). A recent study on complete-SCI patients has demonstrated that tonic drive to the lumber spinal cord by epidural electrical stimulation can induce coordinated muscle activities in lower limb muscles, which are considered to be generated by a combination of multiple locomotor modules (Danner et al., 2015). This result was consistent with recent animal studies using spinalized vertebrates, which demonstrated that extracted modules were organized in the spinal neural circuits (Saltiel et al., 2001; Saltiel et al., 2005; Hart and Giszter, 2010).

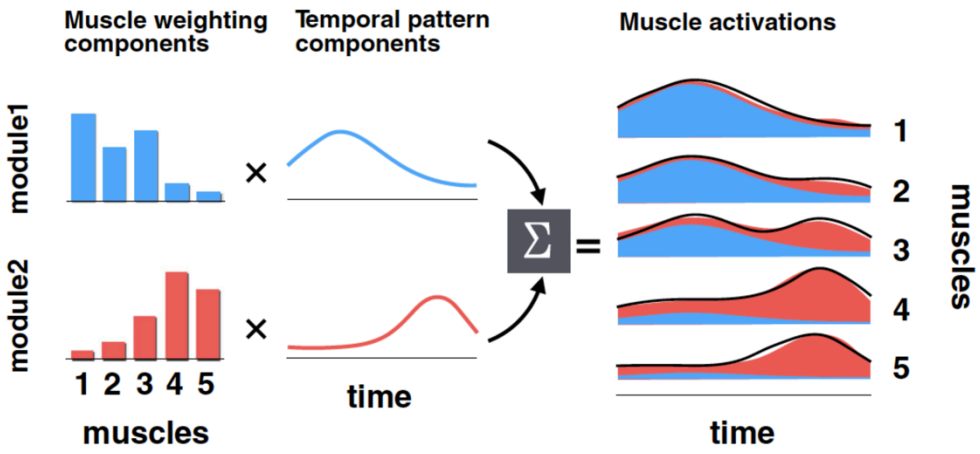

Figure 2-1. Schematic model of EMG reconstruction by the sum of muscle activation generated by different modules (five muscles and two modules, for example). The output of each module (areas filled with blue or red in the right panel) is explained by the product of the muscle weighting component (bars in the left panels; showing activation level of each muscle) and the temporal pattern components (lines in the middle panels). Consequently, the total muscle activation (black lines in the right panel) is explained by the sum of muscle activations generated by each module (filled areas).

Regarding speed- and mode-dependency of locomotor modules, previous studies in humans have examined those characteristics from the following aspects: 1) mode-dependency (i.e., differences between walking and running); 2) speed-dependency in walking; and 3) speed-dependency in running. As to mode-dependency, a previous study showed changes in muscle weighting of a trunk muscle module (Cappellini et al., 2006). In contrast to the mode-dependency, it is generally accepted that the similar modules are utilized regardless of walking speed (Ivanenko et al., 2004; Cappellini et al., 2006; Clark et al., 2010; Chvatal and Ting, 2012). Although the majority of walking modules were certainly shared at a wide range of speeds (Ivanenko et al., 2004; Cappellini et al., 2006; Chvatal and Ting, 2012), some differences in the components of the modules were found between different walking speeds in these previous studies (Ivanenko et al., 2004; Chvatal and Ting, 2012). For example, more than half of the participants used at least one different muscle weighting component of modules between slow walking and self-selected speed

walking (Chvatal and Ting, 2012). Regarding speed-dependency in running, although it has been shown that similar temporal activity patterns of modules were utilized in a slow speed range (Cappellini et al., 2006) (5–12 km/h [1.39–3.33 m/s], considered as jogging (Keller et al., 1996; Greiwe and Kohrt, 2000)), the differences in the organization of modules (i.e., muscle weightings) are not well established. Thus, it remains unknown whether walking modules are truly unchanged regardless of the speed, and more specifically, whether or not there are faster running modules in humans. Therefore, the present study was designed to reveal whether different locomotor modules are recruited with speed changes in walking and running. In the present study, I extracted locomotor modules from EMGs in walking and running over a wide range of speeds. Although the presence of speed-dependency in human locomotor modules has been debatable, based on the existence of the mode- and/or speed-dependent neural mechanisms of locomotion in animals, I hypothesize that different numbers and types of modules would be extracted from EMGs during walking and running, and also at different speeds in the same locomotor mode. The acceptance of this working hypothesis would provide indirect evidence of mode- and/or speed-dependency of neural networks in human locomotion.

2. 2. Methods

2. 2. 1. Participants

Eight healthy volunteers (ages 20–31 yr, all male) participated in the study. In addition, to examine faster running speeds, eight well-trained college runners (ages 20–24 yr, all male, experience of intensive running training for 5–11 yr) were also recruited. Each participant gave written informed consent for his participation in the study. The study was in accordance with the Declaration of Helsinki and was approved by the local ethics committee of the National Rehabilitation Center for Persons with Disabilities and Graduate School of Arts and Sciences, The University of Tokyo.

2. 2. 2. Experimental setup and design

All participants walked or ran on a treadmill (Bertec, Columbus, OH, USA) with linearly increasing speed (ramp speed condition, acceleration was set to 0.01 m/s^2). The speed range was adjusted to each group safely but as widely as possible (0.3–4.3 m/s in the non-runner group, 0.3–5.0 m/s in the runner group). These speed-ranges were set as fast as possible within the safe limits ascertained in preliminary experiments. Participants were instructed to either walk or run on the basis of their preference under the given speed. The transition speed from walking to running for all participants ranged from 1.9 to 2.3 m/s. Because the acceleration was very small and the maximum speeds were set as safe per group separately, locomotor movements in all participants were always stable during the experiment.

2. 2. 3. Data collection

Three-dimensional ground reaction force (GRF) data were recorded at 1000 Hz from force plates under each belt of the treadmill. Surface EMG activity was recorded from the following 16 muscles on the right side of the trunk and leg as that for kinematic recording: tibialis anterior (TA), gastrocnemius lateralis (LG), gastrocnemius medialis (MG), soleus (SOL), peroneus longus (PL), vastus lateralis (VL), vastus medialis (VM), rectus femoris (RF), biceps femoris (long head, BF), semitendinosus (ST), adductor magnus (AM), tensor fascia latae (TFL), gluteus maximus (GM), gluteus medius (Gmed), rectus abdominis (RA), erector spinae (ES). The EMG activity was recorded with a wireless EMG system (Trigno Wireless System; DELSYS, Boston, MA, USA). The EMG signals were bandpass filtered (20–450 Hz), amplified (with 300 gain preamplifier), and sampled at 1000 Hz.

2. 2. 4. Analysis of general gait parameters

GRF data were low-pass filtered with a zero-lag Butterworth filter (5-Hz cut-off). The times of foot-contact and toe-off were determined on a stride-to-stride basis from the vertical component of

GRF. Based on the timing of foot-contact and toe-off, stance duration, swing duration, stride duration and double support duration were calculated. Walking and running were defined by the presence and absence of double support time, respectively.

2. 2. 5. EMG processing and extraction of locomotor modules

The EMG data were divided into 0.1 m/s bins based on the treadmill speed. As the treadmill speed was continuously increasing and the acceleration was set at 0.01m/s^2, each speed bin contained 10 seconds' data. Therefore, there were 40 and 47 speed ranges for non-runners and runners, respectively. In each speed range, the first five to eight consecutive gait cycles (as many as possible in the range, almost eight except at the very slow speed) of the EMG data were used for extraction of locomotor modules. The EMG data were digitally full-wave rectified, smoothed low-pass-filtered with a zero-lag Butterworth filter. The low-pass cut-off frequency influences the smoothing of EMG patterns and thus influences the number of extracted modules (Hug, 2011). To adequately compare EMG envelopes (i.e., EMG patterns with the same smoothing) of movements performed at different speeds, the low-pass cut-off frequency must be adjusted to each speed condition (Shiavi et al., 1998; Hug, 2011). Therefore, the cut-off frequency was adapted to the stride rate in each speed range for each individual to obtain the same pattern smoothing across each speed (Hug et al., 2011; Ivanenko et al., 2013) according to the following formula: 10 × stride rate (Hz). The low-pass cut-off frequency ranged between 4.5 to 13.1 Hz. The smoothed EMG data were then time-interpolated over a time base with 200 points for each gait cycle. Then, the EMG amplitude of each muscle was normalized to the maximum value for that muscle over all speeds.

By using NMF, locomotor modules were extracted for each participant from the two types of EMG datasets: each speed range EMG matrix was composed of 16 muscles × (number of stride × 200) variables (i.e., time points) and whole-speed EMG matrices composed by each speed range EMG matrices connected in the direction of time points (i.e., the matrices were composed of 16 muscles × the summation of time points of all 40 [or 47] speed range EMG matrices). NMF has

previously been described as a linear decomposition technique (Lee and Seung, 1999; Ting and Macpherson, 2005; Tresch et al., 2006), according to equation (2-1):

$$M = W \cdot C + e, \qquad (2\text{-}1)$$

where M ($m \times t$ matrix, where m is the number of muscles and t is the number of samples, with the spatiotemporal profiles of muscle activity) is a linear combination of muscle weighting components, W ($m \times n$ matrix, where n is the number of modules), and temporal pattern components, C ($n \times t$ matrix), and e is the residual error matrix. Before the extraction of modules, each muscle data vector was normalized to have unit variance (i.e. standard deviation of each muscle data vector = 1) so as to equally weight the EMG activity across all muscles (Chvatal and Ting, 2012). This normalization was removed after module extraction to rescale the data to the original scaling and to present small activation of muscle as small. The normalization before module extraction and the removal of normalization is reasonable to reflect small activation of muscles on locomotor modules and provide small but clear patterns (Chvatal and Ting, 2012; Hagio and Kouzaki, 2014).

The module extraction was iterated 10 times for each possible n from 1 to 12, and the variance accounted for (VAF) by the reconstructed EMG (M) was calculated at each iteration. The iteration with highest VAF was kept. VAF was defined as 100 × uncentered Pearson's correlation coefficient (Zar, 1999; Torres-Oviedo et al., 2006). Then, I defined the optimal module number n as the number fulfilling the following three criteria. First, n was selected as the smallest number of modules that accounted for > 90% of VAF (Torres-Oviedo et al., 2006). Second, n was the smallest number to which adding an additional module did not increase VAF by > 5% of VAF (Frere and Hug, 2012). Third, n was selected using the "cusp" method, as named by Cheung et al. (2009) . The cusp method selects the smallest n such that the increase of VAF derived from an additional module is lower compared with the increase of 75% of the almost constant VAF slope calculated for random EMG data (i.e., the number beyond which any further increase in the number of extracted synergies yields a VAF increase <75% of that expected from chance). In brief, the VAF

curve (a plot of the VAF against the number of modules from 1 to 12) was created from both the original EMG matrix and an unstructured EMG matrix generated by randomly shuffling the original data matrix across muscles and times (i.e., the unstructured EMG dataset has no regularity). Then, *n* was selected as the number at cusp, at which the slope of the original VAF curve falls below 75% of the slope of the shuffled VAF curve. The selected number *n*, beyond which any greater increase in the number of modules contributes to an increase in VAF smaller than 75% of that likely stemming from chance, may be regarded as a reasonable selection for the number of modules.

The number of modules were compared among the whole speed and the six representative speeds in each participant group (nearest speed to 20%, 50%, and 80% of the walking and running speed range in each participant, for the "slow walk", "moderate walk", "fast walk", "slow run", "moderate run", and "fast run", respectively, corresponded to 0.60 ± 0.53, 1.18 ± 0.64, 1.69 ± 0.64, 2.49 ± 0.64, 3.19± 0.64, and 3.85 ± 0.53 m/s in non-runners, and 0.70 ± 0.00, 1.28 ± 0.35, 1.79 ± 0.35, 2.74 ± 0.52, 3.60 ± 0.00, and 4.40 ± 0.00 m/s in runners).

2. 2. 6. Clustering the modules across participants

To quantify the similarity of modules among participants at each speed, I sorted the extracted modules using hierarchical clustering analysis (Ward's method) (Ward 1963) of muscle weighting components. The sorting was performed for all participants for each speed condition (the whole speed and the six representative conditions) per group separately. The optimal number of clusters was determined by the gap statistic (Tibshirani et al., 2001). Subsequently, the muscle weighting components in each cluster were averaged across participants. If two components from a participant were put in a same cluster, we retained only one of them (that which had the higher similarity to the cluster average) in that cluster (Hagio and Kouzaki, 2014). Although the module having a lower similarity to the cluster average was excluded from the analysis about sorting across participants, these modules were used for the other analyses (EMG reconstruction [described later]

and number of modules). Then, correlations were calculated for all pairs of the averaged muscle weighting components between those at the whole speed and for each representative speed. A pair was regarded as the same type of components if it had an *r*-value larger than 0.623 (Chvatal and Ting, 2012).

In addition, corresponding temporal pattern components were also grouped based on the results of the clustering of muscle weighting components. To evaluate activation pattern modulation within a gait cycle, each temporal activation pattern component was averaged across strides. Then, these activation patterns within a gait cycle were averaged across participants with each cluster. Finally, to quantify the similarity between the averaged temporal pattern components among speeds and between modes, the timing of the main peak was calculated for the muscle weighting components.

2. 2. 7. Reconstruction of EMG across all speeds with a set of modules

The above-mentioned analyses can evaluate changes in the number of modules and the components of modules (i.e., differences among each module). However, it remains unclear that the quantitative differences between sets of modules among speeds and modes. For example, in my study, the number and types of extracted modules were different between slow walking and fast walking, while only the types of modules were different between fast walking and slow running (described later in the Results section). However, it was difficult to determine which difference is greater using only the evaluation based on the number and component of characteristics. To evaluate differences between sets of motor modules among different conditions, some previous studies (d'Avella et al., 2006; Clark et al., 2010; Berger et al., 2013; Oliveira et al., 2014) assessed how well a set of modules in one condition reconstructed muscle activities in other conditions. In the present study, I performed EMG reconstruction analysis to evaluate quantitative differences between sets of modules among different locomotor modes and speeds. A detailed schema of this method is shown in Figure 2-2. First, I reconstructed EMG activity across all speeds by fixing one

set of muscle weighting components extracted from one speed and while optimizing only temporal pattern components to reduce the error between the original and reconstructed EMG for each speed (Fig. 2-2a). Then, the reconstruction accuracy was evaluated based on the VAF between the original and reconstructed EMG (Fig. 2-2a, right panels). In this analysis, EMGs had to be reconstructed with a high VAF among the speeds where similar modules were recruited. The procedure was iterated for all speed EMGs for one module set at a certain speed; that is, 40- (or 47-) dimensional reconstruction accuracy vectors were calculated for each module set at 40 (or 47) speeds. Next, reconstruction accuracy matrices (Fig. 2-2b, heat map) were constructed by vertically combining the reconstruction accuracy vectors as row vectors for each speed (Fig. 2-2b, an example vector is surrounded by a white dotted line). In the heat map, one line of values on the x-axis indicates the reconstruction accuracy to all speed EMGs of one module set. Subsequently, the matrices were averaged across participants separately for each participant group. Here, assuming that homogeneous module sets have similar trends in EMG reconstruction accuracy, I evaluated changes of modules among speeds and modes based on the extent to which a component set at a certain speed can reconstruct all speed EMGs. If a specific set of modules is recruited for a certain range of speeds, the reconstruction accuracy vectors should change at the border between the ranges of the speeds (Fig.2-2b, arrows denote speed ranges of a specific set of modules). Therefore, to quantify the changes in the reconstruction accuracy vectors among speeds, the vectors were grouped by hierarchical clustering (Ward's method). The optimal number of clusters was determined by the gap static method (Tibshirani et al., 2001).

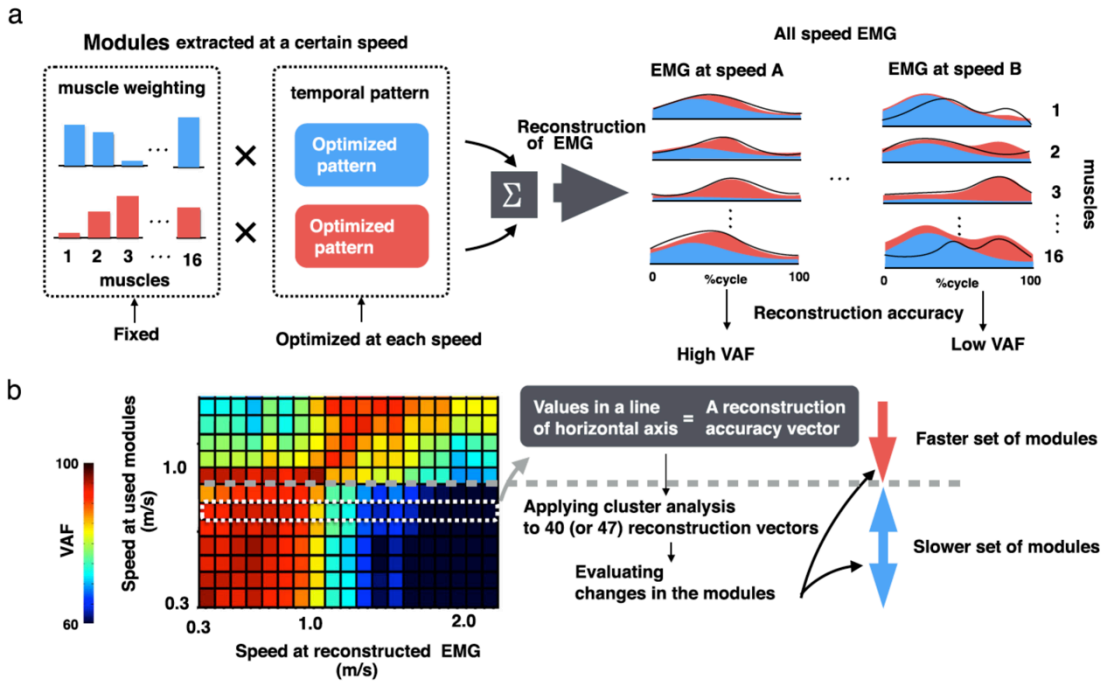

Figure 2-2. Schematic of the EMG reconstruction method (a) and the evaluation of shifts in components of modules based on reconstruction accuracy vectors (b). (a) EMG reconstruction was accomplished by fixing muscle weighting components (blue and red bars in the left panels) while optimizing the temporal pattern components (blue and red rectangles in the left panels) to reduce the error between the original EMG (black waveforms in the right panels) and reconstructed EMG (areas filled with blue or red in the right panels). Then, variance accounted for (VAF) was calculated between the original and reconstructed EMG. If the components are able to reconstruct the EMG signal with high accuracy, the VAF represents high value (at speed A, left waveforms and filled area). Otherwise, the VAF represents low value (at speed B, waveforms and filled area). This procedure was performed for one set of components at all speeds. That is, a 40- (or 47-) dimensional reconstruction accuracy vector was created for 40 (or 47) speeds. (b) The reconstruction matrices (heat maps) were created from the reconstruction accuracy vectors across all speeds. Values in a line along the horizontal axis (surrounded by a white dotted line) represent a reconstruction accuracy vector. The shifts of components of modules (at 0.9 m/s in this example; a grey dashed crossbar between two arrows) were assessed by cluster analysis applied to the overall speeds of reconstruction vectors.

2. 2. 8. Statistics

Differences in the number of modules were compared among seven speed conditions (whole speed and six representative speeds) per participant group using the non-parametric Kruskal–Wallis one-way analysis of variance (ANOVA) test with the Steel–Dwass post hoc test (nonparametric Tukey's test). Data are presented as the mean and standard error of the mean (mean ± SE). Statistical significance was accepted at $p < 0.05$.

2. 2. 9. Validation of the effect of criterion for the number of modules

In previous studies, criteria to select the module number are broadly classified into two types: "global" and "local" criteria. The "global" criteria is based on the R^2 (coefficient of determination) or the VAF between the overall reconstructed EMG matrix and the overall original EMG matrix and should be greater than some threshold (e.g., global VAF > 90% (Frere and Hug, 2012)). The "local" criteria is based on the R^2 or VAF between reconstructed EMG and original EMG for each individual muscle and needs to be greater than some threshold (e.g., all each muscle VAF > 75% (Chvatal and Ting, 2012)). A large number of studies, including the present study, used the "global" criterion (Ivanenko et al., 2005b; Ting and Macpherson, 2005; Dominici et al., 2011; Frere and Hug, 2012; Danner et al., 2015). While many other studies use a combination of "global" and "local" criteria (Clark et al., 2010; Chvatal and Ting, 2012; Hagio and Kouzaki, 2014). It has been reported that different criteria may lead to different module numbers and components (de Rugy et al., 2013). Therefore, I determined whether the present results would be the same using the criterion combined with global and local VAF. Locomotor modules were extracted from the above-described EMG data based on the same criteria used in a study by Chvatal and colleagues (Chvatal and Ting, 2012) (global VAF > 80% and all each muscle VAF > 75%). Using these extracted modules, I performed the above-mentioned analyses (i.e., comparison of the number of modules, and clustering the modules based on weighting components and EMG reconstruction). In addition, it should be noted that there is a possibility that there is less variability in the EMG

patterns in slow walking and that all modules used in faster walking are not extracted from slow walking EMG, especially at the same criterion. Thus, I extracted five locomotor modules at all speeds (five modules condition) and tested whether the same modules were extracted among the different modes and speeds. First, five locomotor modules were extracted from the above-described EMG at all speeds. Then, using these extracted modules, the same analyses (i.e., clustering the modules based on weighting components and EMG reconstruction) were performed.

2. 3. Results

2. 3. 1. Changes in EMG pattern depending on locomotor speed and mode

I recorded EMG activities from the 16 muscles on one side of the trunk and leg. The EMG activity from a typical participant is shown in Figure 2-3. Changes in the EMG patterns depending on locomotor speed and mode were roughly divided into three types based on visual inspection, with the exception of a few others (TA, RF, and AM). In the first type, the peak activation level gradually increased with increasing speed regardless of locomotor mode, while the activation timing was nearly constant throughout the majority of proximal leg muscles (GM, VL, VM, BF, and ST) and the trunk muscles (RA and ES). In the second type, the activation level increased with increasing speed regardless of locomotor mode, while the activation timing abruptly shifted to an earlier phase at the walk-to-run transition in the triceps surae (SOL, MG, and LG) and the PL. In the third type, clear activity was seen from the slowest walking speed, and the activation durations were gradually shortened with acceleration regardless of locomotor mode in the Gmed and the TFL.

2. 3. 2. Extracted locomotor modules at different speeds

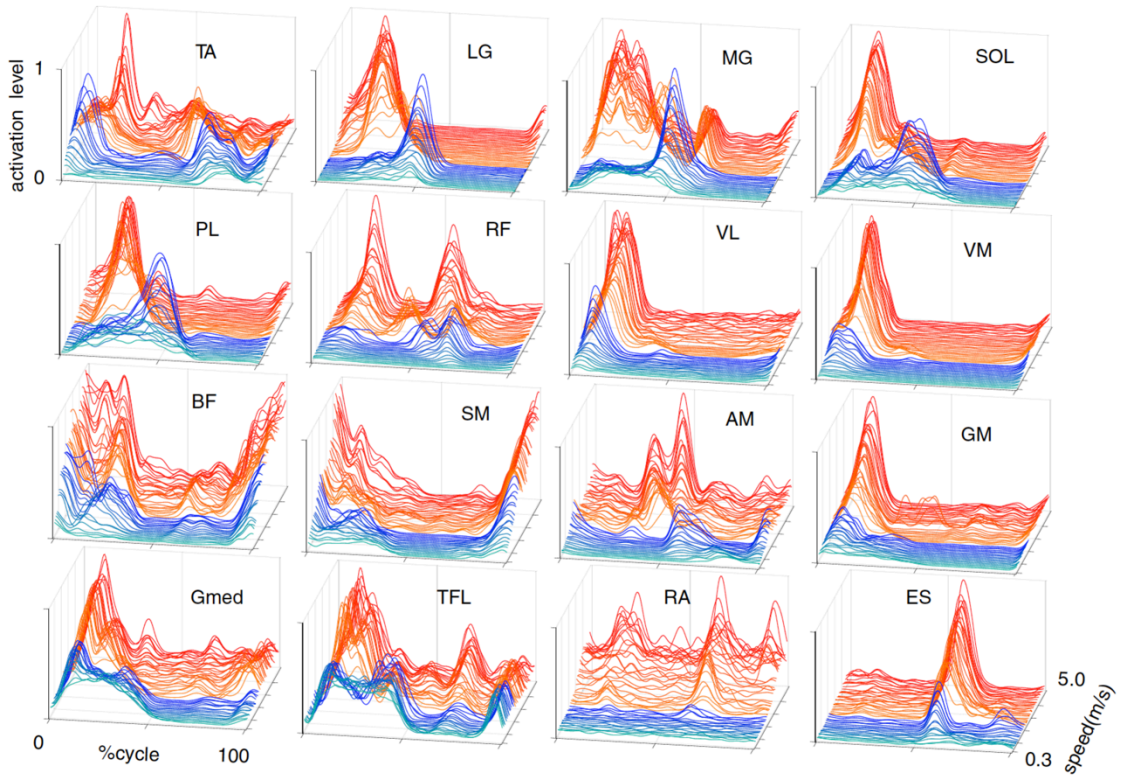

Figure 2-3. Muscle activation patterns during gait cycles over the course of speeds. Each waveform represents the ensemble average of the first six gait cycles in each speed range in a single participant (runner). The amplitude is normalized to the maximal value for each muscle over all speed ranges in this participant. The waveforms shown in blue and red represent walking and running, respectively.

Using NMF, locomotor modules were extracted in each participant from the two types of EMG datasets: a whole-speed EMG matrix and each speed range EMG matrix. Here, I found that (1) the number of extracted modules changed depending on the locomotor mode and speed (Fig. 2-4), and (2) different sets of modules, which were extracted from the whole-speed dataset, were recruited depending on locomotor mode and speed (Table 2-1 and Figs 2-5 and 2-6).

Figure 2-4 shows the number of extracted locomotor modules in each speed range. Approximately four to five modules were extracted over the range of 1.0–5.0 m/s (Fig. 2-4a), while there were nearly three modules in the slow walking speed range (0.3–1.0 m/s, Fig. 2-4a). Subsequently, I compared the number of modules among the whole-speed and six representative

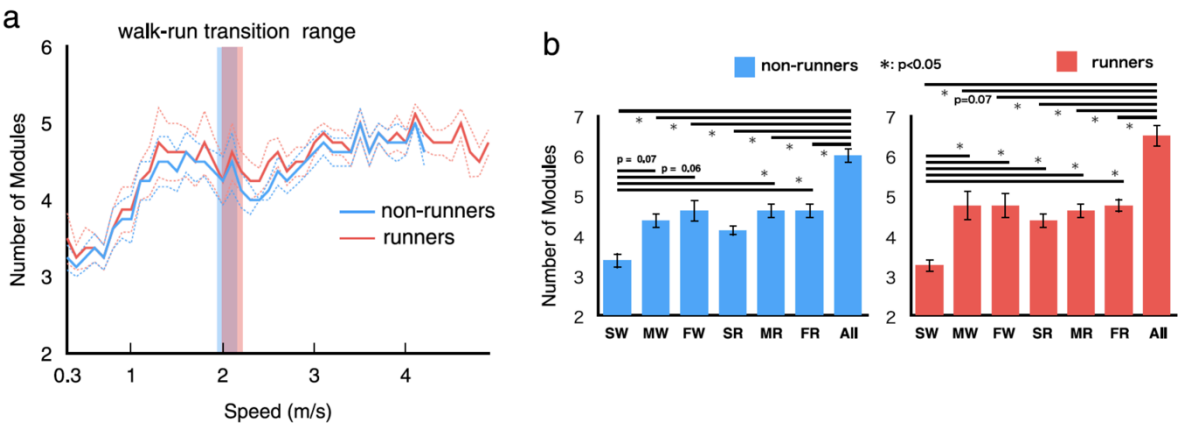

Figure 2-4. Number of modules over the course of speeds, (a) all speed and (b) at six representative speeds in non-runners and runners. (a) Average number of modules across participants in all speeds per group (thick lines) and their standard errors (SE, dotted lines) are represented. Translucent areas represent walk-run transition speed range for non-runners (blue) and runners (red). (b) The average number of modules at six representative speeds (corresponding to the speeds nearest to 20%, 50%, and 80% over the course of speeds for walking and running in each participant, respectively, for the "slow walk", "moderate walk", "fast walk", "slow run", "moderate run", and "fast run") for non-runners (blue) and runners (red). Ranges of speed of each representative speed in all participants are shown below the condition names. Error bars indicate the SE. SW: slow walking, MW: moderate walking, FW: fast walking, SR: slow running, MR: moderate running, FR: fast running, Whole: whole speed.

speeds (i.e., slow, moderate, and fast walk and slow, moderate, and fast run) independently in non-runners and runners. As the ranges of speeds in walking and running were different among participants, the six representative speeds were defined individually for each participant (see Methods, section 2.2.5.). The number of locomotor modules was significantly different among the six representative speeds in non-runners and runners ($p < 0.001$ for both groups, Kruskal–Wallis one-way ANOVA). Specifically, the number of modules in slow walking was significantly lower than that in moderate run, fast run, and whole speed in non-runners, and the number of modules in slow walking for runners was significantly lower than that in all other conditions (Fig. 2-4b; $p = 0.074$ [0.030], 0.056 [0.031], 0.11 [0.036], 0.036 [0.021], 0.036 [0.014], and 0.0079 [0.0081] for moderate walk, fast walk, slow run, moderate run, fast run, and whole speed in non-runners

[runners], respectively; post hoc Steel–Dwass test). Additionally, the number of modules in the whole-speed dataset was significantly higher than those at all other conditions except in moderate walking in runners (Fig. 2-4b; p = 0.0079 [0.0081], 0.013 [0.074], 0.049 [0.044], 0.0069 [0.0091], 0.018 [0.0091], and 0.018 [0.0081] for slow walk, moderate walk, fast walk, slow run, moderate run, and fast run in non-runners [runners], respectively).

Figure 2-5 shows a typical example of the extracted components of locomotor modules (muscle weighting components [Fig. 2-5, bars] and their corresponding temporal activation patterns [Fig. 2-5, waveforms]) in the six representative speed and whole-speed conditions from a representative participant. In this participant, seven types of modules were extracted in the whole-speed condition, and different sets of the whole-speed modules were extracted for the six speeds.

Next, I examined whether the same types of modules were used among participants and speeds using the hierarchical clustering method. As a result, seven types of modules were extracted from the whole-speed datasets in both groups (Table 2-1 and Fig. 2-6). For the six representative speeds, different sets of the whole-speed modules were extracted with changing speed (Table 2-1 and Fig. 2-6). Figure 2-6 shows each type of muscle weighting component of the modules from the whole-speed datasets (bars on the left column) and their corresponding temporal activation patterns for each representative speed (waveforms on the right of the muscle weighting components). As the speed increased, the temporal activation patterns of each module increased in amplitude. Although sorted based on the similarity of muscle weighting components, the peak timings of temporal activation patterns in the same types of modules were also similar among participants (grey waveforms) and speeds (displayed in the same colour). Nevertheless, there were some differences in the peak timings of M3 and M7 depending on mode and speed. In M3, the peak timing was substantially shifted from a peak at around 45% of the cycle during walking to around 20% of the cycle during running. Although M7 has two clear peaks (at initial stance and initial swing) during slow running in runners, the intensity of the first peak diminished during fast running.

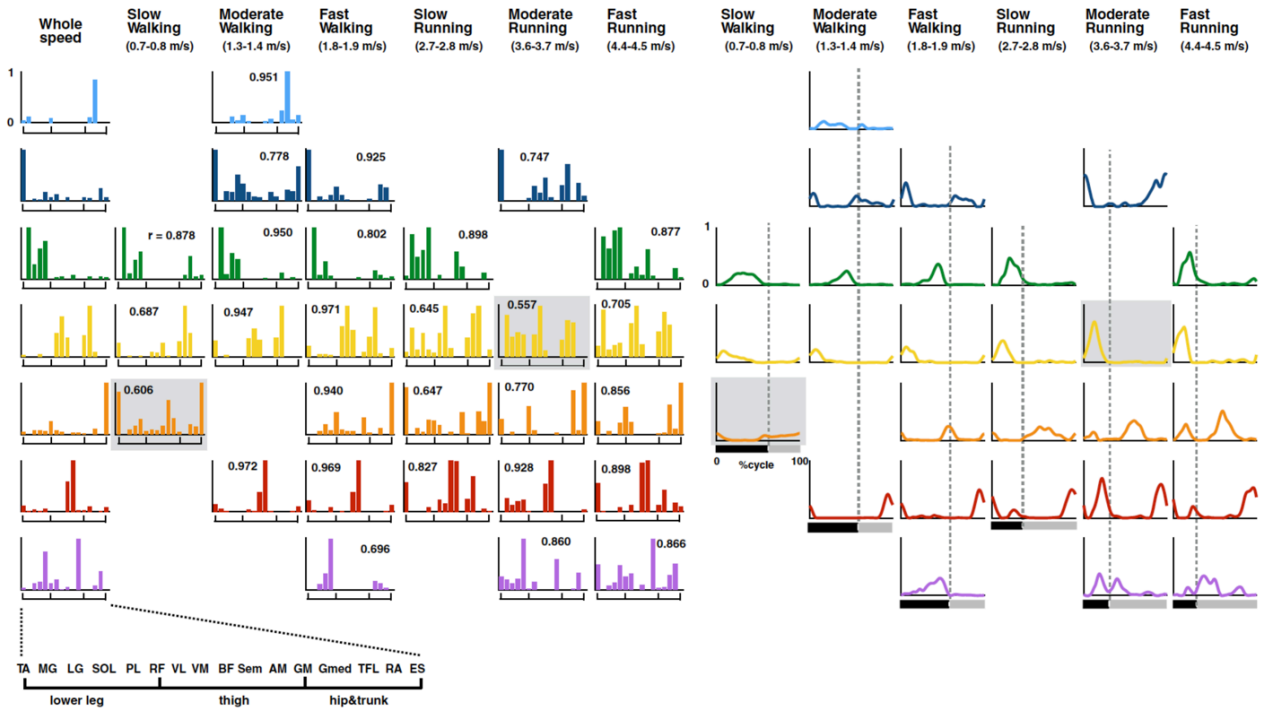

Figure 2-5. Extracted muscle weighting components and corresponding temporal patterns in whole speed and each representative speed in a representative participant. Each bar height represents the relative level of activation of each muscle within the muscle weighting components. Correlation coefficients between modules for the whole speed and for the representative speed in the same row are shown. The same types of components are represented by the same colour ($r > 0.623$, $p < 0.01$). One module indicated with a grey background has $r > 0.497$ ($p < 0.05$), but < 0.623. An enlarged view of the x-axes is shown in the bottom left corner. Temporal pattern components (waveforms) are placed in the corresponding position to their muscle weighting components. The speed for the representative participant is shown below the condition names. The underbars denote stance phase (black) and swing phase (grey) in a gait cycle. The dotted lines denote the transition timing from stance phase to swing phase.

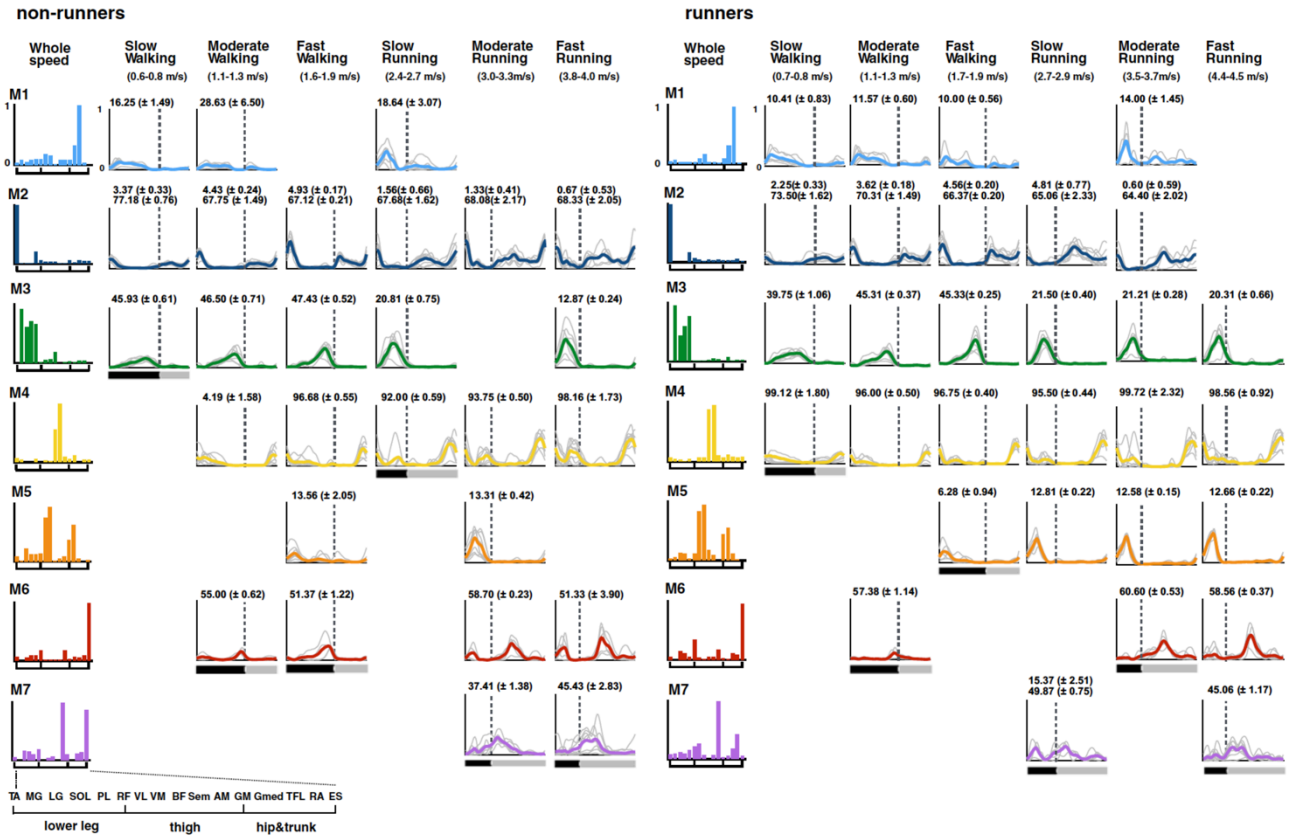

Figure 2-6. Seven types of muscle weighting components from whole-speed datasets in all participants per group, and shifts in the active components depending on speed and mode and their corresponding temporal pattern components. The averages of each cluster of muscle weighting components from whole-speed datasets are shown in the left column (M1–M7). An enlarged view of the *x*-axes of these components is shown in the bottom left corner. If the components are used in the representative speeds (see Table 2-1), corresponding temporal pattern components are shown to the right of these components. The peak timings (% cycle) are shown just above each temporal component. Ranges of speed of each representative speed for all participants are shown below the condition names. The underbars denote average stance phase (black) and swing phase (grey) in a gait cycle across participants. The dotted lines indicate the average transition timing of stance phase to swing phase across participants.

Table 2-1. Characteristics of modules and number of participants within the clusters of module

			Number of participants within clusters (non-runners/runners)						
	Timing	Major Muscles	Whole	SW	MW	FW	SR	MR	FR
M1	Early stance	TFL, Gmed	7/8	5/6	4/7	-/4	7/-	-/4	-/-
M2	Initial stance/Mid swing	TA	8/8	8/8	8/8	8/8	8/8	6/5	6/-
M3	Mid-late stance	MG, LG, SOL, PL	8/8	8/8	8/8	8/8	8/8	-/7	8/8
M4	Late swing-Early stance	BF, SM	8/7	-/4	8/7	4/6	7/7	8/7	8/8
M5	Early stance	RF, VL, VM, GM, Gmed, TFL	4/6	-/-	-/-	8/7	-/8	8/6	-/6
M6	Late stance/Mid swing	ES, RF	5/8	-/-	4/4	8/-	-/-	5/5	6/8
M7	Initial swing	AM, RA, ES	4/6	-/-	-/-	-/-	-/4	6/-	7/8

Whole: whole speed, SW: slow walking, MW: moderate walking, FW: fast walking,

SR: slow running, MR: moderate running, FR: fast running

2. 3. 3. EMG reconstruction

The above-presented results demonstrate that the number and the components of modules changed depending on locomotor speed and mode. To further quantify the speed- and mode-dependent differences among sets of modules, I performed EMG reconstruction and cluster analysis. Figure 2-7a shows heat map representations of the reconstruction accuracy matrices for representative participants in non-runners and runners, and Fig. 2-7b shows the averaged data across participants in each group. Because walk-run transition speed was different in each participant, the data at transition speed (non-runner: 1.9–2.1 m/s, runner: 2.0–2.2 m/s) were excluded from these averaged data (Fig. 2-7b). These heat maps show that the reconstruction accuracy vector of set of modules at each speed (i.e. one line of values on x-axis) changed depending on mode and speed. In the averaged heat maps, the reconstruction vectors were divided into walking and running as two large clusters in both groups (Fig. 2-7c). The walking cluster was divided into three sub-clusters in both groups, and the running cluster was divided into two and three sub-clusters in non-runners and runners, respectively (Fig. 2-7c). The structures of the clusters indicate the quantitative differences among sets of locomotor modules. Thus, the results indicate that locomotor modules

change greatly between walking and running, and change within the same locomotor mode (i.e., depending on speed).

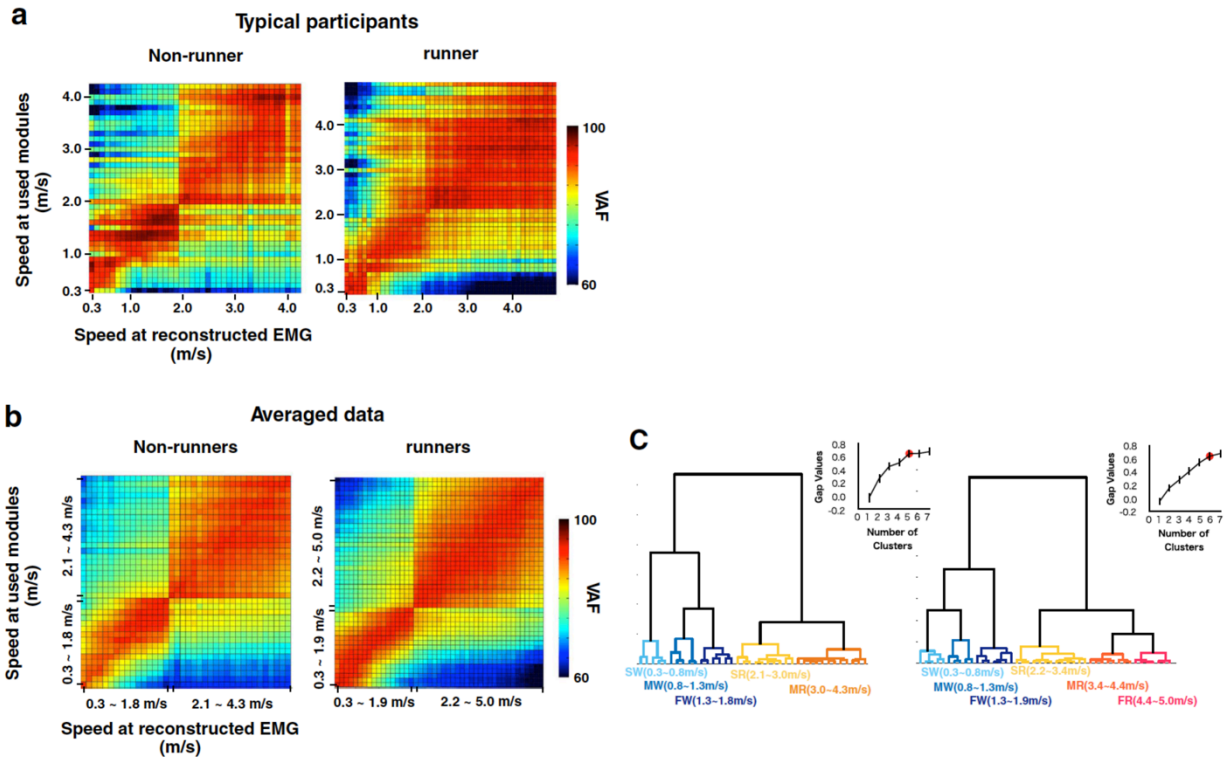

Figure 2-7. Reconstruction accuracy matrices for representative participants (a), averaged data for each participant group (b), and results of cluster analysis applied to the averaged data (c). (a), (b) VAF values in a line along the horizontal axis represent a reconstruction accuracy vector for a particular speed. Changes of the values of the vector indicate changes in the components of modules. A colour scale denotes the VAF value. The data in the walk-run transition speed range were excluded when averaging data. (c) Dendrograms represent the results of cluster analysis (Ward's method, Euclidian distance) applied to the averaged data. The line charts show the optimal cluster number based on the gap statistic values. Error bars indicate the SE. The red circles indicate the optimal cluster number. The same clusters are indicated with the same colour. SW: slow walking; MW: moderate walking; FW: fast walking; SR: slow running; MR: moderate running; FR: fast running.

2. 3. 4. Validation of the effect of criterion on the number of modules

Additionally, I tested whether the above-presented results (Figs 2-4 to 2-7) are observed in different criteria for selection of module number. Figures 2-8 to 2-10 show the number of modules, extracted module types, and reconstruction accuracy vectors in the case of criteria combined with global and local VAF. As this criterion was more severe compared with those for the above results, on average across participants, 6 to 11 modules were extracted in all speeds (Fig. 2-8a). When comparing the six representative speeds and whole speed conditions, the number of modules was different among speeds (Fig. 2-8b). The types of extracted locomotor modules were changed among six representative speeds (Fig. 2-9). In addition, the reconstruction accuracy vectors were divided into three clusters in non-runners (slow and fast walking and running clusters), and four clusters in runners (slow and fast walking clusters and slow and fast running clusters) (Fig. 2-10).

Figure 2-11 and 2-12 show the extracted module types and reconstruction accuracy vectors in the case of five locomotor modules at all speeds. Seven types of modules similar to the above results (Table 2-1 and Fig. 2-6) were extracted, and different types of modules were used among six representative speeds except between moderate and fast running in non-runners, and between slow and fast running in runners (Fig. 2-11). The reconstruction accuracy vectors were divided into four clusters in both groups (slow and fast walking clusters and slow and fast running clusters, Fig. 2-12).

Together, the results obtained under the two different conditions indicate that, although some results were different to the results presented in the above section (Figs 2-4 to 2-7), the main findings were the same regardless of the module number selection method: 1) different locomotor modules were used depending on mode and speed; and 2) reconstruction accuracy vectors differed with changes in mode and speed.

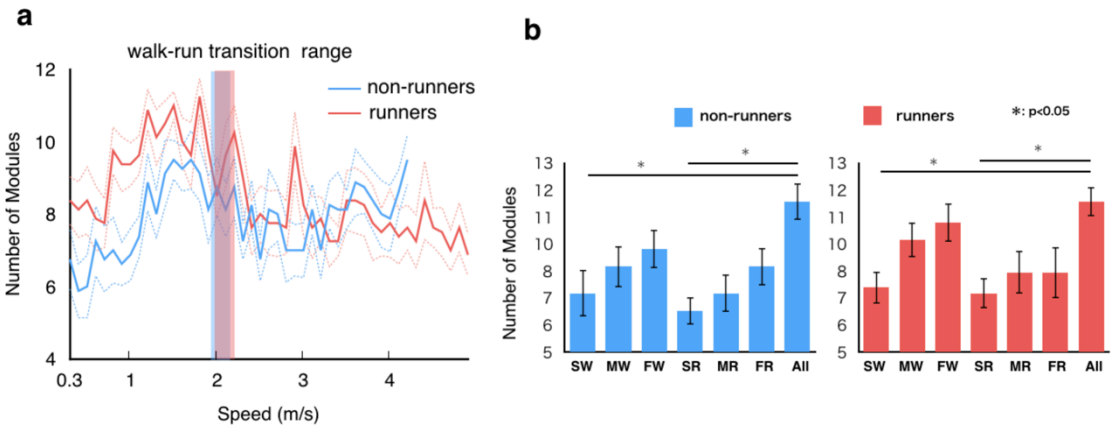

Figure 2-8. Number of modules determined by Chvatal's criterion. (a) Average number of modules across all speeds in each group (thick lines) and their standard errors (SE, dotted lines) are represented. Translucent areas represent walk-run transition speed range for non-runners (blue) and runners (red). (b) The average number of modules at six representative speeds (corresponding to the speeds nearest to 20%, 50% and 80% over the course of speeds for walking and running in each participant, respectively, for the "slow walk", "moderate walk", "fast walk", "slow run", "moderate run" and "fast run") for non-runners (blue) and runners (red). The number of modules was significantly different among the six representative speeds in non-runners and runners ($p = 0.017$ and 0.0045 for non-runners and runners, respectively; Kruskal–Wallis one-way ANOVA). In both non-runners (left) and runners (right), compared among the six representative speeds and whole speed condition, the number of modules in slow walking and slow running was significantly lower than that of the whole-speed condition (p = 0.047 [0.039] and 0.034 [0.040] for slow walking and slow running in non-runners [runners], respectively; post hoc Steel–Dwass test). The range of speeds for each representative speed in all participants are shown below the condition names. Error bars indicate the SE. SW: slow walking, MW: moderate walking, FW: fast walking, SR: slow running, MR: moderate running, FR: fast running, Whole: whole speed.

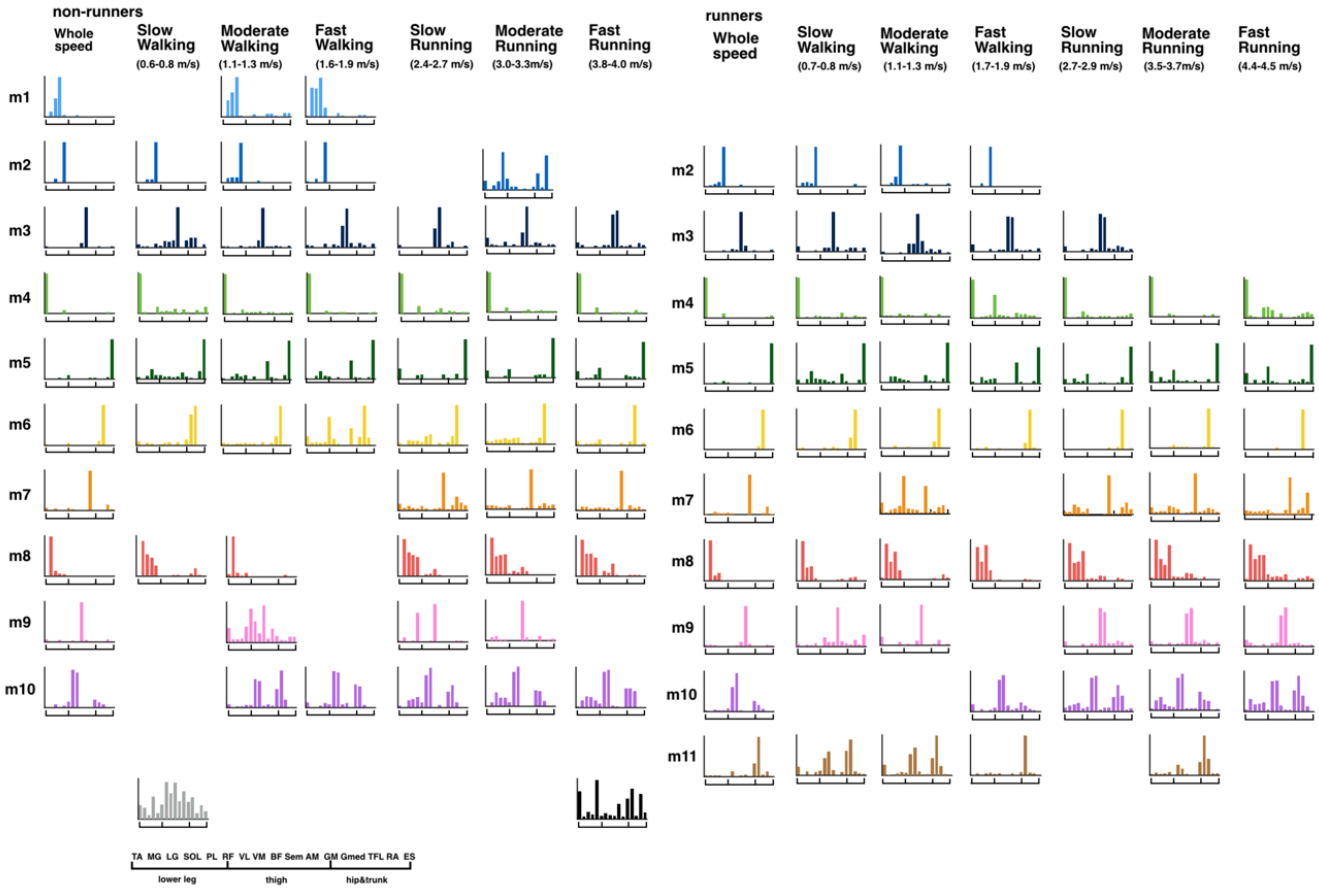

Figure 2-9. Extracted weighting components per group, and change in the extracted components depending on speed and mode in the case of the number of modules determined by Chvatal's criterion. The average of each cluster of muscle weighting components from whole-speed datasets are shown in the left column (m1–m10 in non-runners, m2–m11 in runners). An enlarged view of the *x*-axes of these components is shown in the bottom left corner. The range of speeds for each representative speed for all participants are shown below the condition names.

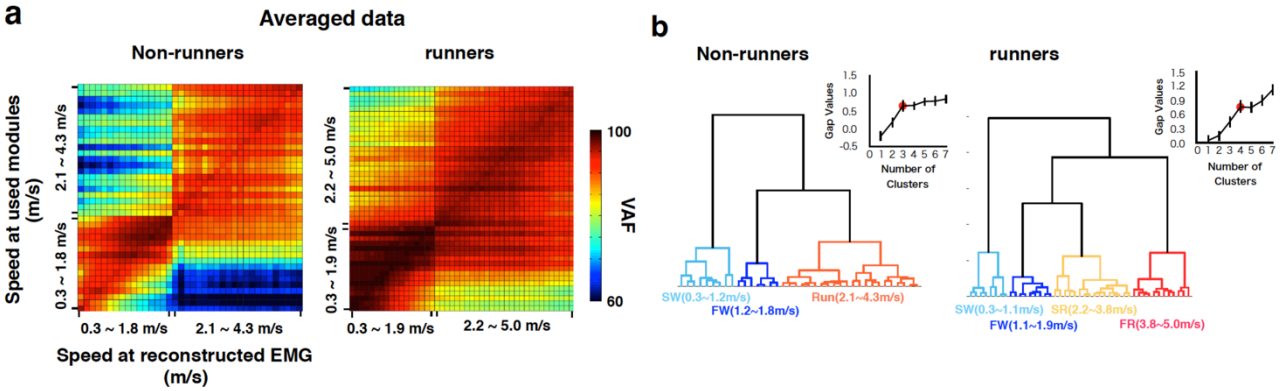

Figure 2-10. Reconstruction accuracy matrices of each component for averaged data for each participant group (a), and results of cluster analysis applied to the averaged data (b) in the case of the number of modules determined by Chvatal's criterion. (a) VAF values in a line along the horizontal axis represent a reconstruction accuracy vector for a particular speed. Changes in the values of the vector indicate changes in the components of modules. A colour scale denotes the VAF value. Data in the walk-run transition speed range were excluded when averaging data. (b) Dendrograms represent the results of cluster analysis (Ward's method) applied to the averaged data. The line charts show the optimal cluster number based on the gap statistic values. Error bars indicate the SE. The red circles indicate the optimal cluster number. The same clusters are indicated with the same colour. SW: slow walking; FW: fast walking; SR: slow running; FR: fast running.

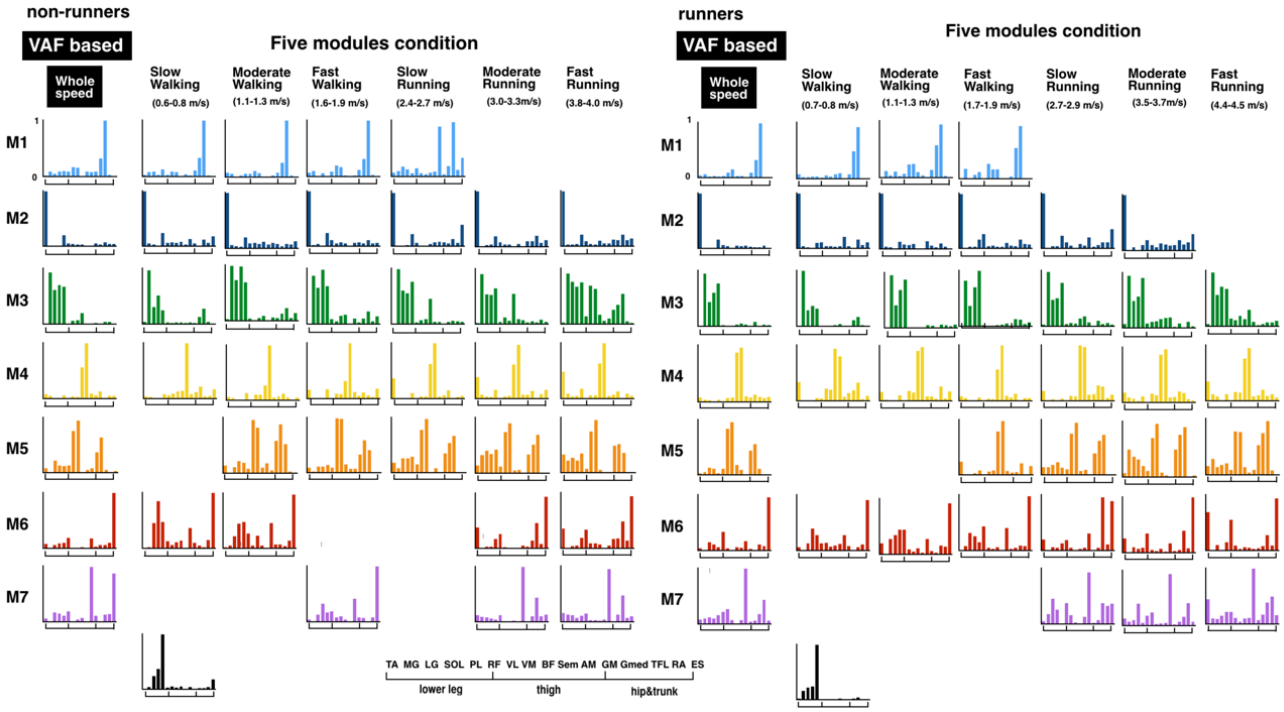

Figure 2-11. Changes in the extracted modules depending on speed and mode in cases where the number of modules was assumed to be five (five modules condition). The modules in the left column (M1–M7) are the different types of modules extracted from whole speed data using VAF based criterion (i.e. same modules presented in Fig. 2-6). Based on these modules, modules under the five modules condition at six representative speeds were sorted in the same way as Fig. 2-6. The range of speeds for each representative speed for all participants are shown below the condition names. An enlarged view of the *x*-axes of these components is shown in the bottom left.

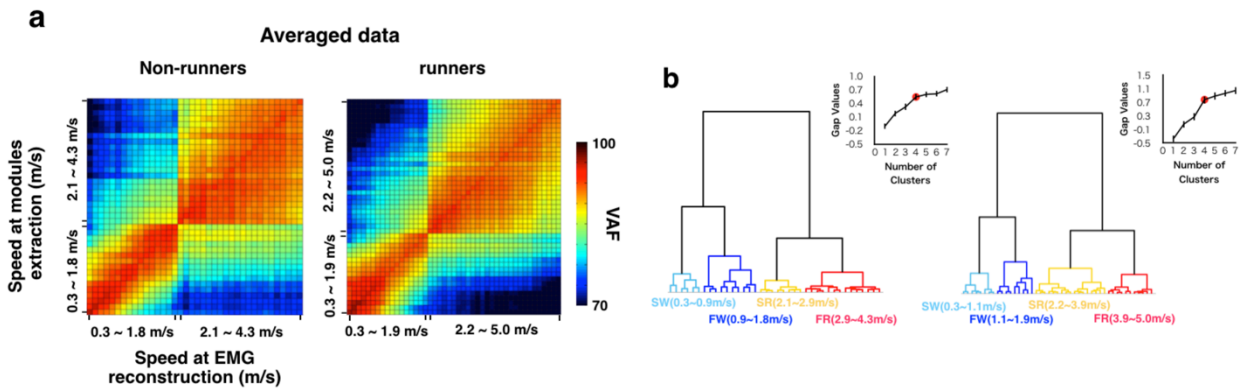

Figure 2-12. Reconstruction accuracy matrices of each component for averaged data for each participant group (a), and results of cluster analysis applied to the averaged data (b) in cases where the number of modules was assumed to be five. (a) VAF values in a line along the horizontal axis represent a reconstruction accuracy vector for a particular speed. Changes in the values of the vector indicate changes in the components of modules. A colour scale denotes the VAF value. The data in the walk-run transition speed range were excluded when averaging data. (b) Dendrograms represent the results of cluster analysis (Ward's method) applied to the averaged data. The line charts show the optimal cluster number based on the gap statistic values. Error bars indicate the SE. The red circles indicate the optimal cluster number. The same clusters are indicated with the same colour. SW: slow walking; FW: fast walking; SR: slow running; FR: fast running.

2. 4. Discussion

In the present study, assuming that human locomotor networks have speed- and mode-dependency as demonstrated in other vertebrates, I tested the following hypothesis using the motor module extraction methods: recruitment patterns of locomotor modules would shift depending on locomotor mode and/or speed. The main results were: (1) the number of modules changed depending on the mode and speed; (2) different types of modules were extracted among all six representative speeds; and (3) the reconstruction vectors were divided into two large clusters of walking and running, and both the walking and running clusters were divided into two or three sub-clusters. The structures of the clusters indicate the quantitative differences among sets of

locomotor modules. In summary, these results suggest that different locomotor modules are probably recruited depending on locomotor speed and mode, which confirms my working hypotheses. The present results provide indirect evidence for mode- and speed-dependency in the neural networks underlying human locomotion.

In the present study, based on mathematically extracted motor modules, I tested speed- and mode-dependency in neural networks for human locomotion. The validity of the procedure is strongly supported by direct evidence that spinal neural networks encode locomotor modules, which has been obtained from spinalized animals (Tresch et al., 1999; Saltiel et al., 2001; Hart and Giszter, 2010; Roh et al., 2011) and SCI patients (Danner et al., 2015). In studies applying factorization algorithms to spinalized animals, it has been suggested that the locomotor modules are encoded in the spinal neural networks (Tresch et al., 1999; Saltiel et al., 2001; Hart and Giszter, 2010; Roh et al., 2011). For example, using a spike-triggered averaging method, Hart and Giszter (2010) revealed direct relationships between the spiking of the spinal interneurons and the output of modules extracted by factorization algorithms. Likewise, it has been suggested that locomotor modules exist in spinal cord using cutaneous (Roh et al., 2011), electrical (Tresch et al., 1999) and neurochemical (Saltiel et al., 2001) stimulation combined with factorization algorithms. Similarly, a study that applied epidural electrical stimulation to the lumbar spinal cord of complete-SCI patients combined with factorization algorithms showed that rhythmic muscle activities of the lower limb were generated by a combination of multiple modules (Danner et al., 2015). Based on these previous studies, mathematically extracted locomotor modules most likely represent spinal neural networks, which underlie coordinated patterns of muscle activity. Therefore, speed- and mode-dependent changes in extracted modules found in the present study strongly suggest that active spinal locomotor networks shift in a speed- and mode-dependent manner.

Assuming that the locomotor modules are encoded in the spinal cord, the speed- and

mode-dependent recruitment of locomotor networks observed in the present study is supported by evidence from some animal studies. Recently, studies using genetic and electrophysiological methods have revealed that spinal interneurons are important components of CPGs, and each interneuron play particular roles in controlling locomotion (Goulding, 2009; Garcia-Campmany et al., 2010). Some vertebrate studies have reported that specific sets of spinal interneurons are recruited depending on locomotion speed and/or mode (McLean et al., 2008; Talpalar et al., 2013; Ampatzis et al., 2014; Bellardita and Kiehn, 2015). For walking in mice, it was demonstrated that two subtypes of interneurons regulating left-right limb alternation could be identified, and differences were found in their contribution to left-right alternation depending on walking speed (Talpalar et al., 2013). Namely, although slow walking and fast walking have been defined as the same locomotor mode, the neural mechanisms underlying slower and faster walking are clearly different in mice. In addition, the larval zebrafish exhibits two different locomotor modes depending on swimming frequency (Budick and O'Malley, 2000), and different classes of spinal interneurons are recruited depending on swimming frequencies corresponding to different locomotor modes (McLean et al., 2008; Ausborn et al., 2012; Ampatzis et al., 2014). Together, these previous results show that appropriate interneuronal locomotor modules are selected and combined within hard-wired modules depending on speed and mode based on the on/off switching of active modules. In the present study, active modules at certain speeds consisted of a combination of parts of modules extracted from whole-speed EMG datasets (Table 2-1 and Fig. 2-6). The results are similar to the characteristics of interneuronal modules in other vertebrates as regards to the recruitment of locomotor modules for speed and mode control. Although it is not clear whether such mode- and speed-dependent recruitment mechanisms of spinal interneurons can be extended to humans, the characteristics of core components of CPGs, which have been mainly derived from a set of embryonic interneurons, are remarkably conserved across different species, even between fish and rodents (Goulding, 2009). In fact, there is substantial evidence that CPG-like neural networks are preserved in humans, and they have been mostly observed in patients with chronic

SCI (Calancie et al., 1994; Calancie, 2006; Danner et al., 2015). Also, as in quadrupeds, long projecting propriospinal neurons connect the cervical and lumbar enlargements in humans (Nathan et al., 1996). Additionally, during gait, coordination and patterns of reflex mediated at the spinal cord are quite similar in humans (Berger et al., 1984) and cats (Gorassini et al., 1994). Based on these observations, the coordination of human gait seems to be controlled by the spinal neural mechanisms in much the same way as gait in other vertebrates. Similarly, if the mode- and speed-dependent recruitment mechanisms of spinal interneurons for locomotion are phylogenetically preserved in humans, this would explain the speed- and mode-dependent specificity of locomotor modules found in the present study.

Some previous studies on human locomotion compared locomotor modules among modes and speeds (Ivanenko et al., 2004; Cappellini et al., 2006; Clark et al., 2010; Chvatal and Ting, 2012). Between walking and running, a study of them changes in the muscle weighting component of trunk extensors/adductors (correlation of the modules between walking and running: $r = 0.38$, $p > 0.05$) (Cappellini et al., 2006). Conversely, regarding speed-dependency, some prior studies have argued that similar locomotor modules have been extracted while walking in various speeds, in contradiction to my results (Ivanenko et al., 2004; Clark et al., 2010; Chvatal and Ting, 2012). Nevertheless, a study extracting locomotor modules from self-selected (1.2–1.5 m/s) and slow walking speeds (0.6 m/s) reported that one locomotor module was only used at one walking speed in six out of nine participants (Chvatal and Ting, 2012). Thus, minor differences in locomotor modules that depended on speed and mode were found in these previous studies.

Methodological differences may have caused the differences in the results between the previous studies and this study. It has been proposed that the extracted modules are affected by the number of muscles, and which muscles are recorded (de Rugy et al., 2013). Some of the previous studies did not record Gmed (Ivanenko et al., 2004) or TFL (Clark et al., 2010) activities, which are major muscles in a module mainly extracted in slow and moderate walking (Fig. 2-6, M1). Therefore, it might not have been possible to sufficiently demonstrate the differences between slow

(or moderate) walking and fast walking modules in these studies. In addition, the criteria used to determine the number of modules may also be a factor in the differing results. Indeed, it has been reported that different criteria lead to different module numbers and structures (de Rugy et al., 2013). Therefore, differences in the criteria adopted between the previous and present studies might lead to the difference in the results related to speed dependency. Nevertheless, my findings were consistently observed under the three different conditions for selecting the number of modules global VAF criterion (Figs 2-3 to 2-7), criterion combining global and local VAF (Figs 2-8 to 2-10) and the five modules condition (Figs 2-11 and 2-12). Based on the results, my findings are most likely not methodology-dependent.

Regarding the speed-dependency of locomotor modules, the present method that uses EMG reconstruction with clustering provides additional information about the quantitative differences between the sets of modules among speeds and modes. In some previous studies (Ivanenko et al., 2004; Chvatal and Ting, 2012), the differences among speeds at each module level (i.e., the number of modules and the characteristics of components) were the main targets of analysis. Using these parameters, it has been difficult to compare the quantitative differences among sets of modules, particularly in cases where two sets have a different number of modules. In the present study, using EMG reconstruction methods, one set of modules at a speed was evaluated by reconstruction accuracy to muscle activities of wide speed locomotion. The reconstruction accuracy vectors were divided into walking and running as two large clusters, then the walking and running clusters was divided into two or three sub-clusters (Fig. 2-7). The structure of the clusters indicates quantitative differences among sets of modules, thus the results mean that the locomotor modules greatly differed between walking and running, and were also different among the same locomotor mode because they depended on speed. Conversely, in many previous studies, the similarity of the modules has been evaluated based on the correlation coefficient between each module. If two different behaviours use multiple similar modules just barely exceeding the criteria of similarity, the modules of the two behaviours would have been different as a whole set of

modules. By using the present EMG reconstruction method combined with clustering, the qualitative difference of component sets can be identified. Therefore, if my method had been used in previous studies (Ivanenko et al., 2004; Chvatal and Ting, 2012), the walking modules might have been divided into different clusters depending on speed.

Regarding the speed-dependency of locomotor modules, a previous study (Clark et al., 2010) performed a similar EMG reconstruction method to my method. The study reconstructed the walking EMGs over a wide range of speeds (0.3–1.8 m/s) with a high accuracy, using only one module set extracted from a self-selected speed (1.25 m/s on average). They assumed that "if the reconstruction of Y by using X is conducted with a high accuracy, then that generally means that X and Y recruit the same modules", and therefore they concluded that the same locomotor modules are recruited in various walking speeds. In my EMG reconstruction method, I did not assume the same principle because it is inappropriate for my results. For example, as the moderate speed walking modules contained almost all of the modules in slow walking (Fig. 2-6 and Table 2-1), the moderate walking speed modules could reconstruct EMGs at slow walking with a high accuracy (Fig. 2-7b). On the contrary, as the slow walking modules contained only some of the modules used in moderate speed walking (Fig. 2-6 and Table 2-1), these modules could not well reconstruct EMGs in moderate speed walking (Fig. 2-7b). Therefore, I evaluated the reconstruction vectors from another viewpoint. Assuming that homogeneous module sets have similar trends in EMG reconstruction accuracy, I evaluated the changes of modules among speeds and modes based on the extent to which a module set at a certain speed can reconstruct all speed EMGs by using hierarchical clustering. This method enabled evaluating important information about the similarity of modules among speeds and modes in the reconstruction vectors. For example, the sets of modules in slow walking (0.3–0.8 m/s) reconstructed running EMGs with only low accuracies (about 60% VAF) (Fig. 2-7b). On the other hand, those of fast walking (1.3–1.8 m/s) reconstructed running EMGs with fairly high accuracies (about 80% VAF) (Fig. 2-7b). This means that modules in fast walking contained those required in running, and suggests that there are clear differences

between slow walking modules and fast walking modules. In this method, although the clusters of reconstruction vectors were divided mathematically (Fig. 2-7c), each set of modules in each representative speed, which corresponded to speed range of each cluster, had different sets of locomotor modules (Fig. 2-6). For example, fast walking modules contained a large portion of slow walking modules (2/3 modules in non-runners, 4/4 modules in runners, Table 2-1 and Fig. 2-6), while slow walking modules did not contain many fast ones (2/5 modules in non-runners, 4/5 modules in runners, Table 2-1 and Fig. 2-6). It has been shown that each type of motor module has a particular biomechanical function, and it has been suggested that the modules act as basic neural control elements (Tresch et al., 1999; Ting and Macpherson, 2005; Neptune et al., 2009). Thus, as discussed in previous studies at each muscle level (den Otter et al., 2004b; Neptune et al., 2008), the results suggest that the different modules were recruited among different walking speeds to presumably meet additional functional demands with a speed increase (e.g., deceleration of the leg in late swing [M4] and large loading response in initial stance [M5]). Therefore, it is considered that the differences among the clusters of reconstruction vectors have important physiological relevance to the speed-dependent recruitment of locomotor modules.

Although the present study mainly focused on the muscle weightings of modules (i.e., spatially fixed muscle synergies), Ivanenko and colleagues have extensively studied the timing patterns of locomotor modules with regard to speed dependency and mode dependency (Ivanenko et al., 2004; Cappellini et al., 2006). Their studies showed that the peak timing shift of the locomotor module activities depended on the speed and mode. One of their studies indicated a peak timing shift of a temporal pattern component of ankle extensors between walking and running (~45% of the cycle during walking, 20%–30% of the cycle during running) (Ivanenko et al., 2004; Cappellini et al., 2006). Concerning speed dependency, another study showed a main activity peak of a type of temporal component mainly controlling BF and ST shifted from the late swing phase at 2, 3, and 5 km/h (0.56, 0.83, and 1.39 m/s) to the early stance phase at 1 km/h (0.28 m/s) (Ivanenko et al., 2004). In addition, the activity peaks of all types of temporal components shifted earlier

about 9% on average, depending on acceleration from 1 to 5 km/h (0.28–1.39 m/s) (Ivanenko et al., 2004). Similarly, in my study, some changes in the timing patterns of the modules were found (Fig. 2-6). The peak timing of M3 was substantially shifted from a peak at around 45% of the cycle during walking to around 20% of the cycle during running. Additionally, M7 had two clear peaks (at initial stance and initial swing) during slow running in runners; however, the intensity of the first peak diminished during fast running. In addition, as the speed increased, the temporal activation patterns of each module increased in amplitude (Fig. 2-6). Thus, on the basis of the prior studies and present results, the temporal activity patterns of each type of spatially fixed locomotor modules are adjusted depending on speeds and modes. These results suggest that the temporal and spatial aspects of locomotor pattern generation are separately and hierarchically organized, and the observation is consistent with a simulation study of locomotor CPGs that demonstrate that temporal rhythm generators in the spinal cord control the networks of spatial pattern formation (McCrea and Rybak, 2008).

Between non-runners and runners, different sets of modules were extracted at all representative speeds (Fig. 2-6, Table 2-1). In addition, another faster running sub-cluster of EMG reconstruction accuracy vectors was observed in runners compared with non-runners (Fig. 2-7). Although locomotor networks have inherent neural mechanisms (Dominici et al., 2011), plastic changes occur in the networks with locomotor training (Reisman et al., 2005; van den Brand et al., 2012). The present participants in the runners group have undergone intensive locomotive training for at least 5 years. Therefore, the possibility remains that long-term training causes plastic changes in locomotor modules. In a study targeting chronic stroke patients, it was demonstrated that alterations of modules in the stroke-affected arm reflect a fractionation of the unaffected-arm modules (Cheung et al., 2012). It was also demonstrated that the use of existing modules is an efficient way to adapt to perturbations in a study of upper-limb movement (Berger et al., 2013). Likewise, in the present study, specific sets of modules in runners were constructed using the modules extracted at other speeds or from non-runners (Fig. 2-6, Table 2-1). It is possible that the

acquisition of novel locomotor movement following long-term training is achieved via the reorganization of locomotor networks consisting of existing locomotor modules. However, one possible limitation is that the two groups were compared under different speed ranges. As the maximum speed for runners was set to faster (5.0 m/s) compared with non-runners (4.3 m/s) to examine faster speed running, the representative fast running speed differed greatly between non-runners and runners. However, the representative slow walking, fast walking, and slow running were approximately the same speed between the two groups. Therefore, it seems valid to conclude that extracted modules in the two groups were different at these three representative speeds.

In conclusion, my results revealed that different numbers and types of modules are utilized depending on the speed and the mode. This result strongly suggests the existence of mode- and speed-specificity in neural networks for human locomotion.

Chapter 3, Study 2

Speed dependency in α-motoneuron activity and locomotor modules in human locomotion

This study has been published as:

Yokoyama H., Ogawa T., Shinya M., Kawashima N., Nakazawa K.. "Speed dependency in α-motoneuron activity and locomotor modules in human locomotion: indirect evidence for phylogenetically conserved spinal circuits. *Proceedings of the Royal Society of London B: Biological sciences.* 284: 20170290. 2017.

3. 1. Introduction

Locomotor muscle activity is generated by a vast number of motoneurons (MNs) in the spinal cord. Spinal CPGs play a critical role in producing the coordinated MN activity during locomotion (Goulding, 2009; Kiehn, 2016). Recently, evidence for the existence of CPGs consisting of spinal interneurons has been demonstrated by experimental studies using animal models based on electrophysiological, genetic and neurochemical techniques (Goulding, 2009; Kiehn, 2016). Also, in humans, some studies on human spinal cord-injured (SCI) patients (Dimitrijevic et al., 1998) and on healthy participants (Gerasimenko et al., 2010) have demonstrated the ability of the human spinal cord to generate rhythmic and synergistic lower limb muscle activity.

In Chapter 2, I reported that different combinations of locomotor modules, which generate specific combinations of muscle activity (i.e., spatially fixed locomotor muscle synergies), are activated depending on speed and mode of locomotion in humans. The locomotor modules are considered to be encoded in spatial pattern formation networks, which activate multiple MN pools, in the spinal CPGs (McCrea and Rybak, 2008). Thus, Chapter 2 suggests that the CPG output changes in a manner dependent on locomotion speed and mode. Recently, to estimate how the CPG output is directed to the MN pools within each spinal segment, EMG signals were used to map the spatiotemporal MN activity in the lumbosacral enlargement (segments L2–S2) along the rostrocaudal direction (Fig. 3-1a; see the "Methods" for further details) (Ivanenko et al., 2006; Ivanenko et al., 2008). Using this method, previous studies have shown some changes in spatiotemporal MN activity depending on speed and mode in humans (Ivanenko et al., 2006; Ivanenko et al., 2008). For example, at non-preferred speed walking and running, the MN activation patterns demonstrated additional locus of activation compared with those at comfortable speed (Ivanenko et al., 2008). Additionally, mode-dependent MN activation patterns were observed during multiple locomotor modes (walking, running, backward stepping, and skipping) (Ivanenko et al., 2008). In these previous studies (Ivanenko et al., 2006; Ivanenko et al., 2008), relationships between the MN activity and timing pattern of locomotor modules have been extensively

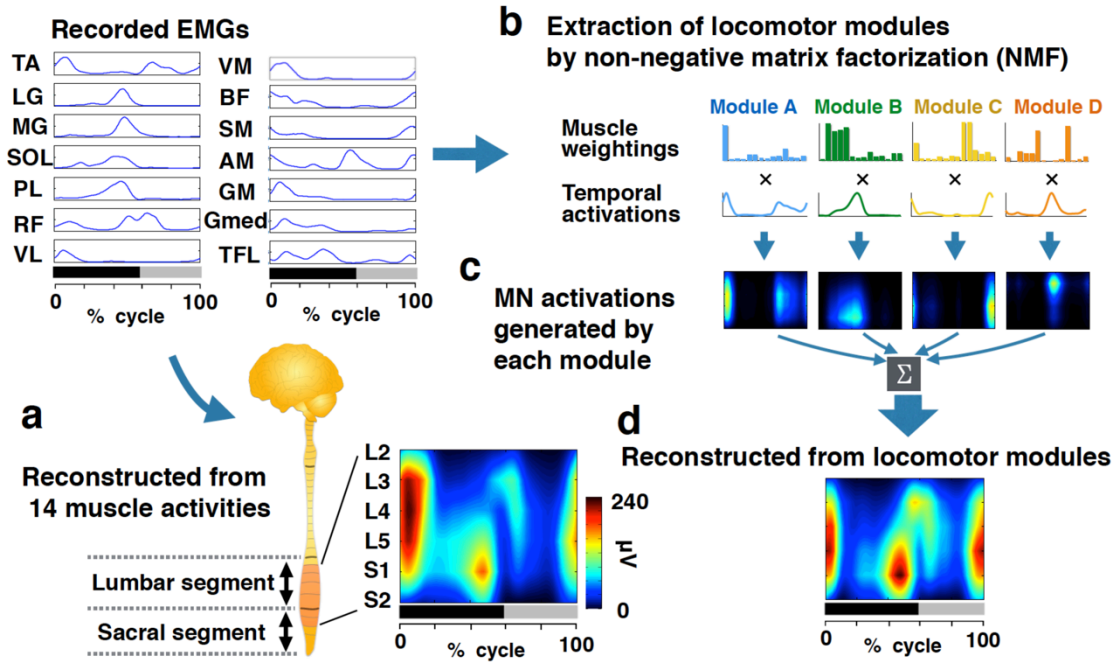

Figure 3-1. Procedures of reconstruction of spatiotemporal activation patterns of motoneurons (MNs) along the rostrocaudal axis of the lumbosacral enlargement from EMGs (a) and locomotor modules (b–d). (a): Activation patterns of MNs in each segment (L2–S2, left vertical scale) were reconstructed by mapping recorded muscle activities (EMGs) based on Kendall's myotomal charts (Table 3-1). (b): Locomotor modules were extracted using non-negative matrix factorization (NMF). The output of each module is explained by the product of the muscle weighting component (bars; specifying activation level of each muscle) and the temporal pattern component (waveforms). The sum of outputs from the modules is approximately equivalent to those of the EMGs. (c): MN activity generated by each module was reconstructed from the output of each module. (d): Activity patterns generated from individual modules were summed into a whole activation pattern. The bar underneath denotes the stance phase (black) and swing phase (grey) in a gait cycle.

investigated. However, relationships between the MN activation patterns and the muscle weightings of modules (i.e., spatially fixed muscle synergies) remain unclear.

Regarding locomotor speed control by the spinal CPGs, previous studies in animal models demonstrated two interesting characteristics. The first is the rostrocaudal gradient of rhythmogenic capacity in the spinal CPGs. Although rhythmogenic capability is widely distributed along the lumbosacral enlargement, the upper segments have a higher rhythmogenic capability (Kjaerulff and

Kiehn, 1996; Cazalets and Bertrand, 2000; Talpalar and Kiehn, 2010). The second is the specific combination of individual classes of interneurons and MNs called a "locomotor spinal microcircuit" (Ampatzis et al., 2014). Ampatzis et al. (2014) showed that three distinct types of these microcircuits are sequentially activated, from slow to intermediate and then fast, with increasing speed. So far, these speed control mechanisms in spinal circuits have not been confirmed in humans.

It has been suggested that CPGs in legged vertebrates emerged during evolution from a common ancestral circuit (Grillner and Jessell, 2009), and a recent EMG-based study showed that the locomotor modules of humans and those of other mammals and birds evolved from similar circuitry (Dominici et al., 2011). As spinal CPG mechanisms are phylogenetically conserved at a cellular level across different species, and even between fish and rodents (Goulding, 2009), the speed control mechanisms of CPGs are probably conserved in humans. Based on the hypothesis that common speed control mechanisms are shared by humans and other vertebrates, I established working hypotheses as follows. 1) MN activity in rostral segments becomes higher compared with in caudal segments with increasing locomotion speed. Additionally, 2) if the MN activation patterns are changed with increasing speed, the distinct MN activation patterns are generated by different locomotor modules. To test the hypothesis, here I mapped the recorded EMG patterns onto the approximate corresponding segments of the MN pools in the spinal cord (Ivanenko et al., 2006; Ivanenko et al., 2008) and extracted locomotor modules using non-negative matrix factorization (NMF) (Dominici et al., 2011) during walking and running over a wide speed range. The acceptance of this working hypothesis would provide indirect evidence that the speed control mechanisms of spinal locomotor circuits are conserved in humans.

3. 2. Methods

3. 2. 1. Participants

Seventeen healthy male volunteers (ages 19–31 yr.) participated in the study. EMGs and

GRF data of 16 participants (eight non-runners and eight runners) out of 17 participants were taken from Study 1 (Chapter 2), which focused on a different topic (namely, on the recruitment of motor modules for different locomotion modes and speeds, in contrast with the present topic: the proportion of the MN activity in rostral and caudal segments). Each participant gave written informed consent for his participation in the study. The study was in accordance with the Declaration of Helsinki and was approved by the local ethics committee of the National Rehabilitation Center for Persons with Disabilities (Tokorozawa, Japan).

3. 2. 2. Experimental setup and design

Participants walked or ran on a treadmill (Bertec, Columbus, OH, USA). The belt speed was linearly increased from 0.3 m/s to 4.3 m/s with an acceleration of 0.01 m/s^2. This speed-range was set as fast as possible within the safe limits checked in Chapter 2. The participants were asked to change their locomotion mode (from walk to run) on the basis of their preference under the given speed. The participants' observed walk–run transition speed ranged from 1.9 to 2.3 m/s.

3. 2. 3. Data collection

Three-dimensional GRF were recorded from force plates under the right and left belts of the treadmill (1000 Hz). Surface EMGs were recorded from the following 14 muscles on the right leg for analysing MN activity patterns and locomotor modules: TA, LG, MG, SOL, PL, VL, VM, RF, BF, ST, AM, TFL, GM, Gmed. I targeted muscles innervated by MNs located in the lumbosacral enlargement, where locomotor CPGs are known to exist (Dimitrijevic et al. 1998). The EMGs were recorded with a wireless EMG system (Trigno Wireless System; DELSYS, Boston, MA, USA). The EMG signals were band-pass filtered (20–450 Hz) and sampled at 1000 Hz. GRF data were smoothed by a low-pass filter (a zero-lag Butterworth filter, 5-Hz cutoff). The timings of heel-contact (HC) and toe-off (TO) were determined based on the vertical component of GRF.

Then the stance time, swing time, and stride time were calculated. Locomotion mode (walk or run) was defined by the presence and absence of double support time.

3. 2. 4. EMG processing

The recoded EMGs were divided into 0.1 m/s bins based on the treadmill speed. Thus, the EMGs data of each participant were divided into 40 speed ranges. As the treadmill speed was accelerated at 0.01m/s^2, each bin contained 10 seconds of data. Then, the EMG data were rectified and low-pass filtered with a zero-lag Butterworth filter. The low-pass cutoff frequency was adjusted to each speed condition according to the following formula: 10 × stride frequency (Hz) as in Chapter 2. Subsequently, the smoothed envelopes were time-interpolated so that they had 200 points for each gait cycle.

3. 2. 5. Spatiotemporal activation patterns of MNs along a rostrocaudal direction within the spinal cord

To characterise the spatiotemporal patterns of the spinal MN activity, the processed EMGs were mapped onto the estimated rostrocaudal location of the MN pools in the spinal cord from the L2 to S2 segments. I adopted Kendall's myotomal charts (Kendall et al., 1993) as in previous studies (Ivanenko et al., 2006; Ivanenko et al., 2008; Ivanenko et al., 2013; La Scaleia et al., 2014). In Kendall's charts, the weight coefficients of innervation level are expressed as *x* (0.5) or *X* (1) (Table 3-1). Based on the charts, the MN activity patterns of the *j*th spinal segment *Sj* was estimated according to the following formula (3-1):

$$Sj = \frac{\sum_{i=1}^{n_j} k_{ij} \cdot EMG_i}{n_j}, \qquad (3\text{-}1)$$

where *nj* is the number of *EMGi* corresponding to the *j*th segment, *EMGi* is the *i*th EMG activity and *kij* is the weighting coefficient of the *i*th muscle for the *j*th spinal segment. Subsequently, the

activity of each spinal segment (*Sj*) was normalized based on the estimated number of MNs in this segment (Table 3-2) (Ivanenko et al., 2013) as in previous studies (Tomlinson and Irving, 1977; La Scaleia et al., 2014). Namely, *Sj* was multiplied by the number of MNs in this segment and was divided by the maximum number of MNs across six segments (i.e., 12,765 in L3). To visualise smooth spatiotemporal activation in the rostrocaudal segments of the spinal cord, I used a filled contour plot (Ivanenko et al., 2006; Ivanenko et al., 2008; Ivanenko et al., 2013).

Table 3-1. Muscle innervation charts.

	GM	Gmed	TFL	AM	RF	VL	VM	BF	ST	LG	MG	SOL	PL	TA
L2				x	X	X	X							
L3				X	X	X	X							
L4		X	X	X	X	X	X		x				x	X
L5	x	X	X	x				x	X				X	X
S1	X	X	X	x				X	X	X	X	X	X	X
S2	X							X	X	X	X	X		

Data are adopted from Kendal et al. (1993). The innervation level is expressed as X (high) and x (low). X and x are weighted with $kij = 1$ and $kij = 0.5$, respectively in equation (2).

Table 3-2. Mean number of lower-limb motoneurons in each segment of the human spinal cord (13–40 years, 12 cases).

Segment height	motoneuron number
L2	5146
L3	12765
L4	12069
L5	12674
S1	10372
S2	4216

Data are adopted from Tomolinson and Irving (1977)

To compare the spatiotemporal activation patterns of MNs among speeds, the patterns across all 40 speed ranges were grouped with hierarchical clustering analysis. First, the activation patterns were averaged across participants at each speed. Then, each data matrix corresponding to 200 time points × 6 segments was transformed into a vector corresponding to 1200 variables. Based on the vectors for each speed, hierarchical cluster analysis (Ward's method, correlation distance)

was performed for the 40 speed ranges. The optimal number of clusters was determined by the gap statistic method (Tibshirani et al., 2001). The MN activation patterns were divided into three speed ranges [slow walking (0.3–1.1 m/s), fast walking (1.1–1.9 m/s) and running (2.2–4.3 m/s), detailed in "Results"], and data in subsequent analyses described below were compared among the middle speeds of each speed range (i.e., 0.7–0.8, 1.5–1.6 and 3.2–3.3 m/s for slow walking, fast walking and running, respectively). Hereinafter, these speeds referred to as "representative speeds".

We checked inter-individual variability of MN activation patterns at the representative running speed, because high inter-individual variability of EMGs during running (Guidetti et al., 1996) may raise a question whether the averaged MN activation patterns during running show representative patterns among participants. To evaluate similarity of the MN activation patterns among participants, we calculated correlation coefficients between individual and averaged data at representative running speed. Firstly, each participant and averaged data matrix corresponding to 200 time points × 6 segments was transformed into a vector corresponding to 1200 variables. Then, the correlation coefficients (r) were calculated between the individual and averaged data vectors.

3. 2. 7. Activation ratio between lumbar segments and sacral segments

To evaluate the relative activation between the lumbar and sacral segments, I calculated the ratio between mean MN activity in the main part of the lumbar (sum of activity from L3 to L4) and the sacral segments (sum of activity from S1 to S2) (Ivanenko et al., 2013). The activation ratios were compared among the representative speeds for each type of MN activation pattern.

3. 2. 8. Spatiotemporal activation patterns of MNs of each locomotor module

Locomotor modules (Fig. 3-1b) were extracted from the processed EMGs in the representative speeds for each type of MN activation pattern, using same method of motor module extraction used in Chapter 2 (see section 2.2.5. for details). Then, spatiotemporal activation patterns of MNs were reconstructed from each extracted modules. First, the motor output of each module was calculated

from the product of the muscle weightings and the corresponding temporal activation patterns (Fig. 3-1b). Then, spatiotemporal activation patterns of MNs generated from individual modules were reconstructed from the motor output of each module (Fig. 3-1c). These activation patterns of individual modules were summed into a whole activation pattern of MNs over a gait cycle at each representative speed (Fig. 3-1d).

3. 2. 9. Statistics

Differences in the activation ratio between the sacral and lumbar segments among the three representative speeds for each MN activation pattern (slow walking, fast walking and running) were compared using one-way ANOVA with Holm's post-hoc test (an updated version of Bonferroni's test). In addition, I compared the number of modules among the three representative speeds by using the non-parametric Kruskal–Wallis one-way ANOVA with the Steel–Dwass post hoc test (nonparametric Tukey's test). Data are presented as the mean and standard error of the mean (mean ± SE). Statistical significance was accepted at $p < 0.05$.

3. 3. Results

3. 3. 1. Spatiotemporal activity patterns of MNs along a rostrocaudal direction in the spinal cord

Using recorded EMGs (typical examples shown in Fig. 3-2) and the myotomal charts, we reconstructed the spatiotemporal activation patterns of MNs along the rostrocaudal direction in the spinal cord over the step cycle. The averaged activation patterns across participants from slow walking to fast running are presented in Fig. 3-3. These patterns were grouped by hierarchical clustering to evaluate the speed-dependent changes (Fig. 3-4a). The activation patterns were grouped into three speed ranges: slow walking (0.3–1.1 m/s), fast walking (1.1–1.9 m/s) and

running (2.2–4.3 m/s) (Fig. 3-4a).

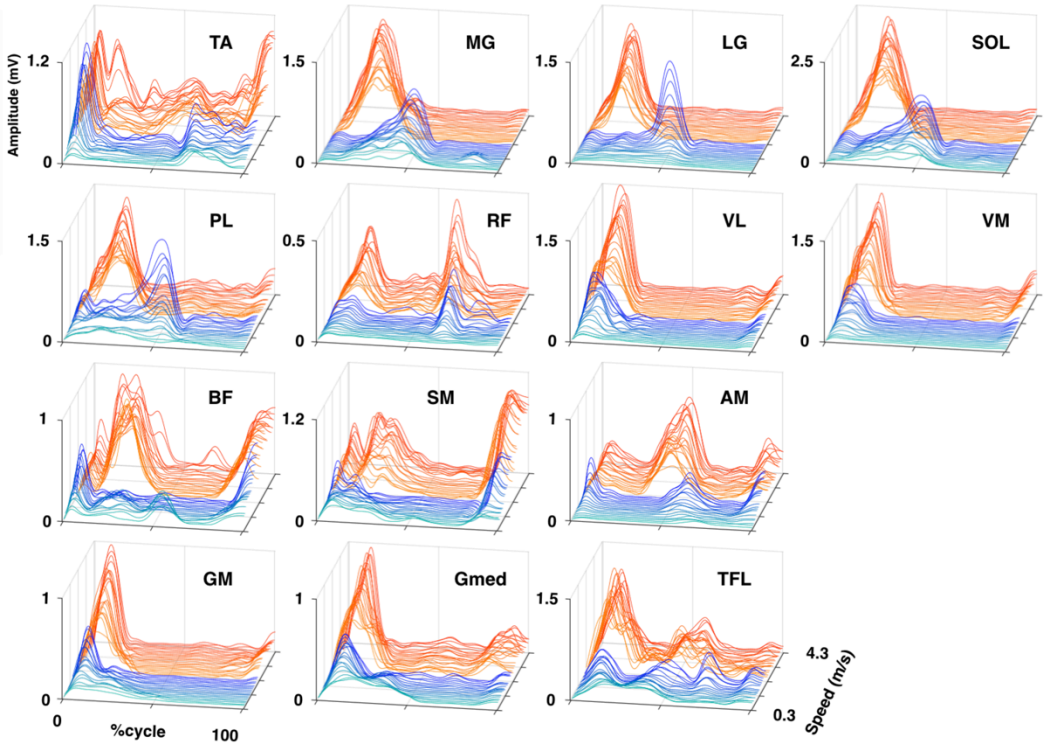

Figure 3-2. Muscle activation patterns during a gait cycle at all speeds. Each waveform shows the ensemble average of the first five to eight consecutive gait cycles (as many as possible in the range, almost eight except at the very slow speed) in each speed range from a single participant. The blue and red waveforms represent walking and running data, respectively.

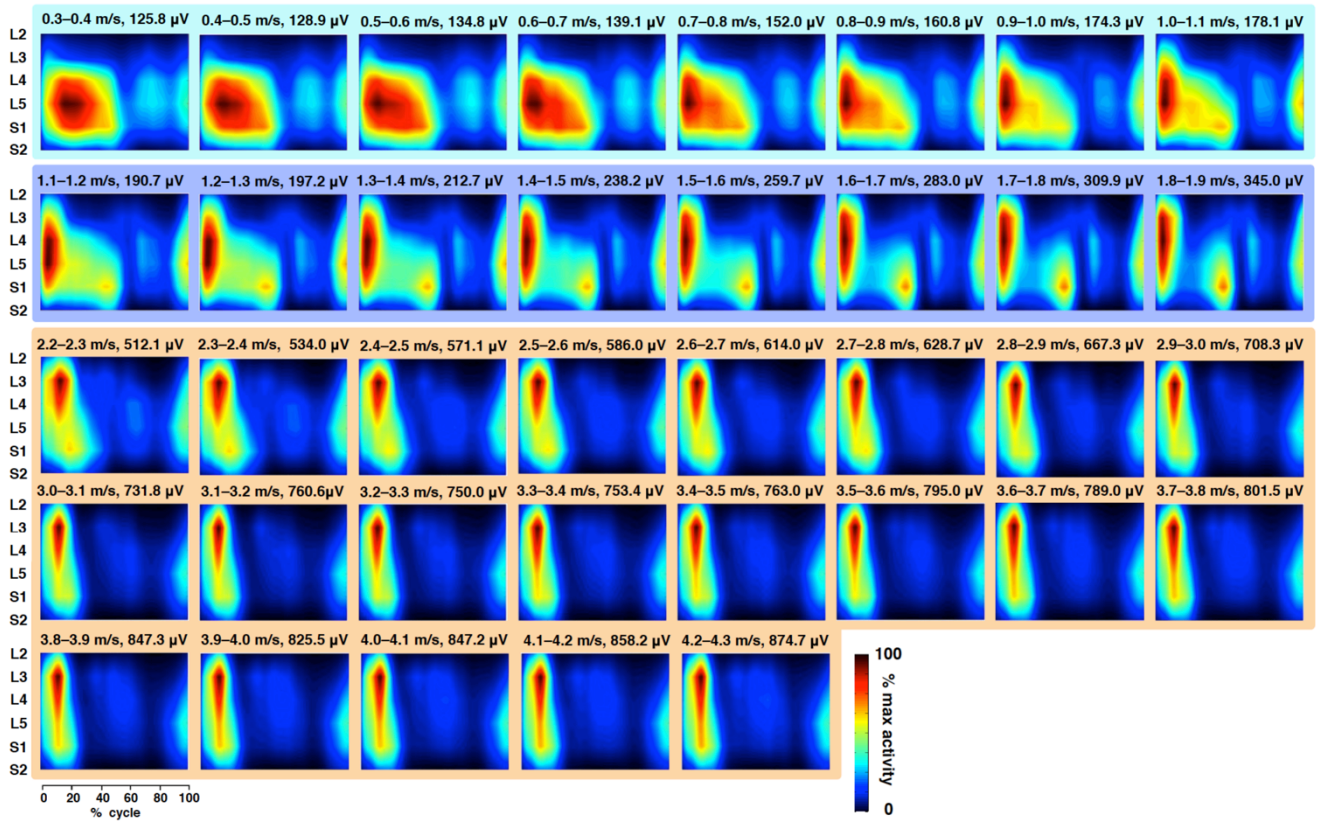

Figure 3-3. Averaged activation patterns of MNs across all participants at all speeds. The speed range and the maximum value of each map are displayed. Colour scale denotes amplitude normalized to the maximum value in each activation pattern. Light blue, deep blue and orange sections the indicate three speed ranges ("slow walking", "fast walking" and "running", respectively) divided by cluster analysis based on the spatiotemporal activation patterns of the MNs shown in Fig. 3-4.

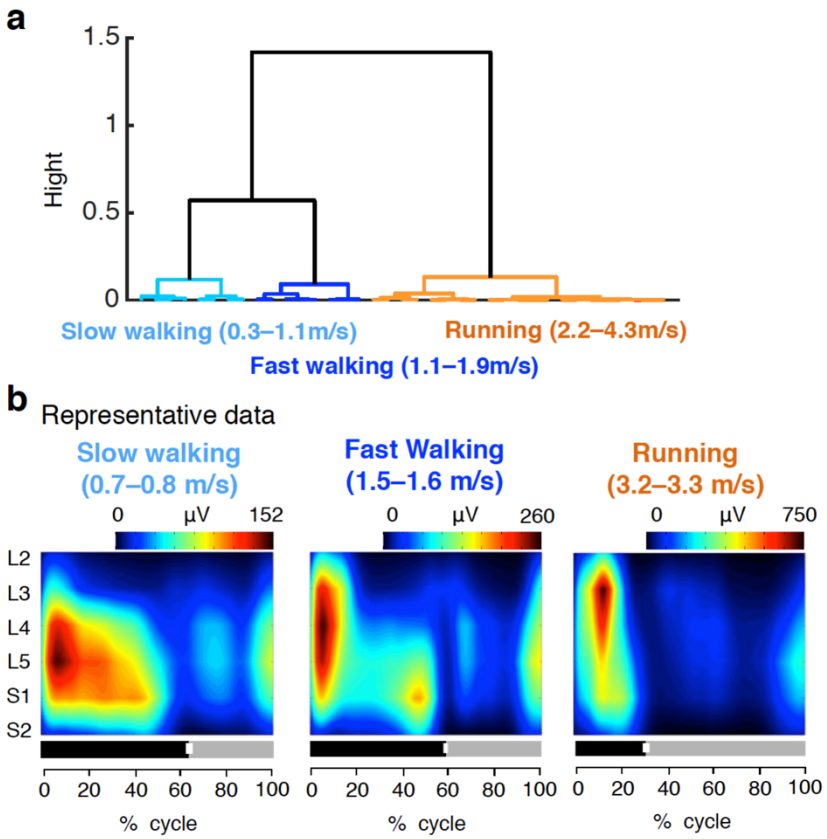

Figure 3-4. Cluster analysis for activity pattern of MNs across all speeds (a) and the representative data from each cluster (b). (a): Dendrograms represent the results of cluster analysis applied to the activation patterns of MNs across all speeds shown in Fig. 3-3. The optimal number of clusters was determined by gap statistics. Three distinct clusters are indicated by light blue, deep blue and orange ("slow walking", "fast walking" and "running", respectively). (b): MN activation maps at the middle speed of each speed range for the three clusters are shown as representative data for the clusters. The bars underneath denote the stance phase (black) and swing phase (grey) in a gait cycle.

Specifically, in slow walking (all data shown in Fig. 3-3, light blue section; representative pattern shown in Fig. 3-4b, left), the patterns showed long-lasting synchronous activation of the lower part of the lumbar (L4 and L5) and sacral (S1 and S2) segments during most parts of the stance phase of the cycle (0–50% of the gait cycle). In addition, weak activation in

segments from L4 to S1 occurred during most parts of the swing phase (60–85% of the gait cycle). At the end of the swing phase (90–100% of the gait cycle), preceding heel contact, segments from L4 to S1 were re-activated with a stronger intensity.

However, in fast walking (all data shown in Fig. 3-3, deep blue section; representative pattern shown in Fig. 3-4b, middle), the stance phase activation was separated into distinct bursts of the whole lumbar [L2 to L5, at around foot contact (0–20% of the gait cycle)] and the sacral segments [S1 and S2, at around toe off (40–55% of the gait cycle)]. Weak activation of segments from L4 to S1 occurred in the first half of the swing phase (60–80% of the gait cycle). At the end of the swing phase (90–100% of the gait cycle), segments from L4 to S1 were also activated as in slow walking.

In running (all data shown in Fig. 3-3, orange section; representative pattern shown in Fig. 3-4b, right), the activity of the lumbar and the sacral segments were synchronous in the stance phase (0–30% of the gait cycle). During the initial swing (30–45% of the gait cycle), weak activity of the rostral lumbar segment (mainly in L3) occurred. Following this narrow segment activation, weak activity in the wide lumbar segments (L2 to L5) occurred in the middle of the swing phase (45–70% of the gait cycle). During the end of the swing phase (90–100% of the gait cycle), the activity of the segments from L4 to S1 occurred similarly to that in slow walking and fast walking. Inter-participant variability in EMGs during running (reported in [Guidetti et al., 1996]) may raise a question about the averaged data of the reconstructed MN activation patterns obtained from individuals. As seen by visual inspection, inter-participant differences in MN activation patterns were quite small at the representative running speed (all individual data are shown in Fig. 3-5). This similarity is supported by high correlation coefficients between individual and averaged data (0.95 ± 0.024 [mean ± SD], Fig. 3-5). Therefore, the averaged running data represent the general trends in the individual data.

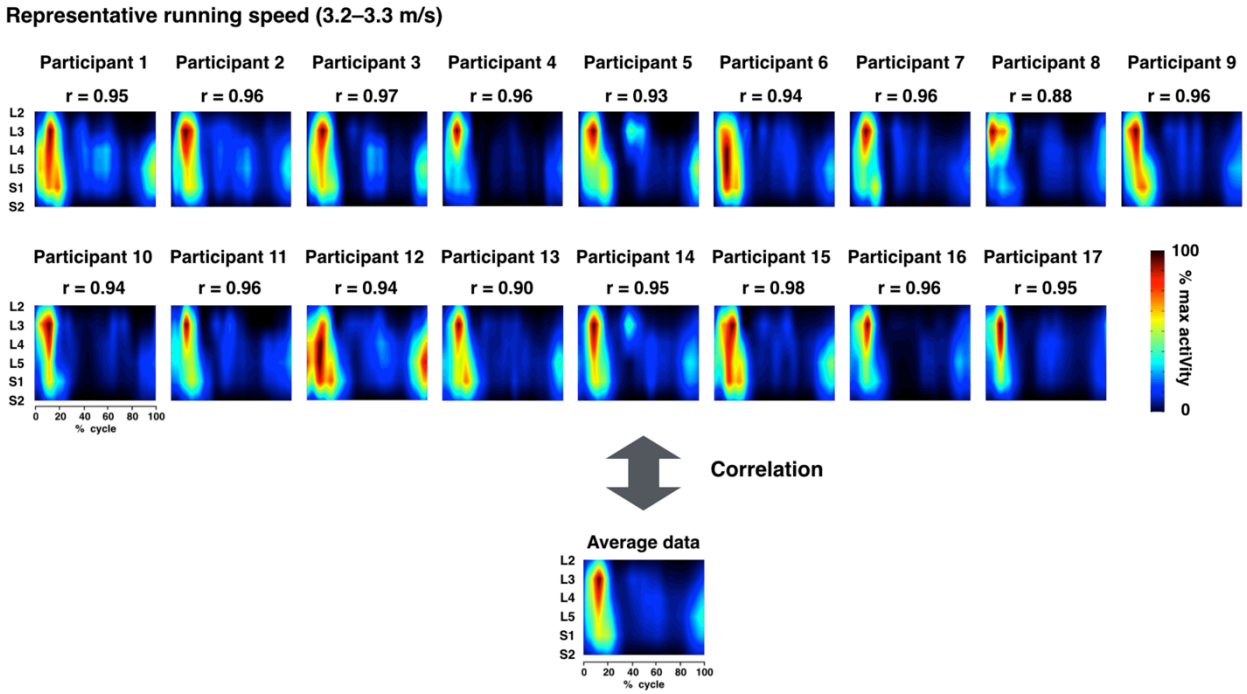

Figure 3-5. Averaged and all individual data of spatiotemporal activation patterns of motoneurons (MNs) at speeds representative of running (3.2–3.3 m/s). Colour scale denotes amplitude normalized to the maximum value in each activation pattern. Correlation coefficients between individuals and averaged data are shown.

3. 3. 2. Activation ratio between lumbar and sacral segments

As locomotion changes from slow walking to fast walking or running, MN activity in the rostral segments was increased relative to that in the caudal segments. This was statistically confirmed by comparing the activation ratio between the lumbar (L3 + L4) and sacral (S1 + S2) segments (Fig. 3-6; ANOVA: $F(2,48) = 18.3$, $p < 0.001$, post-hoc Holm's test: $p < 0.01$).

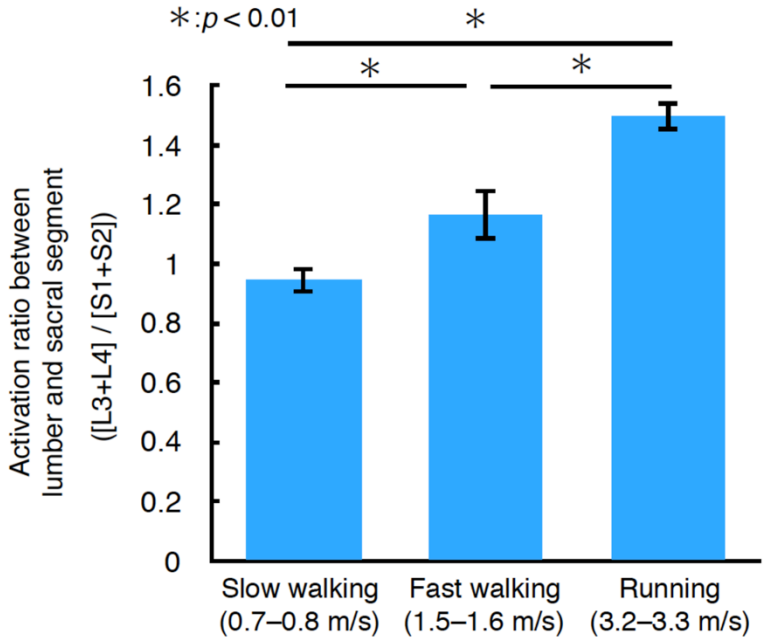

Figure 3-6. Mean activity ratios of lumbar versus sacral segments at three representative speeds. Error bars indicate the SE.

3. 3. 3. Spatiotemporal activation patterns of MNs generated from individual modules

To examine the relationships between the locomotor modules and the activation patterns of the MNs, the modules were extracted from representative speeds lying within the three clusters. The number of extracted locomotor modules was significantly lower during slow walking compared with running (Kruskal-Wallis one-way ANOVA: $H2 = 7.40$, $df = 2$, $p < 0.05$; post hoc Steel–Dwass test: $p < 0.05$, Fig. 3-7). Six types of modules were extracted from the combined dataset of the three representative speeds (M1–M6, Table 3-3, bars in Fig. 3-8 upper row). From these six types of modules, different combinations of modules were used among the three representative speed datasets (Table 3-3).

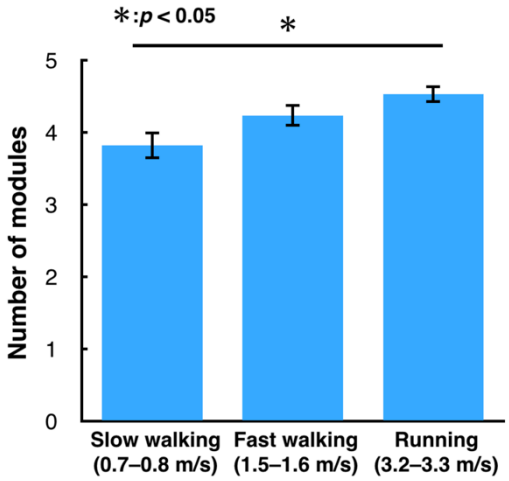

Figure 3-7. Number of modules at three representative speeds for "slow walking", "fast walking" and "running". Error bars indicate the SE.

Table 3-3. Characteristics of extracted locomotor modules.

Module type	Major muscles	Timing	Extracted modules			Peak activation segment
			Slow walking (0.7–0.8 m/s)	Fast walking (1.5–1.6 m/s)	Running (3.2–3.3 m/s)	
M1	TFL, Gmed	Early stance	○	○		L4
M2	MG, LG, SOL, PL	Mid–late stance	○	○	○	S1
M3	TA	Initial stance/Mid swing	○	○	○	L4
M4	BF, SM	Late swing–Early stance		○	○	L5
M5	VL, VM, GM, Gmed	Early stance			○	L3
M6	AM, RA	Initial swing			○	L3

Figure 3-8 shows the spatiotemporal activation patterns of MNs reconstructed from individual locomotor modules at the three representative speeds. Each module activated the MN pools in somewhat narrow segments (2–4 segments) at a specific timing point in the gait cycle (Fig. 3-8, the third to the sixth columns from the left). The MN activation patterns of individual modules at each speed were summed into a total activation pattern over a gait cycle at each speed (Fig. 3-8, the second column from the left). The original patterns were reconstructed with high accuracy by

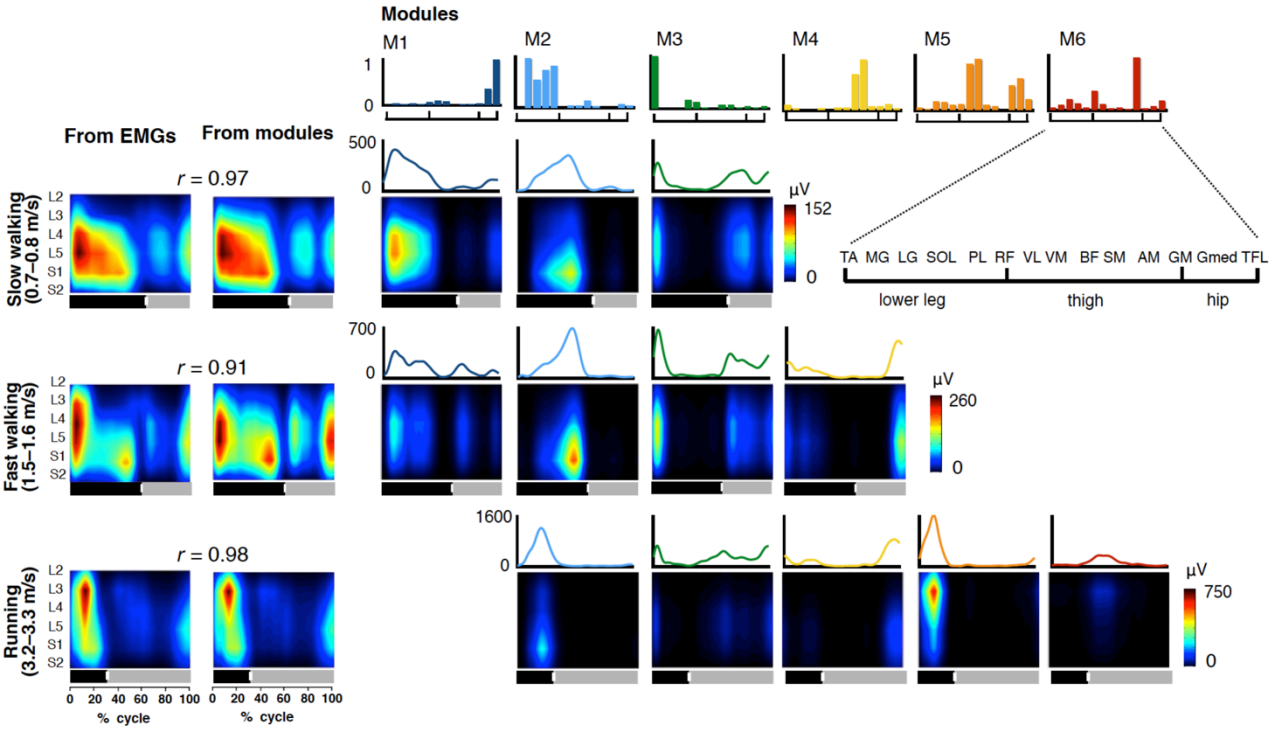

Figure 3-8. Spatiotemporal activation patterns of MNs generated by individual locomotor modules at three representative speeds. The output of an individual module is explained by the product of a muscle weighting component (top bars) and its corresponding temporal pattern component (same colour waveform). Based on the output, MN activity generated by an individual module was reconstructed. The activity patterns generated by the same modules are shown in the same column, while those at the same speeds are shown in the same row. These activity patterns at the same speed were summed into a total activation pattern over a gait cycle (the second column from the left). Correlation between the pattern directly reconstructed from the EMGs (the first column from the left) and the pattern reconstructed from the modules is shown just above these two patterns. An enlarged view of the x-axes of muscle weightings is shown in the upper right. The bars underneath denote the stance phase (black) and swing phase (grey) in a gait cycle.

summation of the activation from individual modules (r = 0.91–0.98). The most strongly activated segments by each module were located at rostral segments, in most cases, of the newly recruited module types as speed increased (Table 3-3). Specifically, in slow walking, one of the three modules (M2) innervated the MN pools in a sacral segment (peak segment: S2). In addition, the other two modules (M1 and M3) activated a lower lumbar segment (peak segment: L4). In fast

walking, the newly recruited modules (M4) mainly innervated lower lumbar and upper lumbar segments, respectively (peak segment: L4). During running, M5 and M6 were newly recruited and they innervated the MN pools in an upper lumbar segment (peak segment: L3).

3. 4. Discussion

The present results confirmed my working hypotheses and demonstrated that (1) MN activity in the rostral segments increased compared with the caudal segments with increasing locomotion speed, and (2) the three different MN activation patterns used in a wide range of speed are generated by distinct combinations of locomotor modules. These results are consistent with the characteristics of the speed control of the spinal CPGs observed in other vertebrates (Kjaerulff and Kiehn, 1996; Cazalets and Bertrand, 2000; Talpalar et al., 2011; Ampatzis et al., 2014). Therefore, my results support the hypothesis that similar basic locomotor neural circuits are used among different vertebrate species even though they have significant morphological differences and exhibit different locomotion styles (e.g., aquatic or terrestrial, non-legged or legged) (Wainwright, 2002; Grillner and Jessell, 2009). Thus my results indicate a possibility that the commonality of the spinal locomotor circuits can be extended to humans.

The present results showed that the MN activation patterns were divided into three speed ranges (slow walking, fast walking and running, Fig. 3-4a). In the fast walking pattern (Fig. 3-4b), two clear bursts occurred at around foot contact (0–20% of the gait cycle) in the lumbar segments and at around toe off (40–55% of the gait cycle) in the sacral segments. This activation pattern was similar to those presented as normal speed walking patterns in many studies (Ivanenko et al., 2006; Ivanenko et al., 2008; Ivanenko et al., 2013; La Scaleia et al., 2014). Additionally, as natural self-selected walking speed is approximately 1.2–1.5 m/s (Chvatal and Ting, 2012; Ivanenko et al., 2013), this activity pattern would be most frequently used as an ordinary pattern in our daily life. Conversely, in the slow walking pattern (Fig. 3-4b), long-lasting synchronous activations of the

lower part of the lumbar segments (L4 and L5) and the sacral segments (S1 and S2) were observed during most parts of the stance phase of the cycle (0–50% of the gait cycle). Such MN activation patterns have been found in several studies at slow speeds (0.28 m/s [Ivanenko et al., 2006]) and low step frequencies (40 steps/min and 40–80 steps/min in young and older adults, respectively [Monaco et al., 2010]). Additionally, the long-lasting synchronous activations of the lower lumbar and sacral segments were also observed in toddlers while stepping (Ivanenko et al., 2013). It has been demonstrated that posture control is an important aspect for the control of locomotion as a common characteristic in slow speed walking (Bauby and Kuo, 2000) and toddler walking (Ivanenko et al., 2005a). Thus, both may represent similar MN activation patterns. Regarding running, to my knowledge, only one previous study (Ivanenko et al., 2008) examined the MN activation pattern in slow speed running (1.38–3.33 m/s, considered as jogging). In the present study, we examined those at a faster speed (–4.3 m/s). As a result, the MNs activation patterns during faster running were almost the same patterns as those during slower running (Figures 3-3 and 3-4a).

Among the three different MN activation patterns, MN activity in the rostral segments was increased relative to that in the caudal segments as the speed increased (Fig. 3-6). Also, the locomotor modules extracted in faster speed (fast walking and running) innervated rostral segments (Table 3-3 and Fig. 3-8). Previous studies demonstrated several functional differences among lumbosacral segments considered to be related to the observed speed-dependent change in MNs activation ratio between the lumbar and sacral segments. A previous study showed that vertebrates have multiple rhythmogenic modules in their entire lumbosacral enlargement (Hägglund et al., 2013). However, rostral segments have a high capacity to generate rhythmic activity of MNs than do caudal segments (Kjaerulff and Kiehn, 1996; Cazalets and Bertrand, 2000). Therefore, although the function of generation of rhythmic MN activity is widely scattered in the lumbosacral

enlargement, the capacity is graded along the rostrocaudal direction. In addition, rostral segments of the lumbar cord play a crucial role in the function of the CPG as a leading oscillator that propagates motor bursts to caudal segments (Saltiel et al., 2015). Also, in humans, the rostral segments have been suggested to work as a leading oscillator (Dimitrijevic et al., 1998; Gerasimenko et al., 2010). From the viewpoint of the rostrocaudal functional gradient, in fast locomotion, high activity of the rostral rhythm generator may be required to achieve a high step frequency. Indeed, non-NMDA receptors, which are responsible for receiving glutamatergic input to the locomotor CPG, exist in more rostral lumbar segments and are indispensable for achieving high frequency locomotor behaviour (Talpalar and Kiehn, 2010). This glutamatergic mechanism for faster locomotion might explain the higher activation in the caudal segments at faster speed locomotion presented in the present study. However, slower locomotion may not require strong locomotor drive from the rhythm generator in the upper segments. Indeed, it has been demonstrated that posture control is an important aspect of the control of locomotion at slow speeds (Bauby and Kuo, 2000). In addition, another study suggested that the locomotor generator in the sacral segments is related to body support through sensory inputs to the foot during walking (Selionov et al., 2009). Therefore, in contrast to the lumbar segment, sacral segment activity might play an important role for posture control, especially in slow walking. Therefore, it is plausible that the observed speed-dependent change in MNs activation ratio between the lumbar and sacral segments reflected these functional differences of the spinal segments.

In the present study, focusing on the relationships between the MN activation patterns and extracted locomotor modules, I found that three different MN patterns were generated by distinct combinations of locomotor modules (Table 3-3 and Fig. 3-8). It is suggested that the locomotor CPG may consist of a timing structure and a spatial pattern formation network (McCrea and Rybak, 2008). The locomotor modules are considered to be encoded in the spatial pattern

formation networks of the spinal CPGs, which activate multiple MN pools (McCrea and Rybak, 2008). Recent molecular and genetic techniques have revealed that CPGs consists of spinal interneurons, and each type of interneuron plays a particular role in controlling locomotion (Goulding, 2009; Kiehn, 2016). In addition, spinalized vertebrate studies have shown that mathematically extracted locomotor modules, like those in the present study, are organized in the spinal interneuronal circuits (Hart and Giszter, 2010; Saltiel et al., 2015). Thus, assuming that the locomotor modules consist of spinal interneurons, my results suggest that each interneuronal locomotor module has specific connectivity with MN pools. Indeed, a recent study in zebrafish revealed the existence of a specific combination of individual classes of interneurons and MNs called a "locomotor spinal microcircuit" (Ampatzis et al., 2014), which has interesting characteristics regarding speed dependency. The authors identified three distinct microcircuits with separate interneuron types innervating slow, intermediate, or fast MNs. Furthermore, the microcircuits are sequentially activated from slow to intermediate and fast with increasing speed (Ampatzis et al., 2014). Thus, this principle of spinal circuit organization represents a neural mechanism to modulate the locomotor speed by stepwise recruitment of different microcircuits. In addition, a study in mice (Bikoff et al., 2016) showed specific connectivity (i.e. microcircuits) between motoneuron subtypes and V1 interneuron subtypes, which regulate locomotor speed (Gosgnach et al., 2006). It is not clear to what extent these findings can be extended to humans. Nevertheless, the greater part of the spinal locomotor networks are conserved across vertebrates (Goulding, 2009; Kiehn, 2011), thus, it is probable that the recruitment patterns of spinal neurons might also be conserved in humans. If the speed-dependent recruitment mechanisms of the microcircuits for locomotion are phylogenetically preserved in humans, this would explain the present result that the different MNs activation patterns were generated by different locomotor modules.

In human walking, generation of muscle activity is largely affected by sensory input (Van de Crommert et al., 1998). In slow walking, as discussed above, large sacral activity in mid-stance is presumably derived from foot-support interactions through load feedback. This sacral activity is most likely related to constancy in triceps surae activity over the speed range and to negative speed dependency in PL activity with regard to load information in slow-speed walking, as discussed in a study by Den Otter et al. (2004). At higher speeds, changes in locomotor muscle activity are clearly related to reinforcement of sensory feedback depending on speed increases. It is assumed that extensor activity during early stance phase (M5 activity and forward shift of activation timing of M2 in running) was related to reinforcing load feedback (i.e. extensor reinforcing reflex) (Duysens, 2002), and hamstring activity at the end of swing (M4 activity) was related to an increase in knee-extension speed (i.e. stretch reflex) (Duysens et al., 1998). Although there was no doubt about the contributions of these reflex-driven muscle activities to control speed in human locomotion, a modelling study showed that reflex-based muscle activity alone without CPGs cannot control locomotor speed (Dzeladini et al., 2014). In addition to reflex control of locomotion, it has been shown that sensory feedback affects lumbar burst generators in CPGs (Gerasimenko et al., 2010; Lev‐Tov et al., 2010). Vibration of leg muscles facilitated locomotor-like muscle activity evoked by spinal electromagnetic stimulation to the lumbar segment (Gerasimenko et al., 2010). A study in mice demonstrated more direct evidence that ascending afferent pathways from the sacral segments to the lumbar segments enhance locomotor bursts (Lev‐Tov et al., 2010). Assuming that similar mechanisms are shared between mice and humans, strong afferent feedback at higher speeds may powerfully facilitate the lumbar burst generators of the CPGs.

Regarding the organization of locomotor networks, Hof et al. (2002) showed that

locomotor EMGs in the speed range of 0.75–1.75 m/s could be estimated by two simple functions, one constant and one proportionally increasing with walking speed (i.e. fixed CPG networks). Nevertheless, this model cannot explain the large activity in the triceps and PL at mid-stance in slow walking or the rapid increase of extensor activity after the walk-run transition. Instead, as Pearson (2004) proposed, CPG networks would be flexibly reorganized by sensory feedback. Reorganization of CPG networks depending on changes in locomotor speed have been revealed in fishes and mice by recent molecular studies (Kiehn, 2016). Thus, regarding speed control in locomotion, sensory input would be related to not only reflex-driven muscle activity, but also rhythmic burst generation and reorganization of CPGs, probably contributing to the speed-dependency of MN activity and locomotor modules observed in the present study.

There are several limitations regarding the method reconstructing the spinal MNs activations. EMG cross-talk is always a potential issue with recordings of surface EMGs. In a previous study, it was demonstrated by modelling the potential effect of different levels of cross-talk in the EMGs that the cross-talk has little effect on the estimation of MN activity patterns (Ivanenko et al., 2013). The study showed that the level of the cross-talk from adjacent muscles increased incrementally (from 10% to 100%); nevertheless, the appearance of a new location of activity or notable temporal shifts of the activity did not occur. Additionally, the number of muscles and the muscle type are also important variables. Regarding this point, it has been demonstrated that the activity patterns, analysed with two different sets of muscles (12 muscles and 20 muscles), are relatively robust (La Scaleia et al., 2014). Presumably, this result stemmed from the fact that each segment in the spinal cord innervates multiple muscles and each muscle is innervated by several segments to the contrary. The activity patterns in the present study were similar to those in previous studies using various sets of muscles (Ivanenko et al., 2006; Ivanenko et al., 2008; Monaco et al., 2010; Ivanenko et al., 2013; La Scaleia et al., 2014). However, it should be kept in mind that the sets of muscles analysed would affect the extraction of locomotor modules

by NMF (Zelik et al., 2014).

Although this study showed the high similarity about spinal locomotor networks humans and quadruped vertebrates by reconstructing MN activation patterns for lower leg muscles, there is high possibility that locomotor networks for forelimbs/upperlimbs are different between them due to difference in biomechanical roles of the forelimbs and upper limbs during walking. Nevertheless, regarding interaction between the fore/upper and hind/upper limb networks, some evidence for similarity between quadruped vertebrates and humans was observed (Dietz 2002). Therefore, even in the level of whole spinal locomotor networks including fore/upper and hind/upper limb networks, it might be that some similar mechanisms are shared by humans and quadruped animals.

In conclusion, I found the following spinal activation patterns regarding speed control of human locomotion: (1) MN activity in the rostral segments increased compared with the caudal segments with increasing locomotion speed; and (2) different MN activation patterns are generated by distinct combinations of locomotor modules. These results are consistent with the speed control characteristics of vertebrate CPGs. This commonality supports the hypothesis that basic locomotor neural circuits are highly conserved across significant morphological differences and phylogenetic distances in vertebrates (Wainwright, 2002; Grillner and Jessell, 2009). Thus, my results provide important insight into not only human locomotor control but also the evolution of vertebrate locomotion.

Chapter 4 study 3

Motor module activation sequence and topography in the spinal cord during air-stepping in human: Insights into the traveling wave in spinal locomotor circuits

This study has been published as:

Yokoyama H., Hagio K., Ogawa T., Nakazawa K. "Motor module activation sequence and topography in the spinal cord during air-stepping in human: Insights into the traveling wave in spinal locomotor circuits". *Physiological Reports*. 5(22): e13504. 2017.

4. 1. Introduction

The timing and pattern of locomotor muscle activities in vertebrates are generated by spinal neural networks referred to as spinal CPGs (Grillner, 1981; Kiehn, 2016). Recent animal studies combining electrophysiology with molecular genetics demonstrated that the CPGs consisted of multiple types of spinal interneurons (Kiehn, 2016). In humans, indirect evidence of the existence of CPGs has been demonstrated by several studies in patients with SCI (Calancie et al., 1994; Dimitrijevic et al., 1998; Danner et al., 2015).

Regarding spinal motor control, the anatomical positions of the MNs, which receive inputs from CPGs, are logically arranged according to the biomechanical characteristics of their target muscles (Romanes, 1964; Jessell et al., 2011). Generally, each muscle is innervated from several spinal segments and each spinal segment innervates several muscles. The anatomical grouping at each segment may reflect synergistic functions at a given hindlimb joint along the rostrocaudal axis of the spinal cord (Romanes, 1964). In addition, MN columns that innervate antagonist muscles are separated spatially along the mediolateral axis of the spinal cord (McHanwell and Biscoe, 1981). Recently, such stereotyped organization of MNs was suggested to simplify the connectivity between MNs and pre-motor inputs for locomotor control in the mouse (Hinckley et al., 2015). In human bipedal walking, specificity in the MN arrangement along the mediolateral axis depending on gait phase (i.e., stance and swing phase) has been suggested (Ivanenko et al., 2008).

Regarding the control of locomotor muscle activity, a small number of motor modules (also referred as muscle synergies) generate complex activities of various muscles (Tresch et al., 1999). The motor modules are encoded in spatial pattern formation networks, which activate multiple MN pools, in the spinal CPGs (McCrea and Rybak, 2008). The CPGs are considered to consist of the pattern formation networks and temporal regulation networks, which send activation commands to the pattern formation networks (McCrea and Rybak, 2008). A recent study by Saltiel et al. (2015) demonstrated that a focal neurochemical stimulation to the frog

spinal cord elicited specific types of motor module activities similar to those used in intact frog locomotion. Interestingly, the locomotor modules exhibited partially overlapping representations along the rostrocaudal direction. Further, the order from rostral to caudal segments corresponded to the activation sequence in a gait cycle. The relationships between the activation sequence of locomotor muscle synergies and their spinal cord topography suggests that the locomotor muscle activity is generated by a wave of neural activation, traveling in the rostrocaudal direction, in the lumbosacral spinal cord. The traveling wave is assumed to be derived from rostrocaudal propagation of electrical activity of dorsal horn neurons and relevant to the temporal regulation networks of CPGs (Cuellar et al., 2009). A simulation model demonstrated that sequentially spacing motor modules from the rostral to caudal regions and the rostrocaudal traveling wave, acted as the pattern formation networks and the temporal regulation networks, respectively, to reproduce actual motor outputs in frogs (Saltiel et al. 2015).

The travelling wave of motor output has been observed among different vertebrates, especially in animals using undulating locomotion, including Lamprey (Wallén and Williams, 1984), fish (Grillner, 1974), and tadpoles (Roberts et al., 1998). Although there is still debate about whether the traveling wave mechanisms exist in legged animals (AuYong et al. 2011; Cuellar et al. 2009; Pérez et al. 2009), evidence for its existence has been observed in frogs (Saltiel et al., 2015), rodents (Cazalets, 2005), and cats (Cuellar et al., 2009; Pérez et al., 2009). However, thus far, the traveling wave has not yet been confirmed in human locomotion. Based on myotomal charts (Kendall et al., 1993), a previous study reconstructed the MN activation during walking in humans (Ivanenko et al., 2006). They demonstrated the rostrocaudal movement of MN activations in the lumbosacral enlargement during a gait cycle based on the locus of the center of activity (CoA) of the MN activity. Although the CoA demonstrated the rostrocaudally traveling wave-like activation of MNs from upper lumbar to lower sacral segments in a swing-stance cycle, the CoA shifted rostrally toward the upper lumbar segments

at foot contact in the middle of the rostrocaudal propagation. The rostral shift of the CoA was induced by a motor module activating the quadriceps and TA muscles at foot contact related to loading response (Ivanenko et al., 2006). A comparative study between humans walking and animal locomotion demonstrated that the large activity of quadriceps and TA at foot contact related to loading response is unique to human upright walking (Vilensky, 1987).

Generally, a large part of the spinal CPGs mechanisms is phylogenetically conserved across different species (Goulding, 2009). Based on the commonality of the locomotor circuits, it is quite possible that the traveling wave of activation exists in the human spinal circuits. The traveling wave of activation in the spinal cord may not have been observed in the previous human walking study (Ivanenko et al. 2006) due to it being masked by the muscle activity induced by loading response at foot contact The air-stepping task has been previously used to examine human locomotor control under the conditions without foot-contact interactions, thus, eliminating body-weight loading (Ivanenko et al., 2002; Ivanenko et al., 2007). By removing foot-contact interactions, the motor output of air-stepping might represent more endogenous activity in the spinal CPGs compared with that during normal walking. Thus, in the present study, by adopting an air-stepping task I examined whether the traveling wave of activation exists in the human spinal circuits based on activation sequence of motor modules and their innervation locations in the lumbosacral enlargement during air stepping. Here, assuming that the traveling wave of activation exists in the human spinal circuits and recruits motor modules during air-stepping, I hypothesized that motor modules would be sequentially recruited from rostral to caudal regions of the spinal cord during each step. The acceptance of this working hypothesis would provide indirect evidence that the traveling wave mechanisms are conserved in humans. My results would contribute to better understanding the human locomotor system and commonality of locomotor neural systems among vertebrates.

4. 2. Methods

4. 2. 1. Participants

Nine healthy male volunteers (age ± standard deviation [SD], 26.1 ± 2.7 years) participated in this study. Each participant gave written informed consent for his participation in the study. This study was carried out in accordance with the Declaration of Helsinki and with the approval of the Ethics Committee of the Graduate School of Arts and Sciences, the University of Tokyo.

4. 2. 2. Experimental setup and design

Participants stepped with the right leg in the air while standing on a stool on the left leg and holding a vertical pole with the left hand for stabilization (Fig. 4-1a). They were instructed to perform 30 strides of one-leg air-stepping at a comfortable cadence as if they walked on the ground. In this condition, all participants performed the step at a pace of 1.34 ± 0.12 s/step (mean ± SD). The step frequency was approximately equivalent to the stride time of slow walking (1.38 sec/stride at 0.83 m/s) (Murray et al., 1984). Prior to the experiment, the participants practiced the task for 5 min.

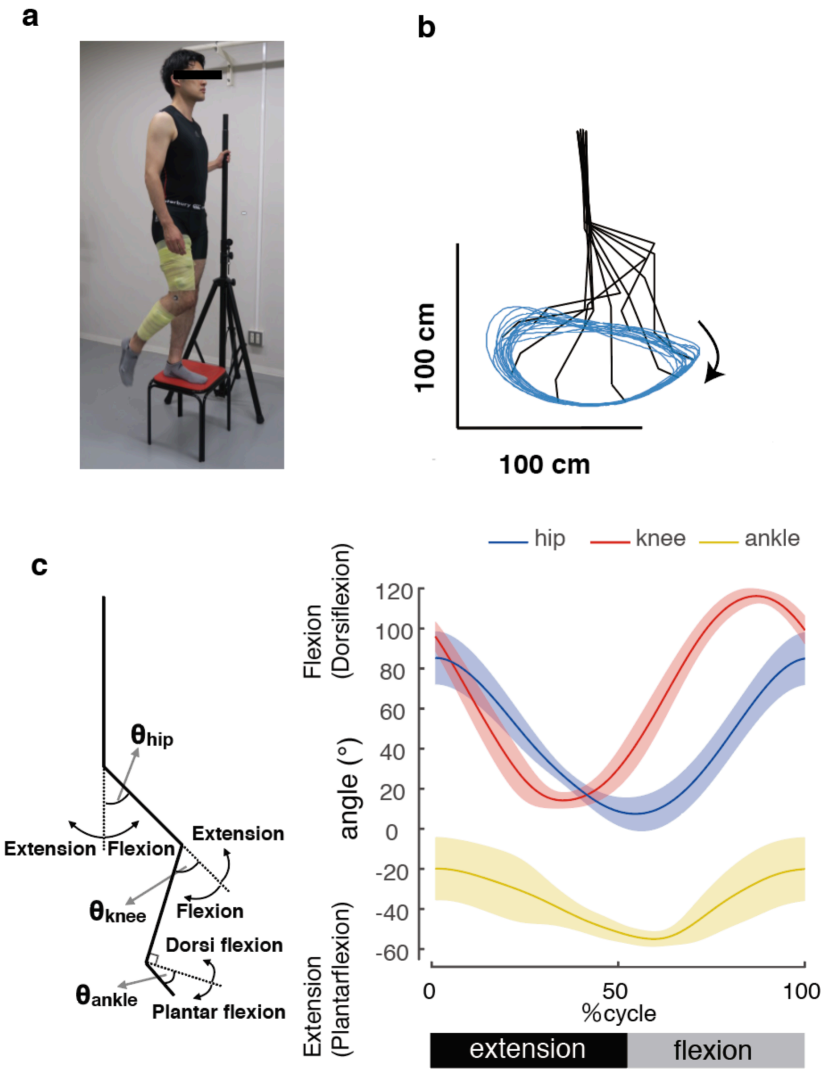

Figure 4-1. Experimental setup of one-leg air stepping and the kinematics pattern. (a) Experimental setup of one-leg air stepping movement. Participants stepped with the right leg in the air while standing on a stool on the left leg and holding a vertical pole with the left hand for stabilization. In accordance with the research ethics of the journal, the individual gave written consent for the publication of this image. (b) An example of kinematics of one-leg air stepping movement. Averaged kinematics patterns over 20 consecutive step cycles are shown at every 10% gait cycle for a single participant. Blue line indicates the trajectory of the toe marker over the 20 consecutive step cycles. (c) Ensemble averages across participants (± standard deviation) of the hip, knee, and ankle angles in an extension-flexion cycle based on the hip angle.

4. 2. 3. Data collection

Surface EMG was recorded from the following 14 muscles on the right leg: TA, MG, SOL, PL, VL, RF, BF, ST, adductor longus (AL), sartorius (SART), iliopsoas (ILIO), TFL, GM, and Gmed. Electrodes were placed in accordance with the recommendation of Criswell and Cram (2011). Although the ILIO is a deep muscle, the superficial area of the ILIO is adequately large for surface EMG recording (Jiroumaru et al., 2014). Nevertheless, EMG signals of the ILIO can be corrupted by cross talk from adjacent hip flexors. Thus, to minimize cross-talk from adjacent muscles, I carefully checked location of the ILIO by manual palpation as outlined by Muscolino (2008) and performed cross-talk tests suggested by Criswell and Cram (2011). The EMG was recorded with a wireless EMG system (Trigno Wireless System; DELSYS, Boston, MA, USA). The EMG signals were band-pass filtered (20–450 Hz) and sampled at 1,000 Hz with the EMG system and a multichannel data-recording unit (PowerLab System, AD Instruments, Sydney, Australia), respectively. Kinematic data were recorded at 100 Hz by using an optical motion capture system (OptiTrack: V100R2, Natural Point, OR, USA) with six cameras. Five spherical markers were placed over the right side of the fifth metatarsal head (toe), lateral malleolus (ankle), lateral femoral epicondyle (knee), greater trochanter (hip), and acromion process (shoulder).

4. 2. 4. Kinematic analysis

The kinematic signals were digitally smoothed with a zero-lag low-pass Butterworth filter (6-Hz cutoff, fourth order). From the marker coordinates, the joint angles at the ankle, knee, and hip were calculated (Definition: Fig. 4-1c, stick diagram). The beginnings of step cycles were defined as the peak flexion timing of the hip joint angle. Of the recorded 30-step cycles, I used 20 cycle data (EMG and kinematics signals) excluding the first and the last five cycles for

subsequent analysis.

4. 2. 5. EMG processing

The EMG data were demeaned, rectified, and smoothed with a zero-lag low-pass Butterworth filter (6-Hz cutoff, fourth order) to obtain the EMG envelopes (Walter et al., 2014). Subsequently, the processed EMG data were time-interpolated so that they had 200 points for each gait cycle.

4. 2. 6. Extraction of motor modules from the EMG data

Motor modules were extracted from the processed EMG data using the NMF methods used in Chapters 2 and 3 (Fig. 4-2a, see section 2.2.5. for details). In this study, Motor modules were extracted in each participant from an EMG dataset organized as a matrix with 14 muscles × 4,000 variables (i.e., 20-step cycles × 200 time points). After the extraction of motor modules, I clustered the extracted motor modules using hierarchical clustering analysis to examine their types (Ward's method, correlation distance) based on the muscle weightings. The clustering analysis was performed for all participants of all motor modules. The optimal cluster number was selected by the gap statistic (Tibshirani et al., 2001).

4. 2. 7. Spatiotemporal activation patterns of MNs within the spinal cord generated by each motor module

Based on the muscle activity generated from each module (i.e., the product of the muscle weightings and the corresponding temporal activation, Fig. 4-2b), spatiotemporal activation patterns of MNs were reconstructed from individual modules of all participants (Fig. 4-2c). The muscle activity generated from each module was mapped onto the estimated rostrocaudal location of the MN pools in the spinal cord from the L1 to S2 segments. I used Kendall's myotomal charts (Table 4-1)(Kendall et al., 1993) to reconstruct MN activation patterns. The

details of the methods for MN activation estimation are descried in Chapter 3 (see section 3.2.5. for details).

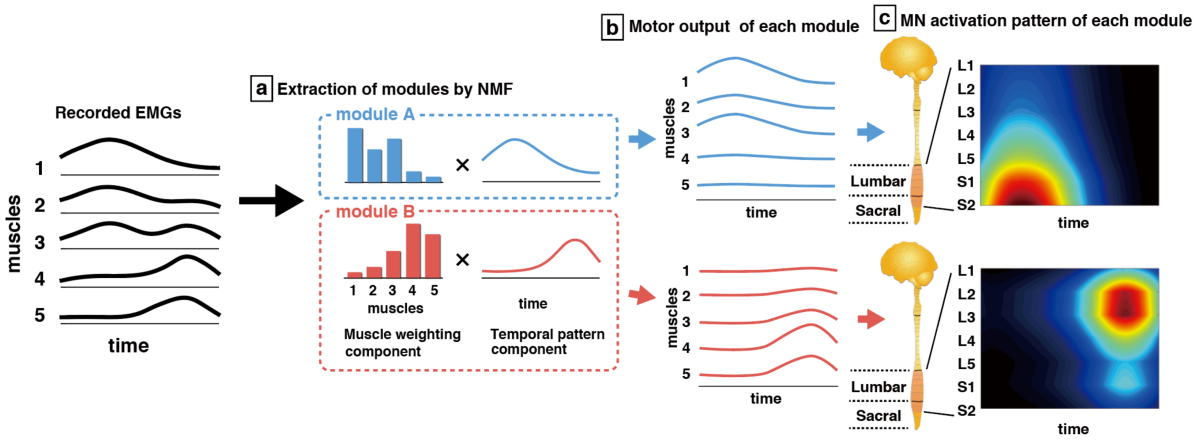

Figure 4-2. Procedures of the reconstruction of the spatio-temporal activation patterns of motoneurons (MNs) along the rostrocaudal axis of the lumbosacral enlargement for individual motor modules from the EMGs. (a) Motor modules were extracted using non-negative matrix factorization (NMF) from EMGs. (b) The output of each module is explained by the product of the muscle weighting component (bars: specifying activation level of each muscle) and the temporal pattern component (waveforms). The sum of outputs from the modules is approximately equivalent to that of the EMGs. (c) The MN activity in each segment (L2–S2, left vertical scale) generated from each module was reconstructed by mapping the output of each module based on Kendall's myotomal charts (Table 1).

Table 4-1. Muscle innervation charts. Data are adopted from Kendal et al. (1993).

	ILIO	GM	Gmed	TFL	SART	AL	RF	VL	BF	ST	MG	SOL	PL	TA
L1	x													
L2	X				X		X	X						
L3	X				X		X	X						
L4	x		X	X		x	X	X		x			x	X
L5		X	X	X					x	X			X	X
S1		X	X	X					X	X	X	X	X	X
S2		X							X	X	X	X		

The innervation level is expressed as X (high) and x (low). X and x are weighted with *kij* = 1 and *kij* = 0.5, respectively in equation (2).

To evaluate the spatial characteristics of the MN activation patterns of each module, the peak activity segment height of the seven (from L1 to S2) lumbosacral segment was calculated in each module. In addition, to evaluate the temporal characteristics of the MN activation patterns of the module, peak timings of the temporal activations were analyzed by using circular statistics (Batschelet et al., 1981; Berens, 2009). Then, the means of the peak timing of temporal activations across participants are calculated in each module type.

4. 2. 8. Effects of normalization methods

Since the number of MNs among each spinal segment is different (Table 4-2) (Tomlinson and Irving, 1977), the spatiotemporal activation patterns of MNs were normalized to the number of MNs in few previous studies (Ivanenko et al., 2013; La Scaleia et al., 2014). This normalization probably affects comparisons of peak activity segment height among each module type. To assess the effects of normalization, the activity of each spinal segment was

normalized based on the estimated number of MNs in the respective segment, according to a previous study (Ivanenko et al., 2013). Namely, the activity of each spinal segment was multiplied by the number of MNs in the respective segment and divided by the maximum number of MNs across seven segments (i.e., 12,765 in L3). From the normalized MNs activation patterns, the peak activity segment height of the seven lumbosacral segments (from L1 to S2) was calculated for each module.

Table 4-2. Mean number of motoneurons in each segment of the human spinal cord (13–40 years, 12 cases)

Segment height	Motoneuron number
L1	806
L2	5146
L3	12765
L4	12069
L5	12674
S1	10372
S2	4216

Data are adopted from Tomolinson and Irving (1977)

Since the activity of some muscles (e.g. triceps surae muscles) during air-stepping was lower than that during walking (Ivanenko et al., 2002; Gerasimenko et al., 2010), their relative activation differed from normal walking. Since the differences in the EMG amplitude affect module extraction by NMF, I assessed whether the results obtained in this study were just derived from the imbalance of EMG amplitude among muscles. Specifically, the EMG amplitude of each muscle was normalized to the maximum value for that muscle over the air-stepping task. Using the normalized EMGs, motor modules were extracted, and then MNs activation patterns were reconstructed using the same methods mentioned above.

4. 2. 9. Statistics

Differences in the peak activity segment height among each module type were compared using

a Kruskal-Wallis test (non-parametric one-way analysis of variance [ANOVA] test) with the Steel-Dwass post hoc test (nonparametric Tukey's test). In addition, differences of peak activation timings (i.e., mean angles of circular observations) among module types were tested by the Watson-Williams test. The p-values were adjusted by Holm's correction for multiple comparisons. Statistical significance was accepted at $p < 0.05$.

4. 3. Results

4. 3. 1. Kinematic data

Figure 4-1b shows a typical example of kinematic pattern of the one-leg air stepping in a single participant. Figure 4-1c shows ensemble averages across participants of hip, knee, and ankle angles of the one-leg air-stepping. In the extension-flexion cycle, the average terminal extension timing (i.e., peak timing of the hip extension angle) was 52.6 ± 1.2%. The temporal characteristics of these joint movements were generally similar to those of walking (Winter et al., 1974; Murray et al., 1984; Kadaba et al., 1990). Nevertheless, there were some differences between air-stepping and walking as described below. In hip joint angle, the maximum flexion angle (83.3 ± 13.2°) was larger compared with that of walking (approximately 45°). The maximum flexion angle of the knee joint (115.4 ± 4.0°) was greater than that of walking (approximately 60°). Additionally, although a small knee flexion occurs after foot contact in level walking (corresponding to the early extension phase in air-stepping), it was absent during air-stepping. In ankle joint angle, the magnitude of the range of motion between air-stepping (36.3 ± 16.5°) and level walking (approximately 30°) was similar, while the central angle in air-stepping was shifted toward plantar flexion compared with that in level walking (39.2 ± 8.0° [planter flexion] in air-stepping, approximately 5° [planter flexion] in level walking). Additionally, the ankle was continuously dorsiflexing during the stance phase and rapidly plantarflexed at the transition timing from the stance to swing phase in level walking; continuous plantar flexion was observed during the extension phase in air-stepping.

4. 3. 2. Motor modules extracted from EMGs

Figure 4-3 shows the EMG patterns generated during the one-leg air-stepping task. From the recorded EMGs (Fig. 4-3), 3.22 ± 0.83 (mean ± SD) motor modules were extracted from each participant. The extracted motor modules were grouped into four types by cluster analysis (Fig. 4-4, upper and middle rows). Module A was activated at the early-mid flexion phase of hip joint angle and mainly recruited the ILIO. Module B was activated at the mid-late flexion phase and mainly recruited the RF, SART, and TA. Module C was activated at twice (i.e., at the early-mid extension and early-mid flexion phases) and mainly recruited the TFL. Module D was activated at the last flexion-initial extension phase and mainly recruited the ST, PL, and MG.

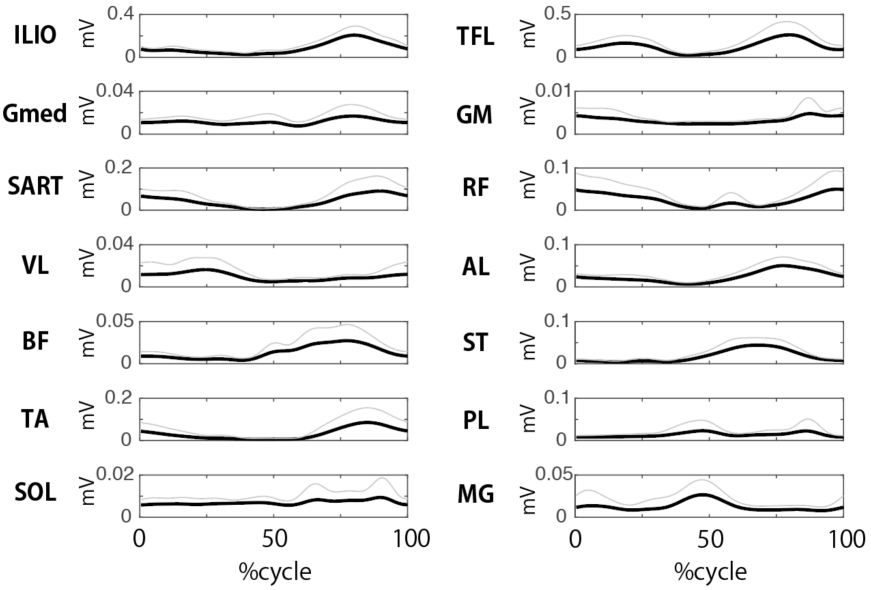

Figure 4-3. Muscle activation patterns during step cycles. Ensemble averaged activity patterns across participants (black lines) and their standard deviations (SD, gray lines) are shown.

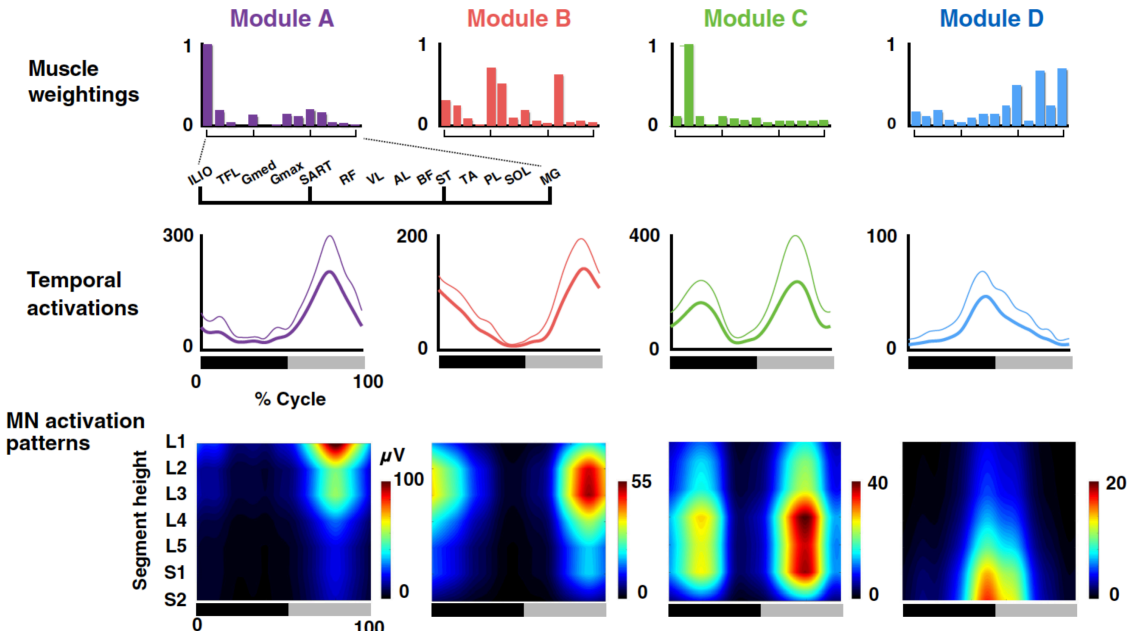

Figure 4-4. Muscle weightings, temporal activation patterns, and motoneuron (MN) activation patterns of extracted motor modules. Average muscle weightings across participants in each type of modules are shown. Each bar height represents the relative level of activation of each muscle within the muscle weighting components. Lines indicate the temporal pattern components of the modules. Average patterns across participants (thick lines) and their standard deviations (thin lines) are represented. Heat map indicates MN activity patterns generated by each module. The bars underneath denote the extension phase (black) and flexion phase (grey) of hip joint angle in a step cycle.

4. 3. 3. Spatio-temporal activation patterns of MNs generated from individual modules

The spatio-temporal activation patterns of MNs were reconstructed from each motor module (Fig. 4-4, lower row). Based on visual inspection, each module activated the MN pools in specific segments at a specific timing point in the gait cycle. To quantify the differences in the activated segments, the peak activity segment heights of in the seven lumbosacral segments

were calculated for each module (Fig. 4-5). Among the four module types, the segment heights of the CoA were high in the order of module A, B, C, and D (Kruskal–Wallis one-way ANOVA: $p < 0.001$; post hoc Steel–Dwass test: $p < 0.05$). Additionally, using the circular statistic, I quantified the differences in peak timings of the temporal activations among modules (Fig. 4-6). As module C had two activation peaks as shown in Fig. 4-4, we separately evaluated the first and second peaks as C1 and C2, respectively. The peak activation timings were different among the module types ($p < 0.05$), except for a pair between modules A and C2. Thus, the sequence of the motor modules during the one-leg air-stepping was in the following order: C1, D, C2+A, and B in the extension-flexion cycle.

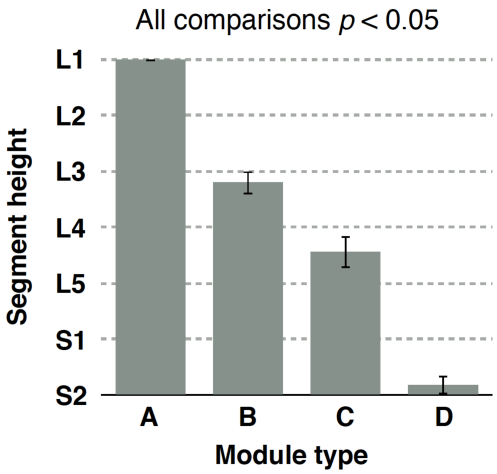

Figure 4-5. Group-averaged peak activity segment height of the MN activity in the seven (from L1 to S2) lumbosacral segments for each motor module. Error bars indicate the standard errors.

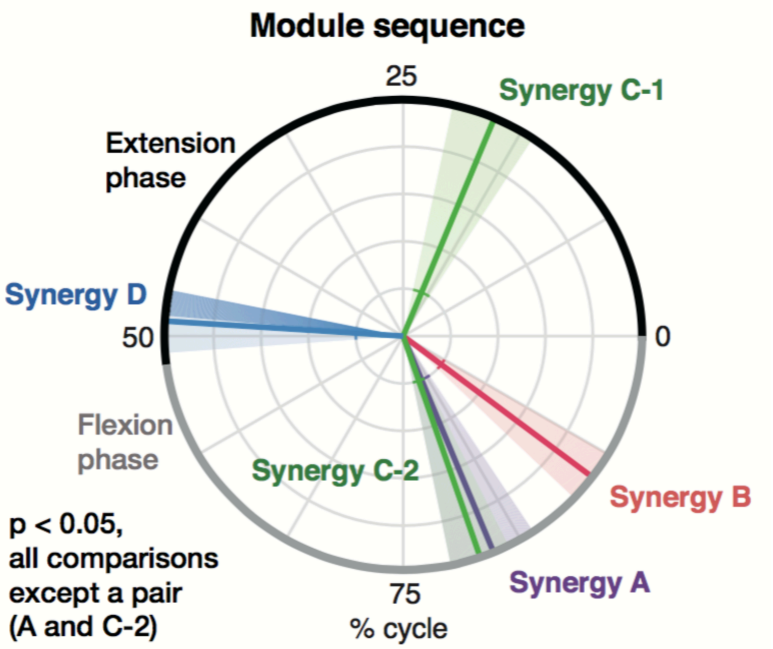

Figure 4-6. Motor module sequence in air stepping. Colored lines in the circular data indicate mean peak activation timings across participants. Translucent areas represent their standard errors.

4. 3. 4. Effects of normalization methods

Figure 4-7 shows the spatiotemporal MN activation patterns (Fig. 4-7a) and peak activity segment (Fig. 4-7b) for each module type after normalization to the MN number. Compared with the non-normalized data (Fig. 4-4), the MN activation patterns were moved toward the center of lumbosacral enlargement. The normalization especially affected to the modules representing MN activations at the end of the lumbosacral enlargement (i.e., module A and D). Although there was no significant difference in the peak activity segment between modules A and B, all the other comparisons showed significant differences ($p < 0.05$) (Fig. 4-7b), which was the same as the non-normalized data (Fig. 4-5).

I extracted modules from amplitude normalized EMGs. As a result, 3.80 ± 0.75 (mean ± SD) motor modules were extracted from each participant, and the modules were

grouped into four types by the cluster analysis, which was the same as in the non-normalized data. Figure 4-8 shows the muscle weightings, temporal activations, and MN activation patterns of the motor modules extracted from the amplitude normalized EMGs. Compared with non-normalized data (Fig. 4-4), the muscle weightings (upper row) of several muscles were highly weighted in modules A–C. The temporal patterns (middle row) represented quite similar patterns. Regarding the MN activation patterns of the modules (Fig. 4-8), the activated segments in module A shifted from L1 (non-normalized data, Fig. 4-4) to L2–L3 (normalized data, Fig. 4-8).

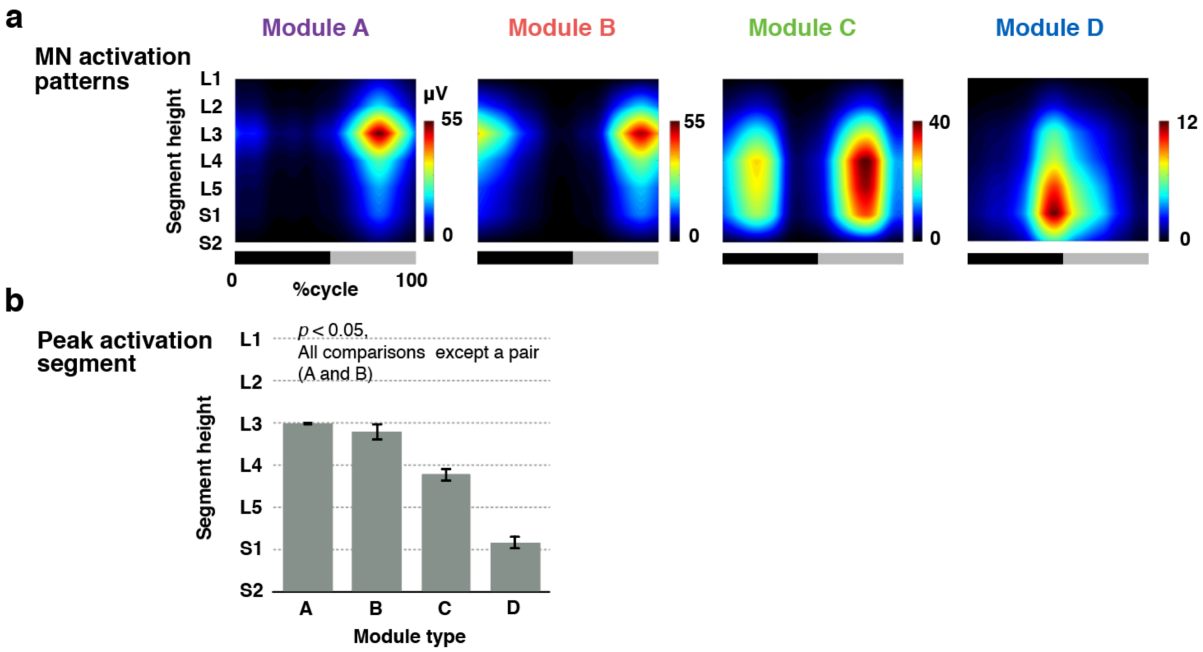

Figure 4-7. (a) MN activation patterns of motor modules normalized to MN numbers in each segment. The bars underneath denote the extension phase (black) and flexion phase (grey) of hip joint angle in a step cycle. (b) Group-averaged peak activity segment height of the normalized MN activation patterns. Error bars indicate the standard errors.

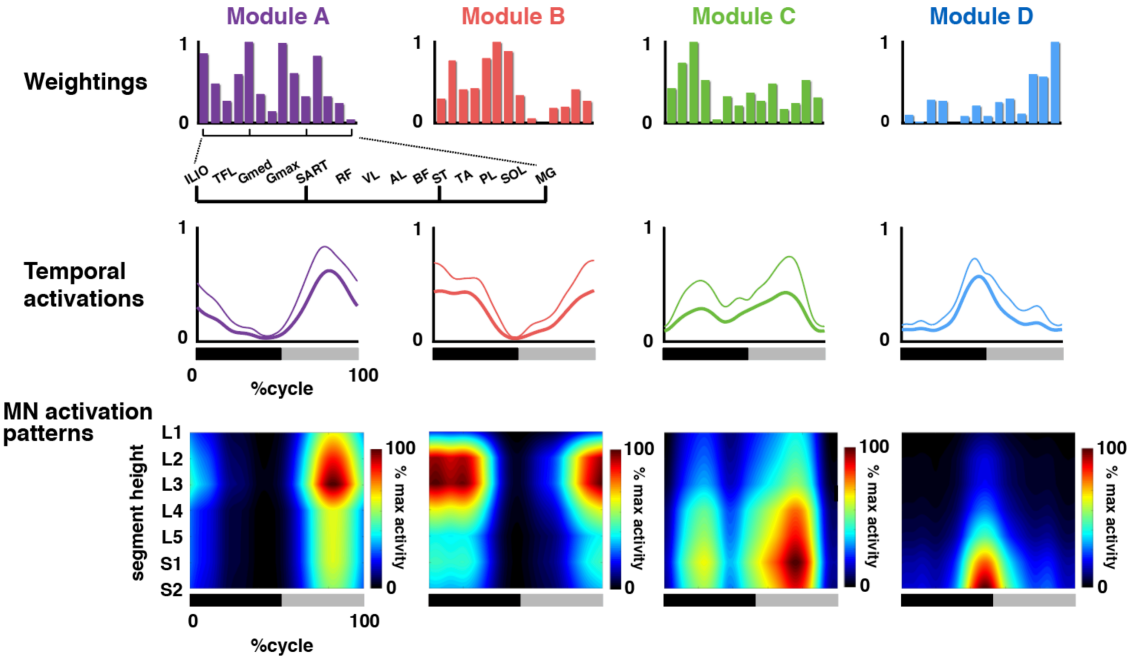

Figure 4-8. Muscle weightings, temporal activation patterns, and MN activation patterns of the motor modules extracted from amplitude-normalized EMGs. Average muscle weightings across participants in each type of modules are shown. Each bar height represents the relative level of activation of each muscle within the muscle weighting components. Lines indicate the temporal pattern components of the modules. Average patterns across participants (thick lines) and their standard deviations (thin lines) are presented. Heat map indicates MN activity patterns generated by each module. The bars underneath denote the extension phase (black) and flexion phase (grey) of hip joint angle in a step cycle.

4. 4. Discussion

In the current study, four different types (module A–D) of motor modules were extracted from muscle activity during air-stepping. Among the module types, the peak activity segment height in the lumbosacral enlargement was high in the order of module A > B > C > D. In addition, the activation sequence of motor modules during the one-leg air-stepping was in the following order: C1, D, C2+A, and B in the extension-flexion cycle. The order can be sorted as "C2+A-B-C1-D" in the flexion-extension cycle. The "A-B-C1-D" sequence corresponded to the

order of the activated segment heights, i.e., "A > B > C > D". Comparing the activation sequence with the topography of the motor modules in the spinal cord suggests the existence of a rostrocaudally traveling wave of activation in human locomotor spinal circuits.

4. 4. 1. Comparisons of bipedal walking and airstepping

Based on the myotomal charts (Kendall et al., 1993), a previous study (Ivanenko et al., 2006) examined the activation of lumbosacral MNs from EMGs during walking in humans. Although Ivanenko et al. (2006) observed rostrocaudal wave-like activation, the activation was shifted rostrally toward the upper lumbar segments around the time of the foot contact timing. Consequently, the MN activations showed rostrocaudal movements with two cycles in a gait cycle. The motor module mainly activated the knee extensor muscles and was considered to be related to the loading response at foot contact.

Therefore, the present study aimed to examine the activation of the lumbosacral spinal cord in a stepping movement, without foot-contact interactions, using an air-stepping task (Ivanenko et al., 2002; Ivanenko et al., 2007). From the muscle activity during air-stepping, four types of motor modules were extracted (Fig. 4-4). As expected, the motor module for the loading response at foot contact (corresponding to the initial extension phase) was not extracted. The four extracted motor modules in the present study were similar to those extracted in previous studies examining motor modules during human locomotion (Cappellini et al., 2006; Neptune et al., 2009; Chvatal and Ting 2012; Yokoyama et al., 2016).

Module A activated at the time of early-mid flexion phase of the hip joint, and it mainly recruited the ILIO (Fig. 4-4). This module acts to accelerate the leg forward in the early swing (Neptune et al. 2009) and showed the highest amplitude activation among the four module types during air-stepping (Fig. 4-4). This characteristic is not seen in walking and would be caused by the greater hip flexion during air-stepping as mentioned in the Results. Module B activated at the time of mid-late flexion phase, and mainly recruited the RF, SART, and TA. This module

was related to toe clearance and leg acceleration in the mid-late swing phase (Neptune et al., 2009). Module C activated at twice (i.e., during the early-mid extension and early-mid flexion phases), and mainly recruited the TFL. During walking, this module activated during walking at one peak timing, i.e., at the early stance (corresponding to early-mid extension), to stabilize the pelvis (Yokoyama et al., 2016). The TFL, major muscle of the module C, was almost inactive at the swing phase of normal walking (Cappellini et al., 2006). However, it would act at the initial swing for additional pelvic stability and supplementary thigh acceleration under a large hip flexion angle during the air-stepping as demonstrated in up-ramp and up-stair walking (Gottschall et al., 2012). Module D activated at the last extension-initial flexion phase of hip joint angle, and it mainly recruited the ST, PL, and MG. During walking, this module play a role in plantar flexion/body support and propulsion at late stance (Chvatal and Ting, 2012).

4. 4. 2.Topography and temporal sequences of MN activations in air-stepping

The difference of the peak activity segment among the modules A > B > C > D (Fig. 4-5) corresponded with the with specificity of encoding locations of motor modules in the spinal cord of frogs (Saltiel et al., 2015) and mice (Caggiano et al., 2016). Regarding the temporal sequence of modules, “C2+A-B-C1-D” (Fig. 4-6), although the peak timings of A, B, C1, and D were consistent with those observed in level walking (Cappellini et al., 2006; Neptune et al., 2009; Chvatal and Ting 2012), C2 is not seen in level walking. If evaluating only the module activations related to level walking (i.e., A, B, C1, D), the order of the activated segment height, “A > B > C > D”, and the activation sequence, “A-B-C1-D”, indicate that motor modules were sequentially activated from the anatomically upper module to the lower module. The locomotor CPG is considered to consist of temporal structures and pattern formation networks, and the motor modules may underlie the pattern formation networks (McCrea and Rybak, 2008). Therefore, the sequential rostrocaudal activation of the motor modules suggests the possibility that rostrocaudally traveling waves of activation exist in human locomotor spinal circuits as a

temporal structure to activate motor modules in proper sequences.

Although the topography and temporal order was corresponded in flection-extension cycle, the temporal order depended on the onset of the gait cycle. Regarding onset of gait cycle, it has been well known that swing onset is regulated by two types of sensory information force afferents of the ankle extensor muscles (Duysens and Pearson, 1980; Whelan et al., 1995) and position afferents from the hip flexor muscles (Grillner and Rossignol, 1978; Kriellaars et al., 1994; Hiebert et al., 1996). Therefore, I consider that the gait cycle is initiated from onset of hip flexion from the viewpoint of neural control. Additionally, my results are consistent with the traveling wave of activations that occurred during the swing-stance cycle in flogs (Saltiel et al., 2015).

4. 4. 3. Traveling wave of activations in the spinal cord in nonhuman vertebrates

The rostrocaudal distribution organization of CPG is supported by theoretical studies (Kaske et al., 2003; Ijspeert et al., 2007) and experimental studies on EMG activity, spinal MNs, and interneurons among many vertebrates including Lamprey (Wallén and Williams, 1984), fish (Grillner, 1974), tadpoles (Roberts et al., 1998), frogs (Saltiel et al., 2015), rodents (Cazalets, 2005), and cats (Cuellar et al., 2009; Pérez et al., 2009). For example, Cuellar et al. (2009) demonstrated a traveling wave of cord dorsum potentials by interneuronal recordings during the fictive cat scratch, indicating the rostrocaudal interneuronal activation in the mammalian spinal locomotor circuits. In rodents, rostrocaudal propagation of MN activation was optically imaged (Bonnot et al., 2002; O'donovan et al., 2008), and the traveling waves were also electrophysiologically recorded from the ventral roots (Cazalets, 2005). In addition, a study by Saltiel et al. (2015) demonstrated a traveling wave in the spinal cord in frog locomotion based on motor module temporal sequences and topography in the spinal cord, which is similar to my results.

Regarding the neural origin of the traveling wave of activation in the spinal cord,

rostrocaudal propagation of spontaneous electrical activity of dorsal horn neurons in the layers III–VI (i.e., cord dorsum potentials) is considered as a temporal structure of CPG networks (Cuellar et al., 2009; Pérez et al., 2009; Kato et al., 2013). Namely, the MN clusters corresponding to each motor modules are probably sequentially recruited from rostral regions to caudal regions by the rostrocaudal propagation of the cord dorsum potentials. In rodents, neurons in the layer III–V have interesting anatomical features that may play a role in propagating the traveling wave (Schneider, 1992). The neurons have an axon running in the rostrocaudal direction, with perpendicular collateral branches that are intermittently spaced apart. If this type of neurons is also present in humans, then it is possible that cord dorsum potentials of the neurons are an underlying mechanism of the traveling wave of activations in the spinal cord, which control locomotion.

4. 4. 4. Possibility of traveling waves in human locomotor circuits

To date, the traveling wave of activation has not been confirmed in human locomotion. Nevertheless, it has been suggested that CPGs in legged vertebrates have evolved from common ancestral circuit for undulatory locomotor behaviors, such as fish and lamprey (Grillner and Jessell, 2009). In addition, EMG-based studies strongly suggested that the motor modules of humans and those of other legged vertebrates share similar circuitries (Dominici et al., 2011). Based on the commonality of spinal locomotor circuits, it is conceivable that traveling waves are the neural mechanisms underlying the motor module sequence and the topography of the motor modules presented in the current study.

In human walking, in addition to the MN activations, which are thought to be related to the traveling wave, MNs in the rostral lumbosacral enlargement are activated around foot contact (Ivanenko et al., 2004). The additional MN activation mainly recruits two modules (Ivanenko et al. 2004), which have essential biomechanical functions to support and decelerate the body during the loading response (Ivanenko et al., 2004; Neptune et al., 2009; Chvatal and

Ting, 2012). One of the modules, which mainly recruits the quadriceps, may be recruited by loading afferent inputs, because the activation of the quadriceps decrease depending on the amount of relief under body-weight supported walking (Ivanenko et al., 2002; Klarner et al., 2010). Another module, which mainly recruits the TA, may be mainly recruited by cortical commands, because the TA has significant connectivity with motor cortex prior to foot contact (Petersen et al., 2012) and the amplitude is not correlated with the amount of body weight relief (Ivanenko et al., 2002; Klarner et al., 2010). Thus, combined motor module activations derived from rostrocaudally traveling waves, sensory inputs and cortical commands may contribute to the generation of coordinated muscle activity during walking.

4. 4. 5. Effect of different normalization methods

Some previous studies normalized the spatiotemporal activation patterns of MNs based on the number of MNs in each segment (Ivanenko et al., 2013; La Scaleia et al., 2014). I examined the effects of this normalization to the peak activity segment (Fig. 4-7). The peak activity segment was significantly different among motor module types in non-normalized data (Fig. 4-4), while the significant difference between module A and B was lost after the normalization (Fig. 4-7). This could be attributed to the fact that this normalization mainly affected on the end segments of the lumbosacral enlargement (L1, L2 and S2), which contained considerably lower numbers of MNs than other segments (Table 4-2). Although there was no significant difference of the peak activity segment between module A and B, the fact remains that activation locations of both modules were upper lumber regions at initial flexion phase. Thus, since MNs activated from rostral region to caudal region during the activation sequence, “A-B-C1-D”, the normalized results still do not refute the existence of a traveling wave of activation in human spinal circuits.

I also examined the effects of EMG amplitude normalization on the motor module extraction and MN activity reconstruction (Fig. 4-8). Compared to the non-normalized data (Fig.

4-4), although the temporal patterns were similar, the muscle weightings were different in modules A–C. Although there was a slight shift in the activated segments in module A, from L1 (non-normalized data) to L2-L3 (normalized data), overall, the MN activation patterns of the other modules (Fig. 4-8) were qualitatively similar to that of the non-normalized data (Fig. 4-4). Even after the normalization, the activation location of module A was the upper lumbar region, indicating that the MNs were activated from rostral region to caudal region during the module sequence. Therefore, the normalized results also do not refute the hypothesis that traveling waves of activation exist in human spinal circuits.

4. 4. 6. Methodological considerations

There are several limitations in this study, which must be noted. I demonstrated the possible existence of the traveling wave in human spinal circuits, using voluntary leg movement. Human locomotor muscle activity is suggested to be generated by the spinal CPGs (Duysens and Van de Crommert, 1998). However, because the cortex controls walking, the possibility that the sequential activation of motor modules in the rostrocaudal direction are independently activated by each corresponding voluntary descending drive cannot be ruled out in humans (Artoni et al. 2017; Petersen et al. 2012). To examine the neural origin of traveling wave, studies on individuals with SCI would provide more direct evidence with eliminating the effects of descending drives. A recent study on SCI showed that the epidural electrical stimulation to the lumbar spinal cord could elicit coordinated rhythmic activities of multiple lower leg muscles innervated from a wide range of lumbosacral segments (Danner et al., 2015). Consistent with my results, this study also showed that four motor modules acting at different peak timings were extracted from the coordinated muscle activities generated by spinal circuits (Danner et al., 2015). Thus, the examination of the topography of the motor modules extracted from patients with SCI would provide more direct evidence of the traveling wave in the human spinal cord.

Another limitation of my study is that I examined locomotor networks using unilateral

leg movements. Although locomotor CPGs have bilateral couplings for left-right coordination (Butt and Kiehn, 2003; Maclellan et al., 2014), unilateral coupling for controlling unilateral leg has been also shown in electrophysiological (Hägglund et al., 2013) and behavioral (Yang et al., 2004; Choi and Bastian, 2007) studies. Therefore, the spinal locomotor CPGs consist of bilateral and unilateral components (Kiehn, 2016). The traveling wave of activation in the spinal cord has been shown as a mechanism for the temporal regulation in the unilateral component of the CPGs (Cuellar et al., 2009; Saltiel et al., 2015). Thus, the results in the present study would reflect the characteristics of the unilateral component of the locomotor circuits in the human spinal cord.

Another important methodological concern is the potential issue of EMG cross-talk. The issue of cross-talk is particularly applicable to the EMG signal of the ILIO muscle in the current study. Although the ILIO is one of the deep muscles, a recent MRI study demonstrated that the superficial region of this muscle in the femoral triangle immediately under the inguinal region is adequately large for surface EMG recordings (Jiroumaru et al., 2014). In the present study, to adequately attach the electrodes on the superficial region, we carefully checked the location by manual palpation (Muscolino, 2008) and cross talk tests (Criswell and Cram 2011). Nevertheless, I cannot completely rule out the possibility that the EMG signal of the ILIO was still contaminated by cross-talk from adjacent muscles, such as the sartorius muscle (SA) and the internal oblique muscle (IO). In this study, as the ILIO was mainly recruited by module A, which was activated from upper lumber segments (Fig. 4-4). Since the SA and the IO are innervated from upper lumber segments and thoracic segments (SA: L2–L3, IO: T7-L1) (Kendall 1993), the module A would be activated from more upper region if the EMG signal of the ILIO was contaminated by the SA and the IO activity. Thus, we believe that the cross-talk in the EMG signal of the ILIO had little effect on the rostrocaudally traveling waves of activation in this study.

4. 4. 7. Conclusions

In summary, I examined whether the traveling wave of activation existed in the human spinal circuits by extracting motor modules and reconstructing the MNs activity of the modules during air-stepping. The present results suggest the possibility that neural mechanisms of rostrocaudally traveling waves of activation are conserved in human spinal locomotor circuits. This neural mechanism would take advantage of activating motor modules in proper sequences to generate locomotor muscle activity in humans. The results would also provide novel information on the spatial arrangement of MNs for movement control, which has been studied over many years (Romanes, 1964; Jessell et al., 2011). In addition, the commonality about the traveling waves of activation between humans and other vertebrates supports the hypothesis that fundamental locomotor networks are conserved across phylogenetic and morphological differences in vertebrates (Grillner and Jessell, 2009; Dominici et al., 2011). Therefore, I believe that the results of the present study advance our understanding of human locomotor control mechanisms, and provide important insights into the evolution of locomotor networks in vertebrates.

Chapter 5 study 4

Neural decoding of locomotor module and muscle activity from EEG signals in humans

5. 1. Introduction

Locomotion behavior is achieved by complex activations of multiple muscles. In quadruped animals, the locomotor muscle activity is mainly generated by subcortical regions and spinal neural networks, while the cortex is considered to have little involvement in the muscle control during steady state walking (Armstrong, 1988). Several studies demonstrated significant involvement of the cortex in locomotor control during visually-guided locomotion and stepping for obstacles avoidance (Armstrong, 1988; Armstrong and Marple-Horvat, 1996; Drew et al., 2004; Drew et al., 2008). Therefore, the motor cortex in quadruped vertebrates has been considered to play a role for only volitional modification during walking when adjusting the stepping movement (Armstrong, 1988).

On the other hand, in humans, neuroimaging studies using functional NIRS and PET indicated that the cortical regions related to motor control have greater activation even during stereotyped walking. The functional NIRS studies demonstrated that oxygenated hemoglobin level is increased in the frontal, premotor, and supplementary motor regions of the cortex during walking (Miyai et al., 2001; Suzuki et al., 2004; Suzuki et al., 2008; Harada et al., 2009). A PET study, which compared imagination and execution of walking, demonstrated that the primary motor and somatosensory cortex were activated during the execution, while the supplementary motor cortex and basal ganglia were activated during the imagination (La Fougere et al., 2010). The task specific differences in brain activity suggested that the direct corticospinal pathway has a role for execution of steady state walking, while indirect motor pathway via a supplementary motor cortex and basal ganglia is involved in planning and modulation of walking (la Fougere et al., 2010). Nevertheless, although these neuroimaging methods revealed large activation of the cortex during walking in humans, they were not able to examine the relationships between the detected locomotor related cortical activity and locomotor muscle activity, which dynamically changes in a stride, because of their limited time resolution.

EEG is a non-invasive brain imaging method which has high temporal resolution

enough to examine the corticomuscular relationship. So far, EEG measurement during dynamic movements has been considered to be difficult, because the EEG signals are easily contaminated by artifacts caused by participant movements. Nevertheless, recently developed artifact removal methods based on ICA (Gwin et al., 2010) and PCA (Mullen et al., 2013) allow EEG measurement during walking. An EEG study on human walking demonstrated significant EEG-EMG coherence between leg sensorimotor area and TA muscle before heel-contact during steady speed walking (Pertersen et al., 2012). In addition, most recent study indicated that causal connectivity from motor cortex to leg muscles during steady state walking (Artoni et al., 2017). These two studies strongly suggested cortical involvement in locomotor muscle control.

Regarding control of locomotor muscle activity, experimental studies using decomposition techniques suggested that the complex locomotor muscle activity is generated from a small set of locomotor modules, which generate basic synergistic activity in multiple muscles (Ivanenko et al., 2004; Dominici et al., 2011). The locomotor modules are considered to be encoded in spinal locomtor networks (McCrea and Rybak, 2008; Danner et al., 2015). Cortical involvement in control of the locomotor modules has been suggested based on discrepancy of the module activations in healthy adults from those in complete patients SCI (Danner et al., 2015) and toddlers (Dominici et al., 2011), who have injured and immature corticospinal system, respectively. However, there is no study showing evidences of the cortico-locomotor module relationships, which is observed from simultaneously recorded cortical activity and locomotor module activity. Moreover, if the cortex is involved in control of locomotor modules, it should be clarified which cortical information is involved in the module control for better understanding of the human locomotor system.

Recently, advances of brain decoding technic, which predict the mental or motor state of a human based on the recorded brain signals, have accelerated for development of brain–machine interfaces (BMIs), particularly as a means for repairing or assisting deficits in cognitive or sensory-motor functions (Patil and Turner, 2008; Lebedev and Nicolelis, 2017).

Regarding locomotor control, previous studies on humans performed decoding of the walking kinematics from the EEG signals (Presacco et al., 2010; 2011). Cortical processing for decoded behavior can be estimated based on contribution of cortical information to the decoding (Nicolelis, 2003). Therefore in this study, applying a brain decoding method, I examined the relationships between the cortical activity and the locomotor module activity. Assuming that the cortex controls multiple muscle activities through a few locomotor modules based on above mentioned indirect evidences (Clark et al., 2010; Dominici et al., 2011), I hypothesized the following working hypotheses: 1) activations of locomotor modules can be decoded from EEG signals, and 2) the decoding accuracy for locomotor modules is greater than that for locomotor muscle activity. The acceptance of the working hypotheses provides indirect evidences for the cortical involvement in control of locomotor modules. Additionally, I examined which cortical information is involved in control of locomotor modules based on the decoding model parameters.

5. 2. Methods

5. 2. 1. Participants

Thirteen healthy male volunteers (age, 22−31 years) participated in this study. Each participant gave written informed consent for his participation in the study. The experiments were performed in accordance with the Declaration of Helsinki and with the approval of the ethics committee of the National Rehabilitation Center for Persons with Disabilities (Tokorozawa, Japan).

5. 2. 2. Experimental setup and design

Participants walked on a treadmill (Bertec, USA) at 0.6 m/s in 7.5 minutes. The slow walking speed was chosen based on two previous studies examining effects of walking speed on movement artifacts of EEGs (Kline et al., 2015; Nathan and Contreras-Vidal, 2016). A study by

Kline et al. (2015), which used an experimental method to isolate and record independently movement artifact with silicone swim cap (nonconductive material), showed large movement artifact in walking speed faster than 0.8 m/s. Another study, which analyzed relationships between head acceleration and motion artifact of EEGs, indicated EEG recording is robust at gait speeds no faster than 3.0 km/h (0.83 m/s) (Nathan and Contreras-Vidal, 2016).

In addition to the walking task, as a static baseline condition, participants sit on a chair in 2 minutes.

5. 2. 3. Data collection

Three-dimensional GRF was recorded from force plates under the right and left belts of the treadmill (1000 Hz). GRF data was smoothed by a low-pass filter (a zero-lag Butterworth filter, 5-Hz cutoff). The timings of heel-contact (HC) and toe-off (TO) were determined based on the vertical component of GRF.

Surface EMGs were recorded from the following 15 leg and trunk muscles on the right side using a wireless EMG system (Trigno Wireless System, DelSys Inc., USA): TA, MG, SOL, PL, VL, VM, RF, BF, ST, AM, TFL, GM, Gmed, RA, ES. The EMGs were amplified (with 300 gain preamplifier), band-pass filtered (20–450 Hz) and sampled at 1000 Hz.

EEGs were recorded at sampling frequency of 1000 Hz and high pass filtered at 0.1 Hz using 31ch spike-shaped active dry electrodes (g.SAHARA, g.tec medical engineering GmbH, Austria) and a wireless EEG amplifier (Livo, Toyota Technical Development Corporation, Japan). The 31ch EEG electrodes were fixed to an EEG electrode cap (g.GAMMAcap, g.tec medical engineering GmbH, Austria) and gathered around the sensory motor area based on the international 10/5 System (Fig. 5-1, the montage) (Oostenveld and Praamstra, 2001), because cortical activity has been identified mainly in sensorimotor area during walking (Wagner et al., 2012; Bulea et al., 2015; Bradford et al., 2016) and cortico-muscular connectivity has been observed between the sensorimotor area and lower leg

muscles (Petersen et al., 2012; Artoni et al., 2017). The EEGs were referenced to the right mastoid, and the ground was placed on the left mastoid.

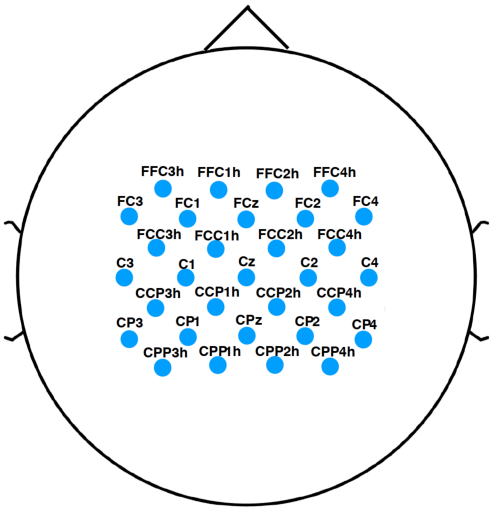

Figure 5-1. EEG electrode montage corresponding to the international 10/5 system (Oostenveld & Praamstra, 2001).

5. 2. 4. EMG processing and Extraction of Locomotor modules

Figure 5-2 shows an overview of my decoding methodology. From the recorded EMG signals, EMG envelopes and locomotor modules were used for the neural decoding analysis.

Firstly the recoded EMG data were high-pass filtered (zero-lag fourth-order Butterworth at 30 Hz), demeaned, full-wave rectified, and smoothed with a low-pass (zero-lag fourth-order Butterworth at 6-Hz cutoff) to obtain EMG envelopes (Walter et al., 2014). Then, the EMG envelopes were resampled at 200 Hz. The amplitude of EMG envelopes for each muscle was normalized to the maximum value for that muscle during the walking task. Then, locomotor modules were extracted from the processed EMG envelopes using the NMF as in Chapter 2 (see section 2.2.5. for details). In this study, locomotor modules were extracted from an EMG dataset organized as a matrix with 15 muscles × 90000 variables (i.e., 200 Hz × [7.5

min]) in each participant.

Then, I clustered the extracted locomotor modules using hierarchical clustering analysis (Ward's method) to examine types of extracted locomotor modules based on the muscle weightings, as in Chapter 2 (see section 2.2.5. for details). The time series activation of each EMG envelope and each locomotor module was then normalized, to produce a standard z-score by subtracting its average value and then dividing by its standard deviation.

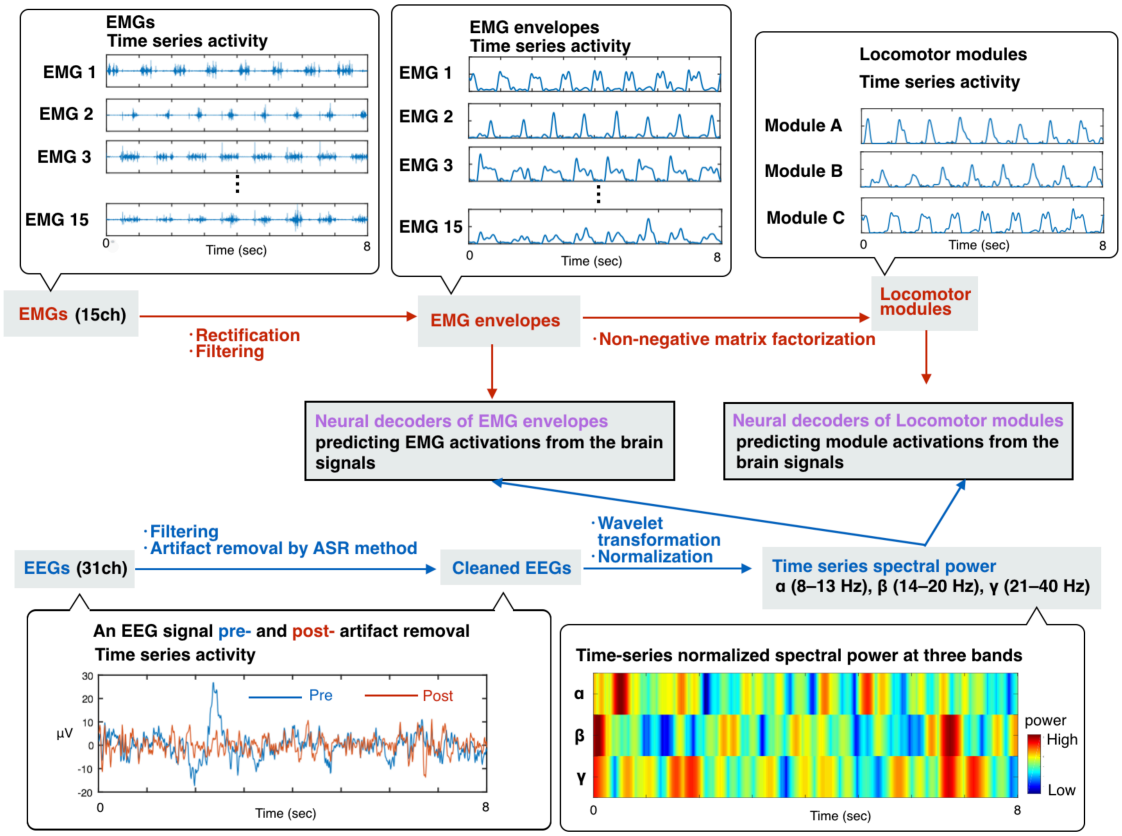

Figure 5-2. Schematic diagram depicting the neural decoding of EMG envelopes and locomotor module activations from simultaneously recorded EEG signals. Examples of simultaneous 8 seconds of raw EMG signals, EMG envelopes, locomotor modules, pre- and post-artifact removal EEG signal from an electrode, and spectral power of the electrode at three frequency bands (α, β and γ) are shown.

5. 2. 5. EEG pre-processing

In this study, from the recorded EEG signals, spectral powers in 3 different frequency bands (α: 8–13 Hz, β: 15–25 Hz, and γ: 30–40 Hz) were used for the neural decoding analysis (Fig. 5-2) as in the previous study by Chao et al. (2010). EEG data analysis was performed using custom-written programs in MATLAB 2016b (The MathWorks, Natick MA) incorporating functions of EEGLAB 14.1b (Delorme and Makeig, 2004). The EEG signals were high-pass filtered at 1 Hz by zero-phase FIR filter (order 7500), and low pass filtered at 200 Hz by zero-phase FIR filter (order 36) (Wagner et al., 2016). Power line noise (50 and 100Hz) was removed using the "cleanline" function in EEGLAB. The EEG data was resampled to 200Hz. Then, I checked noisy EEG channels based on following two criteria adopted from a previous study (Gwin et al., 2011) :1) standard deviation greater than 1000μV, and 2) kurtosis of more than 5 standard deviations from the mean. In this study, no EEG electrode satisfied the criteria in all participants. Then, the EEGs were re-referenced to a common average reference. Then, to remove artifact derived from walking movement, eye blinks, muscle and heart activity, I used an artifact rejection method named Artifact Subspace Reconstruction (ASR) (Mullen et al., 2013) in EEGLAB. Briefly, using a sliding window method, the ASR decomposes EEG data in each window by principal component analysis (PCA). Then, each decomposed components are compared statistically with data from a baseline data which have nominal-variance principal components (in this study, EEG data during sitting). In each sliding window, the principal components, which show significant higher variance, compared to the calibration data are identified as artifact components. The identified artifact components are removed and reconstructed based on the nominal-variance components.

5. 2. 6. EEG scalogram

Spectral power in 3−50 Hz (every 1 Hz) of EEG signals was estimated with Morlet wavelet ("newtimef" function in EEGLAB) at every time points (window size: 149 data points [745

ms]). The wavelet contained 2 cycles at the lowest frequency (3 Hz) and the number of cycles was increasing up to 16.7 cycles at highest frequency (50 Hz). To adjust the data length between the scalogram and the data to be decoded (EMG envelope and locomotor module data), 74 data points (370 ms) at both ends of the EMG envelope and locomotor module data were trimmed. The power of the scalogram was normalized by calculating the standard z-score at each frequency bin. Scalograms were then averaged in three frequency bands: α (8–13 Hz), β (15–25 Hz), and γ (30–40 Hz). That is, a scalogram consisted of 3 frequency bands × time points was calculated for each channel for each participant. Finally, the power of the scalogram were normalized by calculating the standard z-score at each frequency band. Namely the same scale was shared among different frequency band.

5. 2. 7. EEG Decoding of locomotor module and muscle activity

To continuously decode activations of EMG envelopes and muscle synergies from the scalogram, I designed a time-embedded (10 lags, corresponding to from -10 ms to -100 msec) linear decoding model for each EMG and locomotor module data (Carmena et al., 2003; Bradberry et al., 2010; Presacco et al., 2011). The linear model was given by:

$$y(t) = b + \sum_{ch} \sum_{freq} \sum_{lag} a_{ch,freq,lag} \cdot Scalogram_{ch,freq,lag}(t) + e(t), \qquad (5\text{-}1)$$

where $y(t)$ is predicted time series activations of each EMG envelope or locomotor module, b is the intercept, $Scalogram_{ch,freq,lag}(t)$ is the normalized spectral power at electrode *ch*, frequency band *freq*, and time lag *lag*. $a_{ch,freq,lag}$ is the weight for the scalogram component at electrode *ch*, frequency *freq*, and time lag *lag*, and $e(t)$ is the residual error. The parameters of the model were calculated by generalized linear regression using "glm" function in MATLAB (Gaussian distribution condition). Neural decoders were designed separately for each participant and each decoded parameter (i.e., each muscle and locomotor module).

To assess the predictive accuracy of each decoder, a seven-fold cross-validation procedure was performed. That is, the data recorded during the 7 min of the walking task were divided into 7 segments (1 min each). Six segments were used for training data, while the remaining 1 segment was used for testing the decoding model. This procedure was repeated for all the possible combinations (i.e., 7 times). I calculated correlation coefficient (r) between the real activation and the decoded activation at each decoder in each procedure. In addition, to compare overall decoding accuracy between two types of decoders (EMG envelope decoders and locomotor module decoders), overall correlation values in each decoder type were calculated as averaged correlation values across all decoders in each type of decoder separately par participants. To prevent the effect of skewness of sampling distributions in correlation coefficients, each individual correlation coefficient value was averaged after Fisher's Z-transformation (Corey et al., 1998). Then back-transformed to the scale of Pearson's r value.

5. 2. 8. Spatio-spectro-temporal contributions of cortical activity to the decoding

To assess the spatio-spectro-temporal contributions of cortical activity to predict muscle activity parameters, I calculated the following three different quantities from the weights of each decoding model ($a_{ch,freq,lag}$) according to a previous study (Chao et al., 2010):

$$W_s(ch) = \frac{\sum_{freq}\sum_{lag}|a_{ch,freq,lag}|}{\sum_{ch}\sum_{freq}\sum_{lag}|a_{ch,freq,lag}|}; \quad (5\text{-}2)$$

$$W_f(freq) = \frac{\sum_{ch}\sum_{lag}|a_{ch,freq,lag}|}{\sum_{ch}\sum_{freq}\sum_{lag}|a_{ch,freq,lag}|}; \quad (5\text{-}3)$$

$$W_t(lag) = \frac{\sum_{ch}\sum_{freq}|a_{ch,freq,lag}|}{\sum_{ch}\sum_{freq}\sum_{lag}|a_{ch,freq,lag}|}, \quad (5\text{-}4)$$

where $Ws(ch)$ is the percentage spatial contribution of each EEG electrode (ch) across all frequency bins and time lags, $W_f(freq)$ is the percentage spectral contribution of each frequency band ($freq$) across all EEG electrodes and time lags, and $W_t(lag)$ is the percentage temporal

contribution of each time lag (*lag*) across all EEG electrodes and frequency bands.

5. 2. 9. Statistics

The difference between overall correlation value (i.e., decoding accuracy) between two types of decoders (locomotor module decoder and EMG envelope decoder) was tested by a two-tailed paired t-test. For this significance testing, the correlation values were transformed into Z-values using Fisher's Z-transformation and t-test was conducted on the Fisher's Z-values.

Differences in contributions to the decoding among three frequency bands (α, β, and γ) were compared by one-way analysis of variance (ANOVA) test with Tukey's post hoc test separately in each decoder type. Contributions to the decoding in electrodes and time lags were compared to their median values with ANOVA followed by Dunnett's test separately in each decoder type. Statistical significance was accepted at $p < 0.05$.

5. 3. Results

5. 3. 1. Extracted locomtor modules

From the measured EMGs, 3.78 ± 0.60 (mean ± SD) locomotor modules were extracted from each participant. The extracted locomotor modules were grouped into five types by cluster analysis (module A−E, Fig. 5-3). Module A was activated at initial stance phase and throughout swing phase and mainly recruited the TA. Module B was activated at the last swing to early stance phase and mainly recruited the ST, and BF. Module C was activated at the transition timing from stance to swing and mainly recruited the ES and RA. Module D was activated at latter half of the stance phase and mainly recruited the MG, SOL, and PL. Module E was activated at mid stance phase and mainly recruited the TFL, Gmed, and GM.

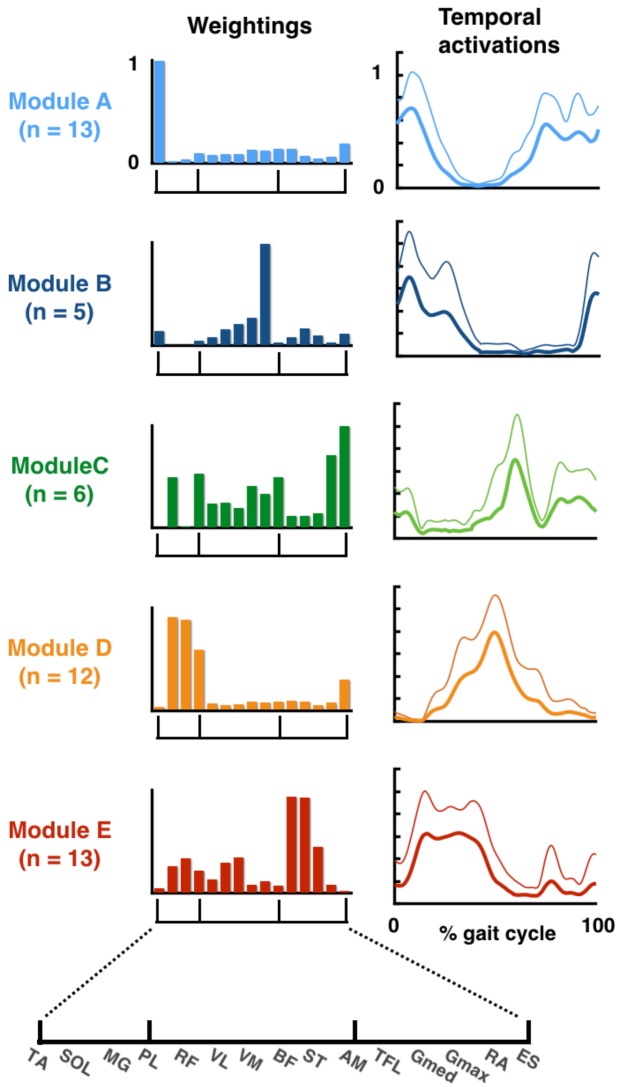

Figure 5-3. Extracted 5 types of locomotor modules. Average muscle weightings (bars) and correspoonding temporal activation patterns (waveforms) across participants in each type of locomotor module are shown. Each bar height represents the relative level of activation of each muscle within a muscle weighting component. An enlarged view of the x-axes is shown in the bottom. Lines indicate temporal activation patters of the locomotor modules. Thick lines indicate average temporal activation patterns, and thin lines indicate their standard deviations (SD).

5. 3. 2. Neural decoding of locomotor module activations and EMG envelopes from EEG signals

Figure 5-4 shows examples of the real and reconstructed locomotor module activations (Fig. 5-4a) and EMG envelopes (Fig. 5-4b), respectively, from a participant. In this participant, all locomotor module activations were well reconstructed (Fig. 5-4a). On the other hand, in each muscle activity level, amplitude modulation was not sufficiently reconstructed in some muscles, such as MG, BF and RA (Fig. 5-4b).

To quantify the decoding accuracy, I computed the Pearson's correlation coefficients (r) between the real and reconstructed activations. Figure 5-5 shows the decoding accuracy (correlation coefficients) for each locomotor module type and each muscle. The mean values across participants were ranged from 0.36 to 0.51 in locomotor module decoders and from 0.21 to 0.47 in EMG envelope decoders. The overall accuracy of the locomotor module decoder was higher than that of the EMG envelop decoder (p = 0.001, paired t-test, Fig. 5-6).

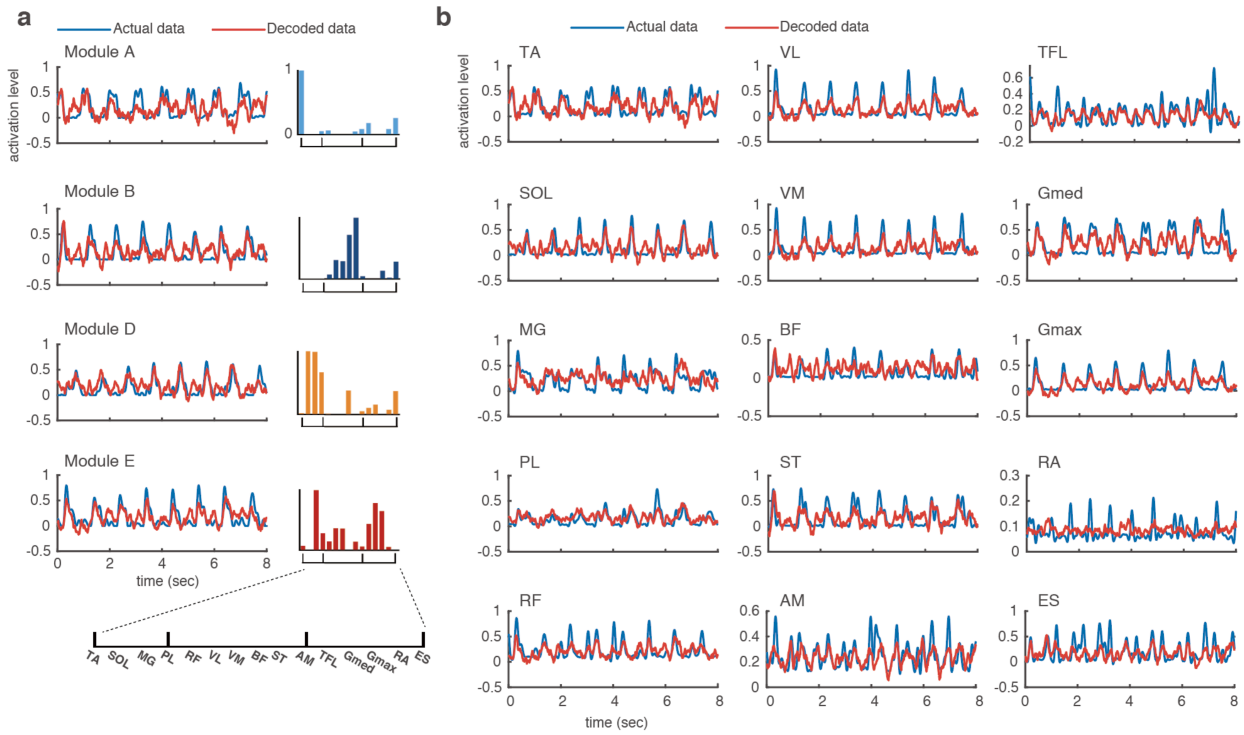

Figure 5-4. Examples of simultaneous 8 seconds of decoded and actual locomotor module activations (a), and EMG envelopes (b) from a participant. Red and blue waveforms indicate decoded and actual activation patterns, respectively. Bars represent the muscle weighting components.

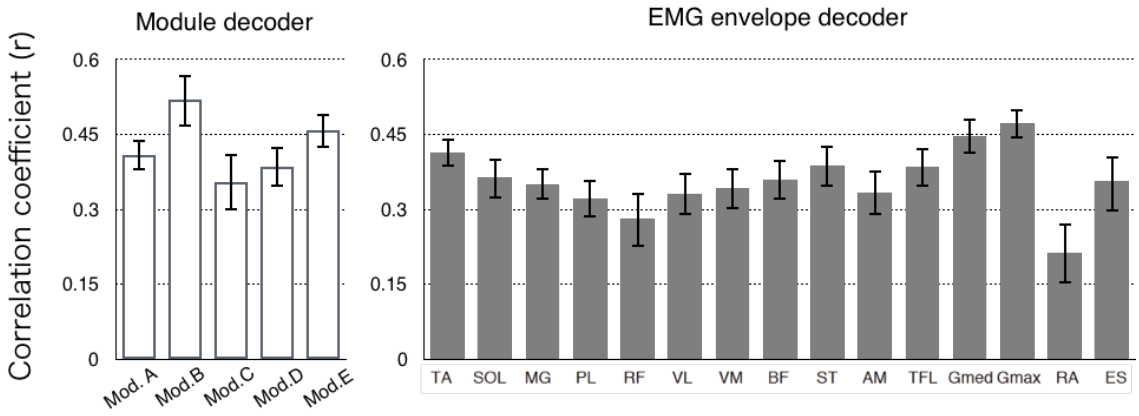

Figure 5-5. Decoding accuracy (correlation coefficient) for each of locomotor module type (left) and EMG envelope of individual muscle (right). The mean and standard error (SE) across participants are shown.

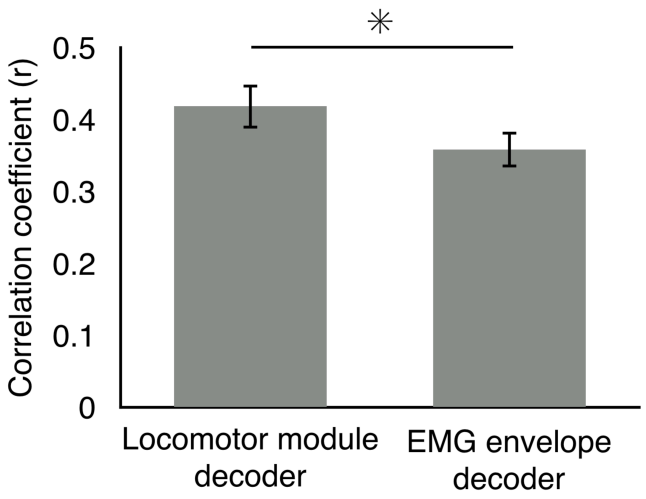

Figure 5-6. Overall decoding accuracy (correlation coefficients) for locomotor module decoders and EMG envelope decoders. The mean and SE across participants are shown. Asterisk indicate significant difference ($p < 0.05$)

5. 3. 3. Spatio-spectro-temporal Contributions of cortical activity to the decoding

Figure 5-7 indicates spatio-spectro-temporal contributions of the EEG signals to the decoding. Spatial contributions, *Ws(ch)*, were significantly greater at Cz and CCP1h (i.e., sensorimotor regions for right leg) than their median in both decoder types (ANOVA: $F_{31,384} = 2.73$, $p < 0.001$ in locomotor module decoder, $F_{31,384} = 2.83$, $p < 0.001$ in EMG envelop decoder; post hoc Dunnett's test: $p < 0.05$; Fig. 5-7a). Regarding spectral contributions, *Wf(freq),* that in α and β bands were significantly greater than that in γ band in both decoder types. (ANOVA: $F_{2,36} = 14.1$, $p < 0.001$ in locomotor module decoder, $F_{2,36} = 12.0$, $p < 0.001$ in EMG envelop decoder; post hoc Tukey's test: $p < 0.05$; Fig. 5-7b). As for temporal contributions, *Wt(lag)*, time lags from -40 to -70 ms from decoded activity (EMG envelope or locmotor module activity) were significantly greater than their median (ANOVA: $F_{10,132} = 143.2$, $p < 0.001$ in

locomotor module decoder, $F_{10,132} = 263.8$, $p < 0.001$ in EMG envelop decoder; post hoc Dunnett's test: $p < 0.05$; Fig. 5-7c)

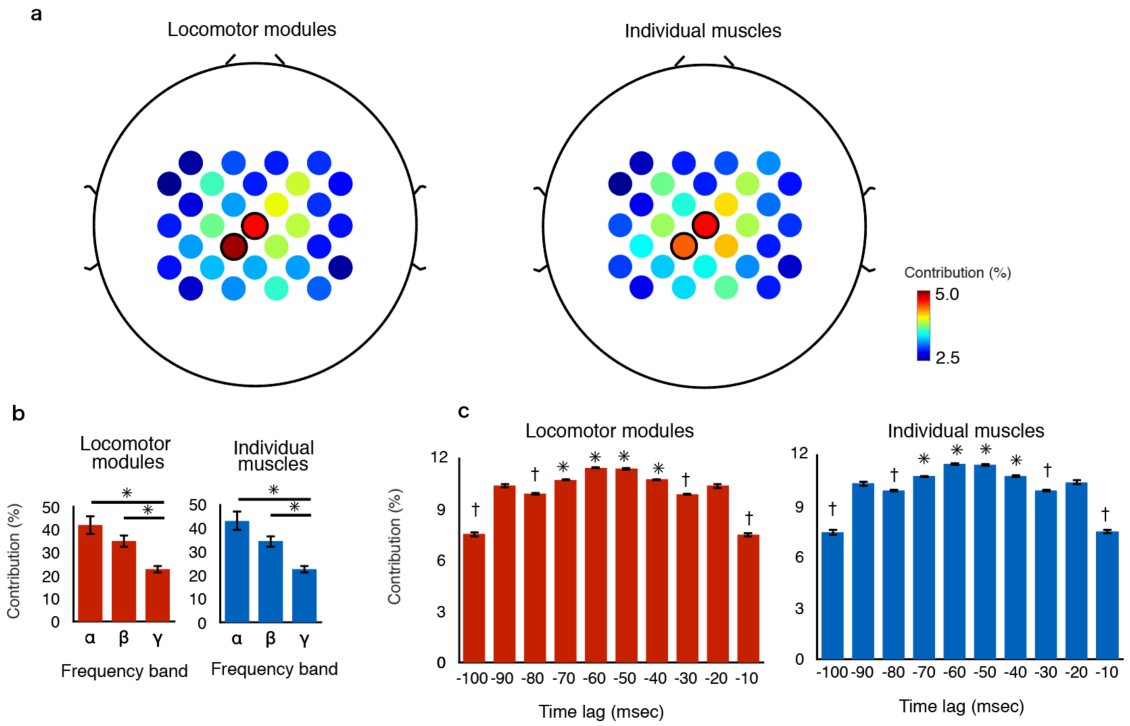

Figure 5-7. Characteristics of the decoding models for locomotor modules and EMG envelopes. (a) Contribution of each electrode. The electrodes with contributions significantly greater than their median ($p < 0.05$) are surrounded by lines. (b) Contributions of each frequency band. Asterisks indicate significant differences ($p < 0.05$). (c) Contribution of each time lag. The time lags with contributions significantly greater than their median ($p < 0.05$) are indicated by asterisks, while those significantly less than their median are indicated by daggers.

5. 4. Discussion

In this study, assuming that the cortex controls locomotor muscle activity through locomotor modules, I tested the following hypotheses using a neural decoding method: 1) activations of

locomotor modules can be decoded from EEG signals, and 2) its decoding accuracy is greater than that for locomotor muscle activity. As a result, locomotor module activations were decoded reasonably well from EEG signals (Fig. 5-5), and the accuracy of the synergy decoder was higher than that of the EMG decoder (Fig. 5-6). In addition, the decoding was mainly contributed by cortical information 40 to 70 ms ahead of the module or muscle activity on leg motor area in α and β bands (Fig. 5-7). These results confirmed my working hypotheses, and therefore suggest that the cortex is involved in control of locomotor modules mainly using the specific cortical information, which had large contribution to the decoding.

5. 4. 1. Cortical control of locomotor muscle activity through locomotor modules

The overall decoding accuracy for locomotor module decoders was greater than that for in EMG envelope decoders (Fig. 5-6). The result suggests cortical control of locomotor muscle activity through locomotor modules. Regarding cortical influences on locomotor module activation, a study on stroke patients demonstrated that the patients use fewer modules resulted from merging of the normal modules observed in healthy adults (Clark et al., 2010), suggesting that the cortex has a role for recruitment of the modules. Other evidences for the cortical control of locomotor modules have been obtained from comparisons of the module activations in healthy adults with those in complete patients SCI (Danner et al., 2015) and toddlers (Dominici et al., 2011), who have injured and immature corticospinal system, respectively. Healthy adults utilize four to five locomotor modules accurately timed around gait cycle events (Ivaneko et al., 2004; Neptune et al., 2009). Nevertheless, the modules extracted from toddlers (Dominici et al., 2011) and complete SCI patients with spinal epidural electrical stimulation (Danner et al., 2015) showed smooth sinusoidal-like activation patterns rather than sharply timed activations. These differences suggest that the cortical descending commands modulate the basic module activation patterns generated by the spinal cord into the sophisticated patterns for human bipedal walking. Thus, based on my results and previous studies, there is a high probability that

the cortex involves in control of locomotor modules in humans.

The decoded locomotor module activations have moderated correlation with the actual activations (Fig. 5-5). This moderate decoding accuracy would have been derived from motor module recruitment via multiple neural pathways, such as the brainstem, the spinal cord and sensory feedbacks (Chvatal et al., 2013; Saltiel et al., 2015; Ting et al., 2015), in addition to the cortex. Namely, although the cortex would be involved in the control of locomotor modules, the contribution may be not dominant. The partial contribution of the cortex in the control of locomotor module would explain the moderate decoding accuracy in this study. Other possible reasons for the not high decoding accuracy are low spatial resolution of EEG and signal contamination between control signals for the legs and upper limbs accompanying the spatial resolution issue.

5. 4. 2. Cortical information involved in the control of locomotor modules

Regarding spatial contribution, the Cz and CCP1h electrodes (i.e., sensorimotor regions for right leg) had large contribution to the decoding in both decoder types (Fig. 5-7a). Similar to the present results, a neural decoding study on non-human primate walking demonstrated that the leg kinematics and EMGs could be decoded from cortical signals from the leg area of the primary somatosensory (S1) and primary motor (M1) cortex (Fitzsimmons et al., 2009). In humans, significant corticomuscular coherence was observed between the leg sensorimotor regions and the TA during walking (Petersen et al., 2012). Although the motor cortex to muscle connectivity during walking has been reported as mentioned above, to my knowledge, the relationships between motor cortex and locomotor modules have been unclear in humans so far. Thus, the present results provide first experimental evidence suggesting that the leg sensorimotor area is involved in control of locomotor modules in humans.

Regarding the frequency domain, the contribution of α and β bands was larger than γ band (Fig. 5-7b). It has been known for a long time that movement related cortical activity in

the α and β bands, which are considered to be related to motor execution and preparation for voluntary movement (Chatrian et al., 1959; Salenius et al., 1997; Feige et al., 2000; Jurkiewicz et al., 2006). In the α and β band frequencies, many walking studies demonstrated spectral modulations depending on the gait cycle phases (Gwin et al., 2011; Chéron et al., 2012; Bradford et al., 2016; Oliveira et al., 2017). In addition, significant corticomuscular coherence in the α and β bands was observed between the leg sensorimotor regions and an ankle flexor muscle during walking (Petersen et al., 2012). Therefore, based on the evidences of sensorimotor related roles in α and β bands, it is possible that cortical activity in α and β bands contain much information regarding control of locomotor modules, and therefore they largely contributed to the decoding.

As for the temporal contribution, cortical information 40 to 70 ms ahead of muscle or module activity had the large contribution (Fig. 5-7c). The time lags were about the same or a little longer compared to latency time of motor evoked potentials (MEP) in leg muscles evoked by transcranial magnetic stimulation (about 35−40 ms), which reflect neural transmission time in the corticospinal tract to muscles (Nielsen et al., 1995; Terao et al., 2000). The difference between the major contributing time lags (40−70 ms) and the latency of MEP for leg muscles (about 35−40 ms) would be explained by involvement of indirect pathways from the cortex to spinal motoneurons through subcortical regions, such as the reticular formation and the basal ganglia, in addition to the direct corticospinal pathways, as suggested by Takakusaki et al. (2008).

5. 4. 3. Methodological considerations

Although the EEG is a suitable brain imaging method to examine brain activity during walking because of the high temporal resolution and the mobility, the potential issue of movement artifact must be noted. Recently, a study examined the gait-movement related artifacts in EEGs

by not allowing to record electrophysiological signals (brain, eye, heart and muscle activity) using a nonconductive layer (silicone swim cap) (Kline et al., 2015). They demonstrated that artifact signals were observed only in δ (0−3 Hz) and θ (4−7 Hz) bands in slower walking, however in the speed faster than 0.8 m/s, the movement artifact occurred up to around β band (−30 Hz). In addition, the artifact was smaller in the electrodes located in the central region (i.e., vertex) than in the peripheral regions, because the movement artifacts were caused by the vertical head acceleration. In the present study, I used EEGs in frequency upper than α band (8 Hz−), at slow walking speed (0.6 m/s), and from electrodes near the vertex for the decoding. Therefore, the movement artifact would not have had major impact to the results.

Additionally, I used a PCA-based artifact rejection algorithm (ASR) to remove the movement artifact, and other artifacts derived from muscle, heart and eye activity. The ASR removes high-variance artifact components from a dataset by comparison to a resting dataset (Mullen et al., 2013). This method has been utilized in studies recoding EEGs during walking to remove the artifacts, and its effectiveness has been demonstrated (Bulea et al., 2014; Nathan and Contreras-Vidal, 2016). Thus, I believe that my decoding results would have been derived not from movement artifact but from cortical signals.

5. 4. 4. Applications to Bran-Machine-Interfaces

The decoding methodology and results in this study could contribute development of more effective locomotor rehabilitation approaches for patients with neural disorders. Recently, brain-machine Interface (BMI) systems, which control stimulators that activate their own muscles through functional electrical stimulation (FES) based on cortical signals, have been used to allow patients for restoring their impaired movement (Bouton et al., 2016). FES is a clinical technique which electrically stimulate patients' muscles to generate functional muscle contractions (Peckham, 1987). As a new stimulation pattern of FES, the effectiveness of a motor module based stimulation pattern has been suggested in upper limb reaching (Muceli et

al., 2010) and locomotion (Alibeji et al., 2015). The present results showed that EEGs contain information about control of locomotor modules, thus providing fundamental information for effective neuroprostheses systems based on a novel concept (e.g., BMI-FES with motor module-based stimulation patterns) to restore locomotion.

5. 4. 5. Conclusions

I found that locomotor module activations was decoded reasonably well from EEG signals, and its decoding accuracy was greater than that for EMG envelope. Additionally, the decoding was mainly contributed by cortical information 40 to 70 ms ahead of the module or muscle activity on leg motor area in α and β bands. These data suggest that the cortex would control activity of multiple muscles through a few locomotor modules mainly using the specific cortical information. The novel knowledge in this study advances our understanding of neural control of human bipedal locomotion. Additionally, the results demonstrate the feasibility of neural decoding of locomotor module activity, suggesting its future contribution to the development of effective brain-muscle neuroprostheses for restoring walking.

Chapter 6 study 5

Strengthening of causal connectivity from the cortex to muscles during voluntary gait modification in humans

6. 1. Introduction

Walking behavior is a very complicated movement which needs coordinated activity of multiple muscles and its modification to fit changes in walking condition. Modification of the walking movement requires accurate control during the execution and proper motor planning to quickly modify one's gait movement fitting the situation (Drew and Marigold, 2015).

It has been established that the cortex has crucial roles for achieving the gait modification by studies in cat locomotion (Liddell and Phillips, 1944; Beloozerova and Sirota, 1988; Drew et al., 1996; Drew et al., 2002; Drew et al., 2008; Krouchev and Drew, 2013; Roemmich et al., 2016). Lesion studies demonstrated that, although cats with damage of the motor cortex can still perform stereotyped walking without any particular problem, they have critical difficulty in performing more challenging walking, such as beam or ladder walking (Liddell and Phillips, 1944; Jiang and Drew, 1996; Drew et al., 2002). Additionally, increased activity of the motor cortex neurons during skilled walking tasks was demonstrated by studies utilizing single-unit recordings (Drew, 1988; Amos et al., 1990; Drew, 1993; Roemmich et al., 2016). The motor cortex is considered to mainly contribute to the execution of the walking modifications rather than its motor planning, because activity of the motor cortex neurons is increased only in the short term during the modification of limb movement (Drew et al., 2008). Moreover, analysis of temporal activation patterns of muscle activity and motor cortical unit activity demonstrated their temporal synchronization during skilled walking, suggesting that the motor cortex would be involved in modification of the timing and amplitude of locomotor muscle activity (Drew et al., 2008).

Regarding cortical activity during gait modification in humans, an EEG study showed large event-related potential in the prefrontal cortex when stepping over obstacles during walking compared to steady state walking (Haefeli et al., 2011). Another EEG study using a cued walking task, which require adjustment of step timing to auditory cue, showed two distinct β band oscillatory cortical networks: decreased β-band power in the parietal and

sensorimotor regions and increased β-band power in the prefrontal cortex (Wagner et al. 2016). These previous studies strongly suggested that the cortical activity significantly involved in walking modification in humans. However, it is still unclear whether and how the cortical activity during walking modification contributes to adjustments of locomotor muscle activity.

Up to now, corticomuscular connectivity during walking has been examined only in steady state walking in humans (Petersen et al., 2012; Artoni et al., 2017). Significant coherence was found in β band frequency between EEG signals of leg motor area and the EMG signals from the TA muscle prior to heel contact (Petersen et al., 2012). Most recent study demonstrated causal connectivity from motor cortex to leg muscle during walking (Artoni et al., 2017). It has been suggested that large parts of corticospinal system for walking control are shared between humans and cats based on fundamentally anatomical and physiological commonality of the corticospinal motor tracts (Drew et al., 2002). Based on this view, assuming that the cortical activity during skilled walking contributes to modification of muscle activity as observed in cat studies (Drew et al., 2008), I established the following working hypothesis: The causal connectivity from the cortex to muscle is enhanced during skilled walking task compared with that during steady state walking. The acceptance of this working hypothesis would provide indirect evidence that cortical activity during skilled walking is involved in the precise lower limb control by modifying muscle activity in humans. It also suggests that strength of cortical to the muscle connectivity is linked to degree of voluntary effort and complexness of the walking behavior.

6. 2. Methods

6. 2. 1. Participants

Thirteen healthy male volunteers (age, 22−30 years) participated in this study. Each participant gave written informed consent for his participation in this study. The experiments were performed in accordance with the Declaration of Helsinki and with the approval of the ethics

committee of the University of Tokyo.

6. 2. 2. Experimental setup and design

The participants performed following two different walking tasks on a treadmill (Bertec, Columbus, OH, USA): 1) normal walking at 0.6 m/s and 2) precision stepping at 0.6 m/s that forced the participants to step on pre-specified positions on the treadmill. Each task duration was 7 minutes.

Figure 6-1 illustrates the experimental setup for the precision stepping task. An ultra short throw LED projector (PH450UG, LG Electronics, Korea), that can project from oblique angles, was placed beside the treadmill, and it presented "stepping bars" (length × width: 15 × 5 cm) specifying the stepping positions. The participants asked to adjust their heel position to center of the stepping bar. During all tasks, a projection board (1.2 m) with the similar appearance to the treadmill surface was attached to the front of the treadmill. This procedure was adopted from Koenraadt et al. (2014). Step length and step width was randomly varied based on 5 and 3 predetermined positions in the anteroposterior and mediolateral directions, respectively. The positions in the anteroposterior direction were defined based on the step length of each participant that was premeasured in a 1-minute treadmill walking task before the precision stepping task. The anteroposterior position was randomly adjusted to −30%, −15%, −0%, +15% or +30% of the individual step length. Position of the stepping bars in the mediolateral direction was defined based on a average step width in humans, approximately 30 cm, demonstrated in previous walking study (Donelan and Kram, 2001). The distance between two consecutive bars in the frontal plane was randomly set to 15, 30 and 45 cm for every step. Once a stepping bar was projected on the projection board, the bars moved synchronized to the belts.

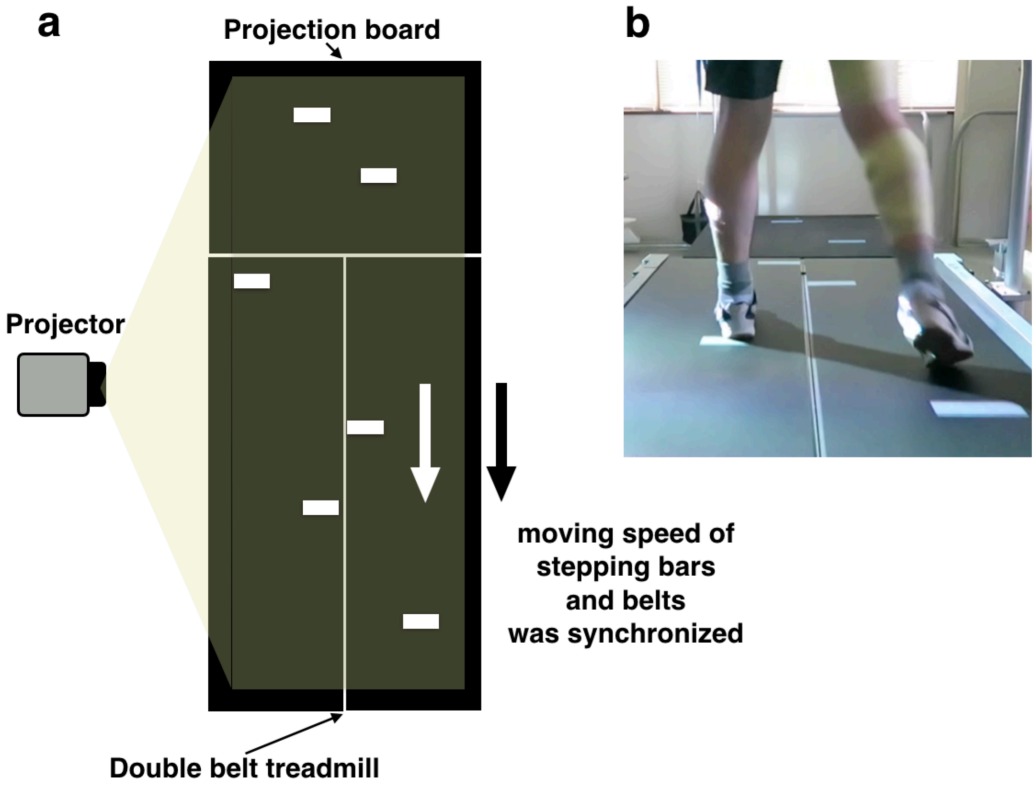

Figure 6-1. (a) Experimental setup for a precision stepping task. (b) An example of experiment view. Participant asked to step on the bar from the heel.

6. 2. 3. Data collection

Three-dimensional ground reaction forces (GRF) of left and right legs were separately measured from two force plates under the right and left belts of the treadmill (1000 Hz). The GRF data was smoothed by a low-pass filter (5-Hz cutoff, a zero-lag Butterworth filter, 4th order). The heel-contact (HC) and toe-off (TO) timings were detected based on the vertical component of GRF.

Surface EMGs were recorded from the following 12 muscles on the right leg using a wireless electrode system (Trigno Wireless System, DelSys Inc., USA): Gmed, GM, SART, BF, ST, RF, VL, AM, TA, PL, SOL, and MG. The EMG data was sampled at 1000 Hz. The recorded EMG data were demeaned, and then digitally full-wave rectified. The EMG data were

then resampled to 500 Hz.

EEG signals were recorded using a portable EEG system (eego Sports system, ANT Neuro, Enschede, Netherlands) with 63 Ag/AgCl electrodes mounted in a cap according to the international 10/10 system (waveguard cap, ANT Neuro, Netherlands). The reference electrode was placed on CPz, and the ground electrode was AFz. The electrode impedances were kept lower than 20 kΩ, which was substantially lower than the recommended impedance for the EEG system (50 kΩ). The EEG signals were sampled at 500 Hz.

6. 2. 4. EEG analysis

6. 2. 4. 1. Preprocessing

Analysis of EEG data was performed using custom-written programs in MATLAB 2016b (The MathWorks, Natick MA) with functions of EEGLAB 14.1b (Delorme and Makeig, 2004). The signal processing methodology for causal connectivity analysis between the cortex and muscles is shown in Fig. 6-2. The recorded EEGs were high-pass filtered (1 Hz cutoff, zero-phase FIR filter, order 7500), and then low pass filtered (200 Hz cutoff, zero-phase FIR filter, order 36) (Wagner et al., 2016). AC power line noise (50 and 100Hz) was eliminated using the "cleanline" function in EEGLAB. The EEG data were then resampled to 200Hz. Then, I checked noisy EEG channels based on following two criteria adopted from a previous study (Gwin et al., 2011) :1) standard deviation greater than 1000μV, and 2) kurtosis of more than 5 standard deviations from the mean. In this study, no EEG electrode satisfied the criteria in all participants. Then, the EEG data were divided into epochs of interest of 800 ms prior and after foot contact of right leg (i.e., an epoch period: 1.6 s). Outlier Epochs were excluded based on the probability distribution of the values over the epochs (mean ±5 SD) (Wagner et al., 2012).

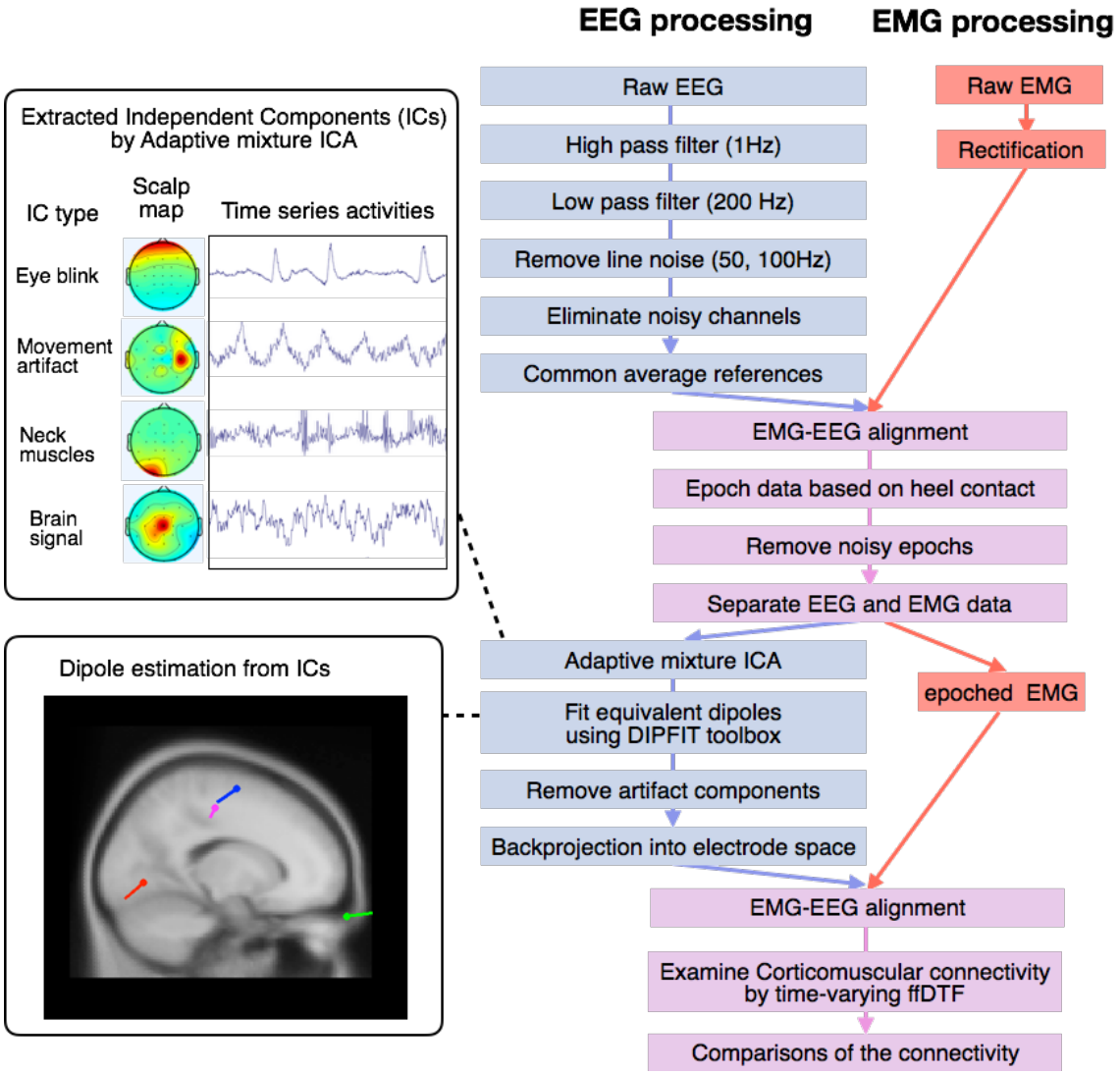

Figure 6-2. Flow-chart indicating the EEG and EMG processing pipeline for corticomuscular connectivity analysis during walking.

6. 2. 4. 2. Removal of non-brain artifact by adaptive mixture ICA and dipole fitting

Then, to identify non-brain source artifacts mixing in the EEGs, the pre-processed EEG data were decomposed using adaptive mixture independent component analysis (AMICA) (Palmer et al., 2006; Palmer et al., 2008). AMICA is a generalization method of the Infomax ICA (Bell and Sejnowski, 1995; Makeig et al., 1996) and multiple-mixture ICA (Lee et al.,

1999; Lewicki and Sejnowski, 2006) to separate EEG data into independent components (ICs) assumed to be spatially static and maximally temporally independent (Palmer et al., 2006, 2008). It has been demonstrated that AMICA is a most effective method to reduce mutual information between components (sources) among many blind source separation methods (Delorme et al., 2012). I performed one AMICA analysis for each participant over both normal walking and precision stepping tasks.

Next, using a standardized three-shell boundary element head model in the DIPFIT toolbox in EEGLAB, the position of a best-fitting single equivalent current dipole was calculated for the scalp projection of each ICs (Oostenveld and Oostendorp, 2002; Delorme et al., 2012; Wagner et al., 2012). The EEG electrode placements were aligned to fit a standard brain model (MNI model). For subsequent analyses, I retained only ICs if the corresponding dipoles were positioned in the head (Wagner et al., 2012; Wagner et al., 2016) and explained at least 80% of variance of their scalp projection (Bulea et al., 2015).

Then, additional artifacts ICs were identified from the remaining ICs based on visual inspection of the scalp maps, time series activity, and power spectrum according to the characteristics of artifact components reported in previous studies (eye and muscle artifact [Jung et al., 2000], walking related movement artifact [Castermans et al., 2014; Kline et al., 2015]). Finally, the identified artifact ICs were removed, and remaining ICs were projected back onto the original scalp channel space.

6. 2. 5. Directed Transfer Function Analysis between EEG and EMG

To investigate causal connectivity (i.e., directional information flow) between EEG and EMG signals, I applied the Directed Transfer Function (DTF), which is a frequency-domain estimator of causal interaction utilizing a multivariate autoregressive (MVAR) model. Signals from a leg sensorimotor EEG electrode (Cz), a non-motor area EEG electrode (AF5), and 12 EMGs from leg muscles were used for the connectivity analysis.

The MVAR model is expressed as:

$$X(t) = \sum_{i=1}^{m} A(i)X(t-i) + E(t), \quad (6\text{-}1)$$

where $X(t)$ is a multidimensional vector of k source signals (2 EEG and 12 EMG signals) at time t, $E(t)$ is a vector of multivariate zero-mean uncorrelated white noise process, $A(i)$ is the $k \times k$ matrix of model coefficients, and m is the model order. The model order was determined based on Akaike's information criterion (AIC).

To examine the frequency domain connectivity between the signals, the MVAR model was transformed into frequency domain based on z-transformation. The transformed model is expressed as:

$$X(f) = A^{-1}(f)E(f) = H(f)E(f), \quad (6\text{-}2)$$

where $H(f)$ is the inverse of the frequency-transformed coefficient matrix ($A(f)$) and is called a transfer matrix of the system, f denotes frequency. From the $H(f)$, the DTF, which quantify interrelations between two signals in relation to all other signals of the analyzed system, can be given by (Kaminski and Blinowska, 1991):

$$\chi_{ij}^2(f) = \frac{|H_{ij}(f)|^2}{\sum_{k=1}^{n}|H_{ik}(f)|^2}, \quad (6\text{-}3)$$

where n is the number of signals. The DTF Values, $\chi^2_{ij}(f)$ (describing information flow from j to i), close to 1 indicate that most of the signal i consists of signal j, while values of DTF close to 0 show that there was no flow from signal j to signal i at a certain frequency. The definition of the DTF as a ratio of transmitted activity is related to its spectral properties. Namely, the DTF values depend on the denominator (formula (6-3)), which specifies inflows to a signal at a certain frequency and varies among frequencies. Therefore, it is difficult to compare the connectivity strength across different frequencies from the DTF values. To overcome the problem, an updated version of the DTF, the full frequency DTF (ffDTF) was proposed

(Korzeniewska et al., 2003). It can be given by:

$$\eta_{ij}^2(f) = \frac{\left|H_{ij}(f)\right|^2}{\sum_f \sum_{k=1}^{n} |H_{ik}(f)|^2}, \quad (6\text{-}4)$$

where n is the number of signals. The ffDTF, η^2_{ij} (f), quantifies the directed causality from signal j to signal i. Since the inflow to signal i was summed across all frequency (1–50 Hz, in this study) in the denominator, the denominator were same among different frequencies. Therefore, ffDTF can evaluate outflow from given signal not depend on the frequency.

Although the ffDFT estimation with MVAR modeling assumes stationarity of the signals, the EEG and EMG activity change dynamically within a gait cycle (i.e., highly non-stationery signals). In the present study, to adapt the nonstationality, the ffDTF was calculated by using a segmentation based (sliding-window) MVAR model (i.e., time-varying ffDTF). Figure 6-3 shows the schematic representation of the time-varying ffDTF with a sliding-window MVAR model. To obtain sufficient data samples for precisely estimating the MVAR model, the analysis utilize multiple epoch data in a same segment timing for calculating the model. In this study, I used 400 ms time window with 5 ms step size. The time-varying ffDTF was computed using SIFT toolbox in EEGLAB (Delorme et al., 2011; Mullen, 2014).

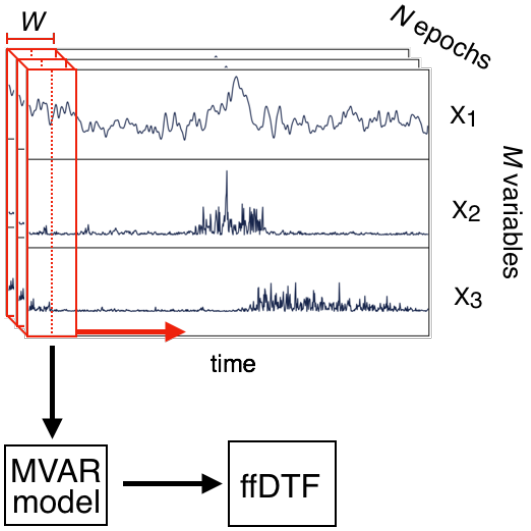

Figure 6-3. Schematic representation of calculation of time-varying ffDTF with sliding window MVAR modeling. *W* is the window length, *N* is the number of epoch, *M* is the number of sources (EEG and EMG signals).

6. 2. 6. Comparisons of corticomuscular connectivity

Statistical significance of causal connectivity (ffDTF value) was evaluated by a non-parametric bootstrapping method using the SIFT toolbox (Delorme et al., 2011). I tested the significance in four types of the connectivity (i.e., motor cortex (Cz)→muscle, muscle→motor cortex, non-motor cortex (AF5)→muscle, and muscle→non-motor cortex) in two walking tasks separately (normal walking and precision stepping).

Then, I examined differences in the connectivity strength between motor cortex→ muscle connectivity and non-motor cortex→muscle connectivity, because any significant connectivity was not observed in muscle→cortex connectivity in all participants (see Results section, for detail). To examine overall directional corticomuscular connectivity across muscles, the peak ffDTF values over frequency and time were averaged across muscles in each participant per connectivity type. Then, the averaged connectivity strength was compared

between the two connectivity types by paired t-test.

As a result, motor cortex→muscle connectivity was stronger than non-motor cortex →muscle connectivity (see Results section, for detail). Thus, subsequent analyses were performed only on the motor cortex→muscle connectivity. To quantify the differences depending on the two walking tasks (normal walking and precision stepping), peak ffDTF values in each three frequency bands (α [8-12 Hz], β [15-25 Hz], γ [30-40 Hz]) were calculated in each muscle. The peak values were separately calculated in two different walking phases (before heel contact [from 600 ms before heel contact to heel contact] and after heel contact [from heel contact to 600 ms after heel contact]). Then, to compare overall trend of connectivity across muscles between two walking tasks, the peak values were averaged across muscles, and the averaged values were compared between two walking tasks by paired t-test. Then, each peak value at individual muscle was compared between two walking tasks by paired t-test.

6. 3. Results

6. 3. 1. Comparisons of directional connectivity strength among different connectivity types

Order of the MVAR model (i.e., *m* in the equation 6-1) was 23.5±2.6 (mean±SD) and 23.9± 2.9 in normal walking and precision stepping conditions, respectively. Since the sampling rate was 500 Hz, the MVAR model predicted future parameters based on past parameters from approximately 40-50 msec before in many cases.

Figure 6-4 shows examples of directional corticomuscular connectivity during normal walking and precision stepping from a typical participant. Significant connectivity was observed in motor cortex→muscle and non-motor cortex→muscle connectivity, while not in muscle→motor cortex and muscle→non-motor cortex connectivity. This difference in significance among the connectivity types was same in all participants. In addition, based on

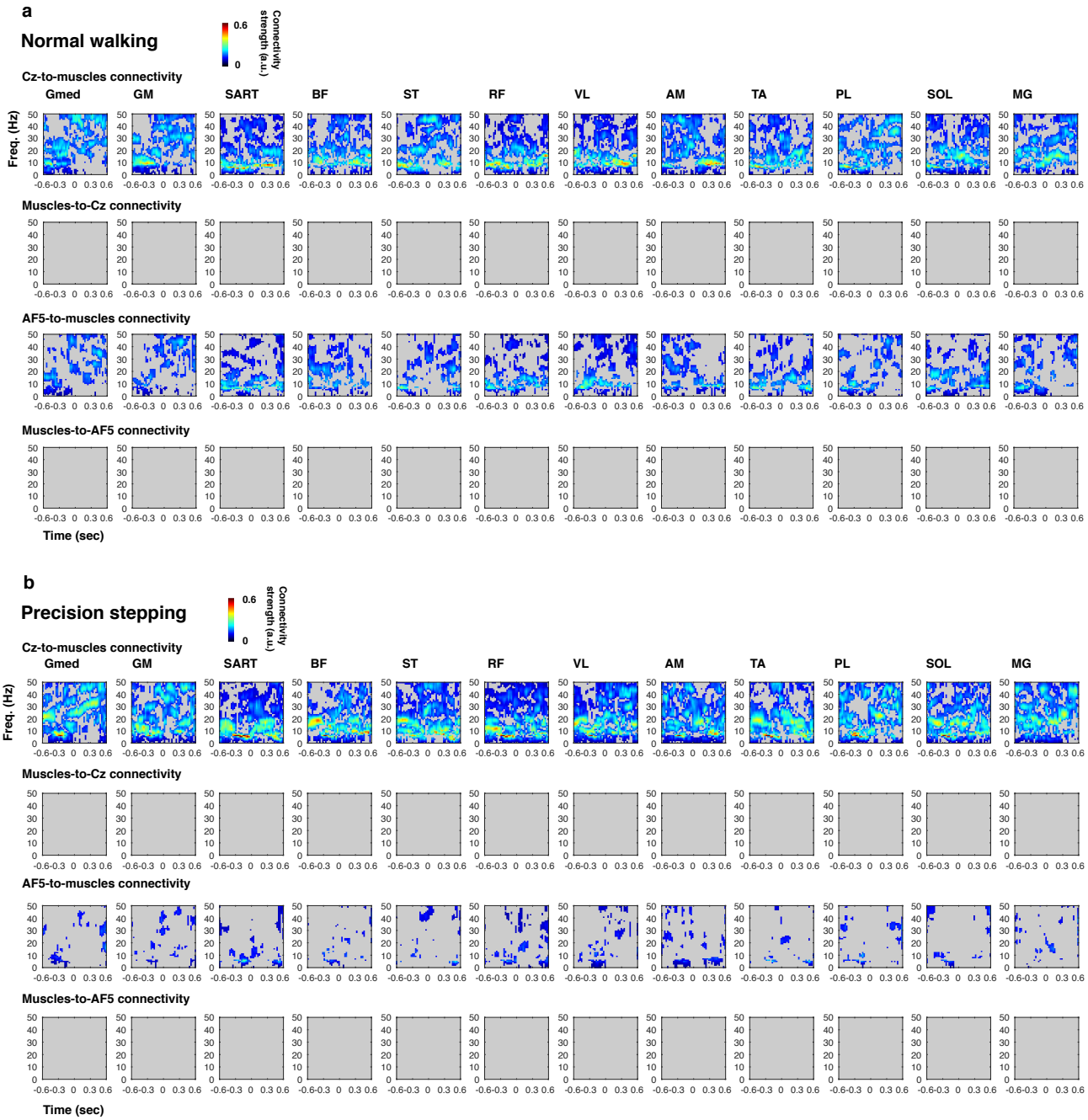

Figure 6-4. Examples of directional corticomuscular connectivity during normal walking and precision stepping from a participant. The following four types of connectivity values of 12 leg muscles are presented: motor cortex (Cz)→muscle (first row), muscle→motor cortex (second row), non-motor cortex (AF5)→muscle (third row), and muscle→non-motor cortex (fourth row). Time 0 means heel contact timing. Non-significant connectivity are masked in gray

visual inspection, the motor cortex→muscle connectivity showed larger strength in frequency higher than approximately 8 Hz in all muscles in both walking tasks compared to the non-motor

cortex→muscle connectivity. The larger connectivity strength of the motor cortex→muscle connectivity than non-motor cortex→muscle connectivity was statistically confirmed by comparing the averaged peak connectivity over the muscles between the two connectivety types (Fig. 6-5, $p < 0.001$ for both tasks).

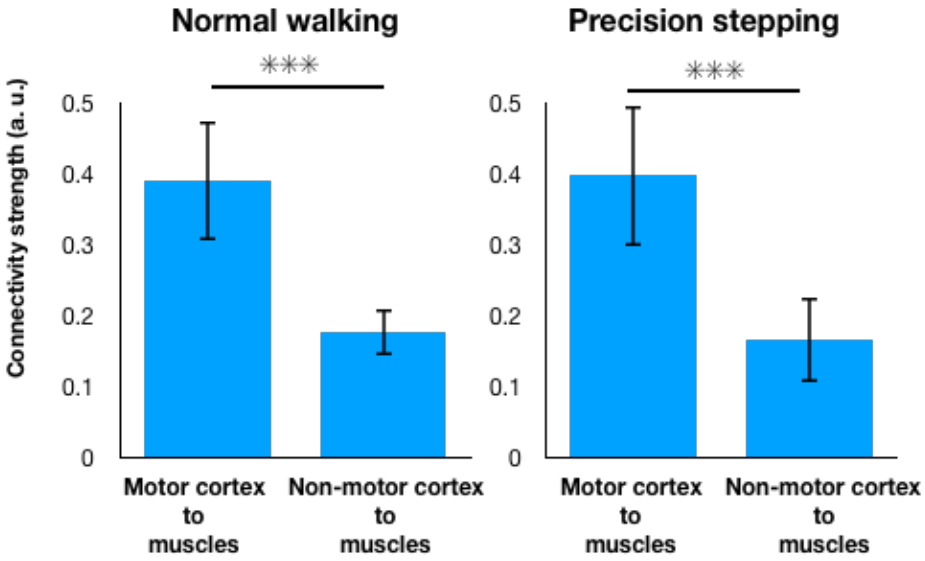

Figure 6-5. Comparisons between two connectivity types (motor cortex (Cz)→muscle and non-motor cortex (AF5)→muscle) of averaged peak connectivity values over muscles in normal walking and precision stepping tasks. ∗∗∗: $p < 0.001$.

6. 3. 2. Comparisons in strength of motor cortex to muscle connectivity between normal walking and precision stepping

Then, I examined the differences of the motor cortex→muscle connectivity between normal walking and precision stepping tasks. Figure 6-6 shows averaged time-frequency representations of motor cortex→muscle connectivity in normal walking and precision stepping

and the differences. Based on visual inspection, it seems that, although smaller connectivity during precision stepping was observed in a few muscles in specific frequency bands (γ band connectivity in the TA and PL and α band connectivity in the SOL), the connectivity strength during precision stepping were generally larger than that during normal walking, especially in β band connectivity. Differences in the averaged connectivity strength over muscles between normal walking and precision stepping in three frequency bands (α, β and γ) in two gait phases (before heel contact and after heel contact) are shown in Figure 6-7. The connectivity in β band before heel contact in precision stepping task was significantly larger than normal walking, while there is no significant difference in other comparisons (Fig. 6-7).

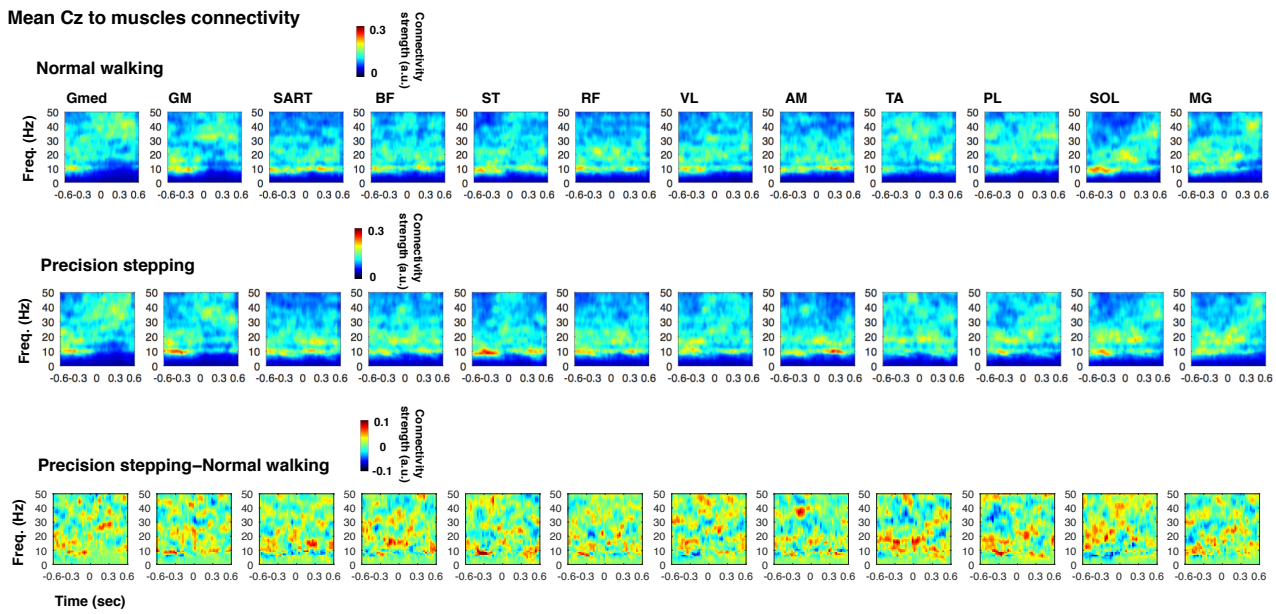

Figure 6-6. Mean unidirectional motor cortex (Cz) to muscle connectivity across participants in normal walking (upper row), precision stepping (middle row) and the differences (precision stepping-normal walking, bottom row). Time 0 means heel contact timing.

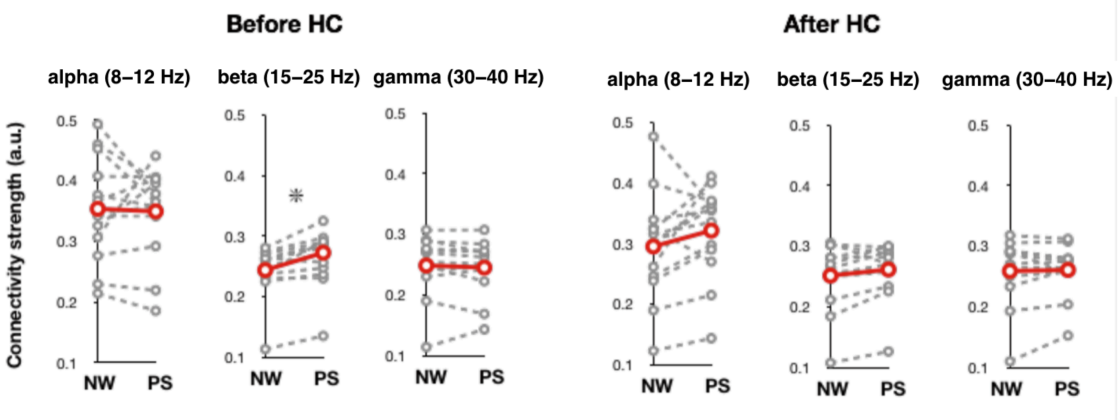

Figure 6-7. Comparisons of averaged connectivity strength over muscles between normal walking (NW) and precision stepping (PS). The values were separately compared in three frequency bands (α、β and γ) in two gait phases (before heel contact (HC) and after HC). Gray dot lines indicate individual data. Red lines indicate mean data across participants. ∗: $p < 0.05$.

Table 6-1 shows statistical results of comparisons of the connectivity strength of individual muscles between normal walking and precision stepping in each frequency band and gait phase. The muscles, which showed the significant differences, are presented in Fig. 6-8. More muscles showed significant changes of the connectivity between the two tasks before heel contact (6 muscles at 3 frequency bands) than after heel contact (2 muscles at 1 frequency band). Specifically, in before heel contact phase, the connectivity increased in many muscles (TA, Gmed, VL, AM, and PL) in β band during precision stepping, while it decreased in VL and SOL in α band, and in TA and PL in γ band. Regarding after-heel contact phase, the connectivity increased in Gmax and ST in α band.

Table 6-1. Comparisons between normal walking (NW) and precision stepping (PS) of motor cortex-to-muscle connectivity in three frequency bands in two gait phases. The *p* values smaller than 0.05 are highlighted in red.

	Before heel contact								
	α (8–12 Hz)			β (15–25 Hz)			γ (30–40Hz)		
	NW	PS	*p (NW vs. PS)*	NW	PS	*p (NW vs. PS)*	NW	PS	*p (NW vs. PS)*
Gmed	0.34(0.13)	0.33(0.096)	0.98	0.23(0.057)	0.27(0.051)	0.030	0.26(0.055)	0.25(0.051)	0.33
Gmax	0.39(0.11)	0.39(0.11)	0.78	0.25(0.048)	0.26(0.062)	0.22	0.26(0.063)	0.24(0.039)	0.24
SART	0.33(0.1)	0.36(0.1)	0.27	0.23(0.05)	0.25(0.075)	0.21	0.24(0.063)	0.22(0.063)	0.17
BF	0.38(0.14)	0.32(0.095)	0.09	0.25(0.061)	0.27(0.068)	0.22	0.24(0.054)	0.27(0.059)	0.0
ST	0.4(0.15)	0.43(0.13)	0.41	0.25(0.056)	0.25(0.068)	0.54	0.24(0.052)	0.25(0.046)	0.36
RF	0.31(0.076)	0.34(0.093)	0.28	0.26(0.062)	0.25(0.053)	0.35	0.23(0.058)	0.23(0.057)	0.81
VL	0.4(0.14)	0.33(0.1)	0.023	0.24(0.058)	0.26(0.054)	0.017	0.24(0.053)	0.25(0.055)	0.59
AM	0.36(0.099)	0.37(0.11)	0.99	0.23(0.052)	0.27(0.051)	0.011	0.23(0.061)	0.23(0.061)	0.87
TA	0.3(0.11)	0.28(0.076)	0.55	0.22(0.061)	0.27(0.055)	0.0098	0.29(0.059)	0.25(0.06)	0.0030
PL	0.29(0.13)	0.33(0.11)	0.18	0.24(0.057)	0.27(0.051)	0.028	0.27(0.068)	0.25(0.056)	0.033
SOL	0.42(0.093)	0.35(0.11)	0.015	0.28(0.065)	0.27(0.055)	0.54	0.23(0.065)	0.24(0.052)	0.27
MG	0.33(0.13)	0.35(0.12)	0.71	0.25(0.072)	0.26(0.057)	0.62	0.26(0.061)	0.26(0.065)	0.85

	After heel contact								
	α (8–12 Hz)			β (15–25 Hz)			γ (30–40Hz)		
	NW	PS	*p (NW vs. PS)*	NW	PS	*p (NW vs. PS)*	NW	PS	*p (NW vs. PS)*
Gmed	0.19(0.15)	0.2(0.11)	0.79	0.24(0.07)	0.23(0.073)	0.47	0.29(0.06)	0.3(0.046)	0.62
Gmax	0.2(0.1)	0.25(0.11)	0.018	0.21(0.067)	0.23(0.068)	0.19	0.28(0.067)	0.29(0.05)	0.63
SART	0.36(0.13)	0.37(0.1)	0.89	0.25(0.064)	0.26(0.068)	0.17	0.23(0.072)	0.22(0.048)	0.10
BF	0.34(0.14)	0.34(0.14)	0.79	0.27(0.063)	0.28(0.06)	0.72	0.25(0.06)	0.25(0.057)	0.76
ST	0.33(0.13)	0.4(0.14)	0.016	0.26(0.074)	0.24(0.05)	0.51	0.24(0.059)	0.24(0.061)	0.84
RF	0.33(0.093)	0.37(0.13)	0.18	0.26(0.063)	0.27(0.062)	0.34	0.23(0.067)	0.25(0.048)	0.40
VL	0.27(0.14)	0.33(0.13)	0.093	0.23(0.063)	0.26(0.059)	0.25	0.26(0.079)	0.26(0.057)	0.76
AM	0.37(0.15)	0.42(0.14)	0.29	0.24(0.055)	0.27(0.052)	0.084	0.23(0.069)	0.23(0.045)	0.79
TA	0.28(0.1)	0.29(0.075)	0.90	0.26(0.074)	0.28(0.064)	0.38	0.26(0.053)	0.27(0.044)	0.93
PL	0.27(0.13)	0.27(0.12)	0.93	0.26(0.087)	0.27(0.051)	0.62	0.3(0.061)	0.28(0.057)	0.16
SOL	0.3(0.098)	0.32(0.091)	0.44	0.26(0.083)	0.28(0.065)	0.56	0.27(0.063)	0.27(0.048)	0.80
MG	0.3(0.084)	0.29(0.08)	0.59	0.28(0.067)	0.28(0.071)	0.92	0.26(0.057)	0.29(0.062)	0.094

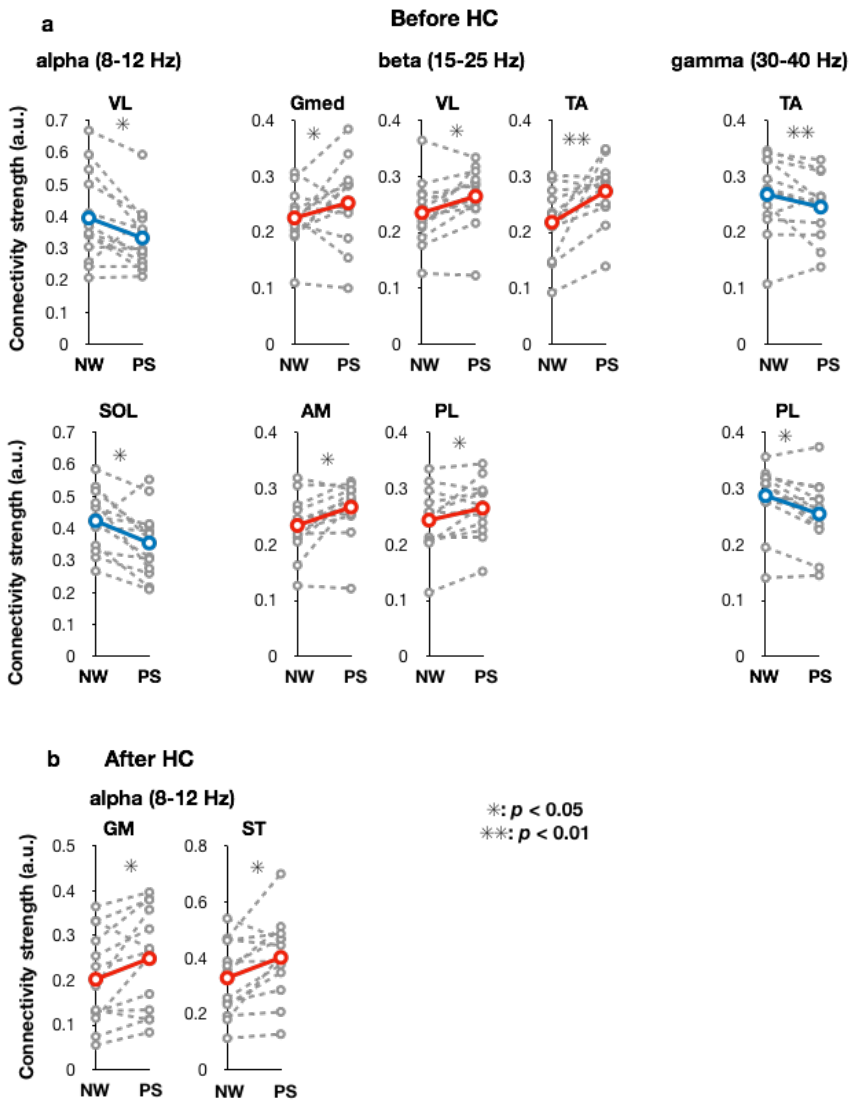

Figure 6-8. Comparisons of corticomuscular connectivity strength for individual muscle between normal walking (NW) and precision stepping (PS). The values were separately compared in three frequency bands (α、β and γ) in two gait phases (before heel contact (HC) and after HC). Only the connectivity, which changed significantly between NW and PS ($p < 0.05$), is shown. All comparison data are indicated in Table 1. Gray dot lines indicate individual data. Red lines indicate the mean value, which was significantly increased from NW to PS. Blue lines indicate the mean value, which was significantly decreased from NW to PS. ∗: $p < 0.05$. ∗∗: $p < 0.01$.

6. 4. Discussion

Here, to reveal how the cortex voluntarily modifies locomotor muscle activity, I examined causal connectivity of EEG and EMG signals during normal walking and precision stepping. I found that large causal connectivity from motor cortex to leg muscles in both walking tasks. Additionally, during precision stepping, the motor cortex→muscle connectivity was enhanced in β band in many muscles (TA, Gmed, VL, AM, and PL) before heel contact. These results confirmed my working hypotheses, and therefore suggest that β band descending commands from the motor cortex is involved in voluntary modification of locomotor muscle activity, especially in the swing phase.

6. 4. 1. Cortical activity during walking and its involvement in muscle control

In cat studies that recorded motor cortex activity, firing rate modulation depending on gait phase was observed during steady state walking (Armstrong and Drew, 1984: Drew et al. 2008). The firing rate modulation in motor cortex during locomotion has also been confirmed in other animals, such as rodents (Rigosa et al., 2015; DiGiovanna et al., 2016) and non-human primates (Foster et al., 2014; Yin et al., 2014). Regarding relationships between the cortical activity and locomotor muscle activity, recent studies using neuronal decoding methods demonstrated that hindlimb muscle activity are able to be reconstructed from firing rate information of the motor cortex in rodents (Rigosa et al., 2015) and non-human primates (Fitzsimmons et al., 2009), strongly suggesting cortical involvement in control of locomotor muscle activity.

In humans, regarding roles of the cortical activity during walking for muscle control, recent EEG studies demonstrated significant corticomuscular coherence between motor cortical EEG and EMG from TA muscle (Petersen et al., 2012) and directional causal relationships from the cortex to muscles (Artoni et al., 2017) during steady state walking. In accordance with previous studies, the present study demonstrated large directional connectivity from motor

cortex to leg muscles (Figs. 6-4 and 6-5). Artoni et al. (2017) showed that sensorimotor regions including primary motor area, supplementary motor area and premotor area had a strong connectivity with leg muscles. The cortical regions are near the EEG electrode, which showed strong connectivity with muscle in the present study (Cz electrode). Given the low spatial resolution of EEG, the Cz electrode would contain combined information from the sensorimotor areas, that had large conrticomuscular connectivity in the previous study (Artoni et al., 2017). In non-human primates, neurons in these motor areas have anatomical connectivity to the motoneurons (Dum and Strick, 2002). Thus, considering the high anatomical commonality of corticospinal systems between humans and non-human primates (Lemon and Griffiths, 2005), such a corticomuscular connection may contribute to the causal connectivity from the motor cortex to muscles in human walking.

6. 4. 2. Cortical involvement in voluntary modification of locomotor muscle activity

In the present study, strength of the causal connectivity from motor cortex to muscles was different between normal walking and precision stepping (Figs. 6-6, 6-7 and 6-8). Strong connectivity was observed in many muscles (TA, Gmed, VL, AM, and PL) in β band before heel contact during a precision stepping task (Fig. 6-8). The precision stepping task can be regarded as a leg reaching task to a target on a treadmill. Therefore, it is considered that the motor cortex-to-muscle connectivity was increased in muscles that have roles in the reaching movement, namely forward swing of the leg and the endpoint control (VL: knee extension, TA and PL: toe clearance and fixation of ankle, Gmed and AM: adjustment of leg movement in mediolateral direction). β band cortical activity has been considered to be involved in motor preparation and execution (Jurkiewicz et al., 2006; Salenius et al., 1997; Pfurtscheller and Lopes da Silva, 1999). The involvement of motor cortex β band activity in voluntary muscle control has also been suggested by significant EEG-EMG coherence in the β band during isometric contraction of leg muscles (Mima et al., 2000; Ushiyama et al., 2010) and bilateral

alternate rhythmic foot movements (Raethjen et al., 2008). Based on these evidences about involvement of β band motor cortex activity in voluntary muscle control, modification of muscle activity during walking may be mainly achieved by β band descending drive from the motor cortex. Therefore, the connectivity strength from the motor cortex to muscles in β band was increased during precision stepping.

The changes of connectivity strength also occurred few muscles in α and γ bands (Fig. 6-8). In the γ band, the connectivity strength was decreased in TA and PL before heel contact during precision stepping (Fig. 6-8). Regarding corticomuscular connectivity in γ band, reciprocal relationship of EMG-EEG coherence between γ and β band coherence has been demonstrated (Mima et al. 1999; Omlor et al. 2007). In the present study, the decreases of connectivity strength in TA and PL in the precision stepping task were associated with increases of β band connectivity in these muscles. Thus, I speculate that the decreases of γ band connectivity were related to the reciprocal relationship between γ and β band. Regarding α band, the connectivity strength was increased in GM and ST after heel contact during precision stepping, while decreased in VL and SOL before heel contact. A previous study, which performed electrical stimulation to afferent fibers tonic, indicated that sensory feedback involved in generating corticomuscular coherence in the α band (Hansen and Nielsen, 2004). The authors considered that the afferent induced corticomuscular coherence may have been related to a cerebellar–thalamic–cortex circuits, based on a evidence that cerebellar nuclei involves in α band rhythmicity (Marsden et al., 2000). In addition, the α band cortical activity would be utilized for information transmissions between motor and parietal areas involving in visuomotor control (Pfurtscheller and Neuper, 1994; Pfurtscheller and Da Silva, 1999; Babiloni et al., 2002). Since the GM and ST activated initial stance phase for loading response (Winter and Yack, 1987), the load afferents and visual information might be integrated through the α band sensorimotor networks. Then, the integrated information might have transmitted to motor cortex, and transformed into descending motor drives. Therefore, the increase of α band

connectivity strength in GM and ST after heel contact during precision stepping in this study might have been involved in the α band sensorimotor networks. On the other hand, decreased in VL and SOL before heel contact in α band might be related to relative decrease of contribution of the α band sensorimotor networks to the muscle control in exchange for the increase of β band voluntary descending drive.

6. 4. 3. Voluntary modification of locomotor muscle activity in quadruped animals

Similar to the present results, the contribution of the cortex for modifying locomotor muscle activity during skilled walking has been presented by a number of cat studies (Beloozerova and Sirota, 1988; Drew, 1988; Amos et al., 1990; Beloozerova and Sirota, 1993; Drew, 1993; Marple‐Horvat et al., 1993; Widajewicz et al., 1994; Drew et al., 1996; Drew et al., 2002). In cat locomotion, although the corticomuscular connectiy during steady state walking has hardly been observed, temporally synchronized activity of hindlimb muscles and motor cortex neurons, which are inactivated during normal walking, were observed during skilled walking (Drew et al., 2008). In addition to the corticomuscular connectivity, cats studies demonstrated that the posterior parietal cortex (PPC) is deeply engaged in motor planning for gait modification during visually guided walking (Beloozerova and Sirota, 2003; Drew et al., 2008; Andujar et al., 2010; Drew and Marigold, 2015). It has been demonstrated that firing rate of large parts of neurons in the PPC become faster during visually guided gait modifications (Beloozerova and Sirota., 2003, Andujar et al., 2010). When stepping over obstacles, the PPC is considered to integrate information regarding interaction between walkers (cats) and walking environment, and therefore has a role for recognition of relative position between walkers and the obstacles (Drew and Marigold, 2015).

The motor cortex sends descending motor commands based on inputs from several cortical and subcortical regions including the PPC, somatosensory cortex, basal ganglia and cerebellum (Drew and Marigold, 2015). Thus, huge cortical and subcortical networks would be

involved in adaptive gait modification during visually guided walking. Therefore, more understanding of the neural control of the gait modification in humans requires detailed examination of information flow in whole brain in future studies.

6. 4. 4. Methodological considerations

Important methodological concern in this study is the potential issue of movement artifact of the EEG recording. Recent studies examining the movement artifacts during walking demonstrated that walking-related artifact are observed especially in lower frequencies, i.e., delta (0–3 Hz) and theta (4–7 Hz) bands (Castermans et al., 2014; Kline et al., 2015). Additionally, the studies also indicated that the artifact become serious in walking faster than 0.8 m/s. Therefore, to ensure reliability of the data, I adopted the slow walking speed (0.6 m/s) and focused on relatively high frequency bands (8Hz–).

Additionally, I performed ICA and source localization techniques (i.e., dipole fitting) on the EEG signals to exclude artifact components. This procedure is an established and most popular artifact removal method for EEG data during walking (Gwin et al., 2010, 2011; Wagner et al., 2012; Wagner et al., 2014; Bruijn et al., 2015; Bulea et al., 2015; Snyder et al., 2015; Bradford et al., 2016; Wagner et al., 2016; Oliveira et al., 2017). To test reliability of the artifact removal procedure, Snyder et al. (2015) applied the ICA and dipole fitting to pure movement artifact signals obtained from an EEG recording set up with a silicone swim cap (non-conductive layer). They showed that ICA and dipole fitting accurately recognized 99% of the independent components as non-brain signals. Another study using the same method to isolate and record only movement artifact showed that the spectral modulation patterns of movement artifact signals are not similar to those in the actual EEG signal (Kline et al., 2015). These results strongly support that present results are obtained from neural activity.

6. 4. 5. Conclusions

In summary, I demonstrated changes in the causal connectivity from the motor cortex to muscles between visually guided skilled walking and normal walking. The changes of causal connectivity were mainly observed in task related muscles in swing phase as the increased connectivity strength in the β band. The present results provide evidences that the motor cortex is involved in control of voluntary skilled walking through modification of muscle activity. Given the cortical involvement in temporally-precise control for lower limb muscle activity during steady state walking as demonstrated in the Study 4 (Chapter 5) and Artoni et al., (2017), my results further emphasize the critical importance of the cortex for control of human bipedal locomotion. In addition to the contribution in understanding of neural control of human walking, the findings of descending command regarding voluntary gait modification would provide fundamental knowledge for development of volitional control system of brain–machine interfaces for walking rehabilitation. Future studies should investigate the information flow in brain networks for the gait modification for further understanding the neural control of human walking.

Chapter 7

General discussion

7. 1. Summary of the results

In the present thesis, I raised following research questions regarding muscle control of human bipedal locomotion based on previous studies.

- **Spinal level: The detail characteristics of human locomotor CPG is remain unclear. Are the neural mechanisms, which were revealed in animal models, conserved in human locomotor circuits?**
- **Cortical level: 1) Whether and how does the cortex control activation of the spinal CPG? 2) How does the cortex modify the muscle activity under conditions that require voluntary adjustment of walking behavior?**

Then, I executed five separated studies to investigate role of the spinal cord and the cortex in muscle control of human bipedal locomotion by solving the questions. I examined the neural control by the spinal cord and the cortex in Studies 1−3 and Studies 4−5, respectively. The following findings and suggestions were obtained from these studies.

In Study 1 (Chapter 2), I tested whether speed- and mode-dependency in the recruitment of locomotor networks, which was revealed in animal studies (Talpalar et al., 2013), exists or not in humans by extracting locomotor module. During walking and running over a wide speed range, locomotor modules, which generate basic patterns of muscle activities and are encoded in the pattern formation networks in the spinal CPGs (McCrea and Rybak, 2008), were extracted from EMGs. The results showed that different combinations of modules were recruited during walking and running, and at different speeds even during the same locomotor mode. These results strongly suggest that, in humans, different spinal locomotor networks are recruited depending on the mode and the speeds.

In Study 2 (Chapter 3), I examined whether characteristics of MN activation for control of locomotion speed observed in animals (Cazalets and Bertrand, 2000; Talpalar and Kiehn, 2010) exist in humans or not. For this purpose, I reconstructed the spatiotemporal

activation patterns of MNs along the rostrocaudal direction of the spinal cord during varied-speed locomotion. The MN activation patterns were analyzed from EMGs. The reconstructed MN activity patterns were divided into the following three patterns depending on the speed: slow walking, fast walking and running. During these three activation patterns, the proportion of the activity in rostral segments to that in caudal segments increased as locomotion got faster. Additionally, the different MN activation patterns were generated by distinct combinations of locomotor modules. These results are consistent with the speed control mechanisms observed in vertebrates, suggesting phylogenetically conserved spinal mechanisms of neural control of locomotion between humans and other vertebrates.

In Study3 (Chapter 4), I examined whether rostrocaudally traveling wave of neural activity in the spinal cord, which is considered to be one of components in the rhythm generation layer of CPGs (Cuellar et al., 2009; Saltiel et al., 2015), exists in spinal locomotor networks in humans as in non-human vertebrates. Assuming that the traveling wave recruits spinal locomotor modules from upper to lower region in the spinal cord, I examined the existence of traveling wave based on the activation sequence of locomotor modules and their topography. In this study I used an air-stepping task to explore activity of a "pure" version of CPG in the absence of afferent modulation derived by foot contact (Ivanekno et al., 2002). I identified four types of locomotor modules. MN clusters innervating each motor module were sequentially activated from the rostral to caudal region in the spinal cord, from the initial flexion to the last extension phase during air-stepping. The rostrocaudally sequential activation of MN clusters suggests the possibility that rostrocaudally traveling waves exist in human locomotor spinal circuits.

In Study4 (Chapter 5), to examine the relationships between cortical activity and spinal locomotor circuits, I performed neural decoding of the activation patterns of locomotor modules and EMGs from EEG signals in three frequency bands (α, β, and γ). As a result, the activations of locomotor modules and EMGs were decoded from EEG signals. The accuracy of

the synergy decoder was higher than that of the EMG decoder. The decoding were mainly contributed by cortical information 40−70ms ahead of the module activity from leg motor area in α and β bands. The higher accuracy of the synergy decoder than that of the EMG decoder suggests that the cortex hierarchically control the locomotor muscle activities through locomotor modules.

In Study 5 (Chapter 6), to examine cortical contribution to voluntary modification of muscle activity during skilled walking, I examined differences in causal connectivity of EEG and EMG signals between normal and skilled walking. The results showed significant causal unidirectional connectivity from contralateral motor cortex to muscles in both walking tasks. During the skilled walking, the unidirectional causal connectivity was enhanced in β band in the muscles related to the stepping task compared with that during normal walking. These results suggest that β band descending commands from the motor cortex involve voluntary modification of locomotor muscle activity.

Together, the results obtained from the five studies indicate following novel knowledge to answer the research questions of the thesis regarding human locomotor control by the spinal cord and the cortex:

1) **The spinal locomotor networks in humans, which generate basic locomotor muscle activity, have high similarity with those in non-human vertebrates (Studies 1-3). (Corresponding to the research question at spinal level)**
2) **The cortex would be involved in hierarchical control of locomotor muscle activity through locomotor modules by using cortical information 40−70 ms ahead of module activity from leg motor area in α and β bands (Study 4). (Corresponding to the research question 1 at cortical level)**
3) **The cortex would contribute to voluntary modification of locomotor muscle activity**

during skilled walking via β band descending commands from leg sensorimotor area (Studies 5). (Corresponding to the research question 2 at cortical level)

The novel knowledge about human locomotor control strongly suggest that human-specific bipedal upright locomotion can be achieved even under challenging walking conditions by the generation of the basic patterns of muscle activity from the spinal cord and the cortical modification of it. The details of the above three characteristics in human locomotor system are discussed in following sections. Then, I also discuss the possible future direction and clinical implications of the present findings.

7. 2. Spinal neural networks for locomotion

In studies 1−3, I examined whether neural mechanisms in the spinal locomotor networks reveled in animal studies are shared in humans using several indirect methods using EMGs. The results in studies 1−3 consistently demonstrated the commonality of the spinal locomotor neural networks in humans and non-human vertebrates. In line with my findings, recent studies demonstrated the similarity of the spinal locomotor networks in humans and animals, focusing on temporal activation patterns of the spinal locomotor modules (Diminichi et al., 2011; Danner et al., 2015). Dominichi et al., (2011) showed activation patterns of the locomotor modules extracted from toddlers, whose developmental stage was considered to be before maturation of the corticospinal system, were significantly similar to those extracted from rat, cat, macaque, and guineafowl. Similarly, Danner et al., (2015) also demonstrated that the locomotor modules extracted from patients with complete SCI exhibit very similar activation patterns with non-human vertebrates. Regarding another common characteristic in the spinal CPGs, it has been founded that rostral regions of the lumbosacral spinal cord have a higher rhythmogenic capacity as burst generators for locomotor muscle activity both in mice (Kjaerulff and Kiehn,

1996; Cazalets and Bertrand, 2000; Talpalar and Kiehn, 2010) and humans (Dimitrijevic et al., 1998; Gerasimenko et al., 2010; Danner et al., 2015; Gerasimenko et al., 2016). Based on my findings and these related recent studies, there is a high possibility that the fundamental mechanisms in the spinal locomotor networks are phylogenetically conserved among vertebrate animals including humans.

My findings are consistent with the idea that fundamental motor patterns (e.g. hunting, feeding and masticatory patterns) conserved across and morphological and phylogenetic differences among vertebrates even after a long period of evolution (Wainwright, 2002). Also in locomotion behavior, spinal locomotor CPGs in legged vertebrates have been considered to be emerged through evolution from a common fundamental circuit for vertebrates performing undulating locomotion (Grillner and Jessell, 2009). Recent studies using novel genetic technics, the similarity of core components of spinal CPGs at the interneuron level has been confirmed across many non-human vertebrates even between fish and rodents (Goulding, 2009; Kiehn, 2016). If the similarity at the spinal interneuron level is conserved in humans, this would explain the high commonality of the spinal locomotor networks between humans and non-human vertebrates.

7. 3. Cortical involvement in control of locomotor muscle activity

Although the spinal locomotor networks are very similar between humans and non-human vertebrates, there are apparent differences in the cortical control of locomotor muscle activity. After lesions of the cortex, although cats have critical difficulty in performing more challenging walking conditions such narrow beam or ladder walking, they can still perform stereotyped walking without any particular problem (Liddell and Phillips, 1944; Jiang and Drew, 1996; Drew et al., 2002). On the other hand, in humans, patients with stroke exhibit gait disturbance even in stereotyped walking in most cases (Perry et al., 1995). Although pure spinal locomotor outputs induced by epidural electrical stimulation to the spinal cord of complete SCI patients

was similar to locomotor muscle activity patterns of quadruped animals, human walking exhibit modulated muscle activation pattern from the spinal outputs (Danner et al. 2015). Based on these previous studies, in human locomotion, cortical tuning of basic locomotor muscle activity generated from spinal networks would be needed even during stereotyped walking.

To support this idea, my Studies 4 and 5 demonstrated greater connectivity between locomotor muscle activity and cortical activity even during stereotyped walking. In Study 5, the connectivity had a significant unidirectional causality from the motor cortex to muscles, suggesting that human locomotor muscle activity is largely modified by descending drives from the motor cortex. Additionally, Study 5 also showed that the causal connectivity was strengthened during visually guided walking in the muscles related to the walking task. Thus, my findings strongly suggest that the cortex modify locomotor muscle activity for both achievement of human specific bipedal locomotion and adjustment to specific tasks during walking, such as precision stepping and obstacle avoidance.

Upright bipedal walking in humans and quadruped walking and exhibit different muscle activation patterns (Vilensky, 1987), due to difference in the biomechanical characteristics (Lovejoy, 1988). Namely, humans probably adapt locomotor muscle activity to human specific upright bipedal walking (Grillner et al. 2011). Foot-contact position of humans is the heel, while that of quadruped vertebrates is their toe in general (Nilsson et al., 1985; Vilensky, 1987). Thus, there is a possibility that genetically conserved spinal networks from non-human vertebrates cannot generate all the locomotor muscle activity in humans, and therefore, following two possible neural contributions are required for the muscle control: 1) developmentally reorganization of the spinal network, and 2) additional cortical involvement. Nevertheless, the latter contribution would be larger to the human locomotor control, because a study on patients with complete SCI, who were injured after 15 years old (mean±SD: 28.2± 11.8), demonstrated that their spinal motor outputs induced by spinal epidural electrical stimulation were similar to muscle activation patterns of non-human vertebrates (Danner et al.,

2015).

As a typical example, cortical involvement in human specific locomotor muscle activity has been observed in TA activity during walking. TA muscle is primarily activated at a swing phase in quadruped animal walking (Engberg, 1964), while in humans its additional activity occurs after heel-contact (Winter and Yack, 1987). The differences would related to the deference in the foot-contact positions (humans: heel, quadruped animals: toe) (Nilsson et al., 1985; Vilensky, 1987). A recent study showed that the human specific TA activity has significant coherence with cortical activity in leg sensorimotor area of the cortex (Petersen et al., 2012). Regarding the control of the TA, Study 5 also suggested that the TA activity was strongly modified by descending drives from the motor cortex during skilled walking. The human specific TA activity related to the biomechanical characteristics of upright walking and neural connectivity between TA and motor cortex supports the hypothesis that additional cortical involvement contributes to humans specific muscle activity to adapt bipedal upright walking.

It is possible that mechanical instability of the upright bipedal walking due to narrow base of support (Kuo, 1999) also requires additional cortical involvement for locomotor control. Actually, an EEG study reported that the cortical activity in premotor regions differed between normal walking and body stabilized walking by elastic bands (Bruijn et al., 2015). Additionally, walking behavior of toddlers, who have immature corticospinal connections, display considerable postural instability (Assaiante et al., 1993; Bril and Brenière, 1993) and different muscle activation patterns from adults (Dominici et al., 2011), suggesting importance of the cortical muscular control for walking stability. Together, the above-mentioned biomechanical specificity of the upright bipedal walking would cause the greater cortical involvement in control of locomotor muscle activity.

In addition to humans, birds walk bipedally. However, walking posture between humans and birds is greatly different. Birds walk with a squatted position touching the ground

from the toe and the leg is bent at the foot contact timing (Alexander, 2004). On the other hand, humans walk erect with a heel-strike and their leg is almost completely extended at the heel contact timing. These different bipedal gaits have evolved independently in two vertebrate lineages, archosaurs and primates corresponding to birds and humans, respectively. Given the different evolutionary processes, for the discussion of the evolution of locomotor networks for mammals from fish to humans, there would be no problem without considering neural mechanisms for the bird bipedal walking.

7. 4. Recruitment of the spinal locomotor modules by multiple neural pathways

Although previous studies detected locmotor related cortical activations during walking (Gwin et al., 2011; Wagner et al., 2012; Bulea et al., 2015), relationships between the cortical activity and spinal locomotor networks have remained unclear so far. Regarding the relationships, study 4 demonstrated activations of the locomotor modules can be decoded from EEG signals. The finding suggested that the spinal locomotor networks are activated or modified by descending commands from the cortex. In line with my finding, a previous study demonstrated that stroke patients can only utilize few number of modules due to a merging of the modules observed in healthy peoples, suggesting the cortical contribution in the recruitment of spinal locomotor modules (Clark et al., 2010).

Regarding the recruitment of spinal locomotor modules, Study 3 suggested that the rostrocaudally traveling wave of activations in the spinal cord are involved in recruitment of locomotor modules in a proper sequence. In addition, recent rodent studies demonstrated that MLR neurons in the brainstem innervate the rhythm generation layer of spinal CPGs, and therefore, the MLR affects the recruitment of locomotor modules (Bouvier et al., 2015). It is not clear whether such contribution of brainstem to locomotor module recruitment can be extended to humans. Nevertheless, there is a possibility that the brainstem system for locomotor module recruitments is conserved in humans, because existence of MLR is strongly suggested (for

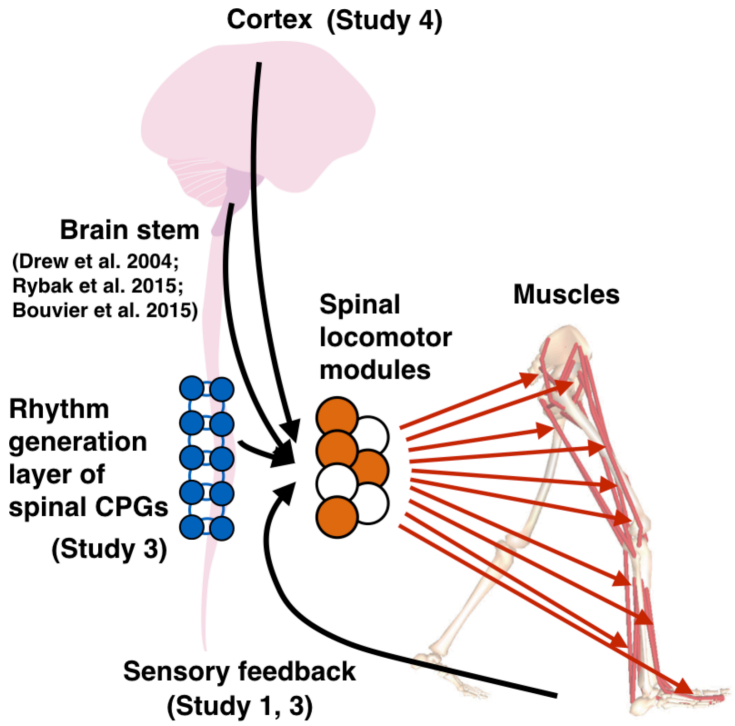

Figure 7-1. Recruitment of locomotor modules by multiple neural pathways. For walking, descending commands from the spinal cord, brainstem, and cortex and sensory feedback are integrated to selectively recruit and modulate spinal locomotor modules. An appropriate combination of locomotor modules is selectively recruited from multiple hard-wired modules for flexible generation of locomotor muscle activity. Circles filled with orange indicate activated locomotor modules and open circles indicate inactive locomotor modules.

details, see section 1.2 in Introduction) (Piallat et al., 2009; Tattersall et al., 2014; Lau et al., 2015). Additionally, comparison of extracted locomotor module types between walking (Studies 1, 2 and 4) and air-stepping (Study 4) suggested that a locomotor module is recruited by loading afferent inputs related to the foot-contact.

Altogether, the locomotor modules can be recruited through different neural pathways including cortical descending drive, rhythm generation layer of the spinal CPGs, brainstem pathways and sensory feedback. The recruitment of locomotor modules by multiple neural pathways is depicted in Figure 7-1. In Study 1, small sets of locomotor modules were selectively recruited from multiple modules depending on locomotor speed. Therefore,

integrated command from the multiple neural pathways would selectively recruits a set of locomotor modules from multiple hard-wired modules to generate appropriate muscle activity for the situation (Fig. 7-1). Thus, I could conclude that humans can easily execute walking and adapt the walking behavior to ever-changing walking environment by the simplification of complex muscle control by spinal locomotor modules as the lower level of the motor control hierarchy and the flexible recruitments of the modules by multiple neural pathways.

7. 5. Future Directions

In the present studies, I examined control of locomotor muscle activity in humans focusing on the role of the spinal cord and the cortex. In addition to the cortex and the spinal cord, it is well known that subcortical regions, such as basal ganglia, limbic system, hypothalamus, brainstem and cerebellum involve locomotor control (Takakusaki and Okumura, 2008). Nevertheless, in humans, role of these subcortical regions for control of locomotor muscle activity remains unclear.

Recently, MRI-Compatible treadmill devices have been developed to examine brain activity during walking (Dalla Volta et al., 2015; Martínez et al., 2016). Locomotor related subcortical regions in humans will be gradually revealed by fMRI measurement during walking thanks to such treadmill devices. Nevertheless, it must be noted that limited time resolution of fMRI is a barrier to explore detail relationships between locomotor muscle activity and detected locomotor related subcortical regions.

Deep brain stimulation (DBS) is a neurosurgical technic which electrically stimulate to a specific area of the brain region. DBS to pedunculopontine nucleus (PPN), which is a MLR region in humans (Piallat et al., 2009; Tattersall et al., 2014; Lau et al., 2015), has recently attempted in Parkinson's disease patients to restore their waling behavior (Fasano et al., 2015). Recently, to examine the role of the PPN for walking control, extracellular single-unit recordings of PPN from the electrodes for DBS has been performed by several studies (Tatssall

et al., 2014; Lau et al. 2015). This method can record electrical signals, which has high time resolution enough to examine the relationships between locomotor muscle activity and brainstem activity. Nevertheless, it should be kept in mind that the recorded signals are obtained from PD patients and therefore it is possible that the recoded activity is different from those in healthy peoples.

In addition, to investigate signals from deep brain regions such as basal ganglia and hippocampus, source estimation from high density EEGs (more than 128 channels) has been utilized (Attal et al., 2007; Attal and Schwartz, 2013; Barzegaran et al., 2016). So far, this source estimation method has been used for static tasks. The applicability of the method to EEG signals recorded during dynamic movement needs further confirmation. If the source estimation method is robust for dynamic movement, it will advance our understanding of the role of subcortical regions for control of locomotor muscle activity in healthy peoples.

7. 6. Clinical implications

The present studies demonstrated the roles of the cortex and spinal circuits in the locomotor muscle control in healthy peoples. The understanding of the neural mechanisms of human locomotion would provide important fundamental knowledge to interpret gait deficits of patients with neural disorders such as stroke and SCI patients and to facilitate their gait rehabilitation.

Additionally, there is a possibility that my findings contribute to development of a novel neuroprosthesis for SCI patients in future. A recent primate study demonstrated that monkeys with SCI have regained the ability for walking thanks to a novel technology that re-establishes communication between the brain and spinal cord (Capogrosso et al., 2016). In this primate study, firstly, spinal electrical stimulation patterns were created based on MN activation patterns estimated by similar method used in my Study 2 (Chapter 3). Then, walking related information was decoded from cortical signals, and the information triggered the

patterned electrical stimulation to the spinal cord. In this present thesis, I obtained detailed information about MN activation patterns for each locomotor module in the spinal cord over a wide speed range using a method based on anatomical evidences (Kendall, 1993) (Studies 2, Chapters 3). Additionally, stimulation patterns based on the traveling wave of neural activation in the spinal locomotor networks (Studies 3, Chapters 4) may contribute to construct effective spinal electrical stimulation systems. In addition, I demonstrated the feasibility of using scalp EEG to reconstruct the locomotor module activations using a brain decoding method based on machine learning (Study 4, Chapter 6). Therefore, based on a similar concept of the primate study (Capogrosso et al., 2016), the findings and technics in the present studies could contribute to develop a novel neural-interface system that re-connect between the brain and spinal cord for patients with SCI (Fig. 7-2).

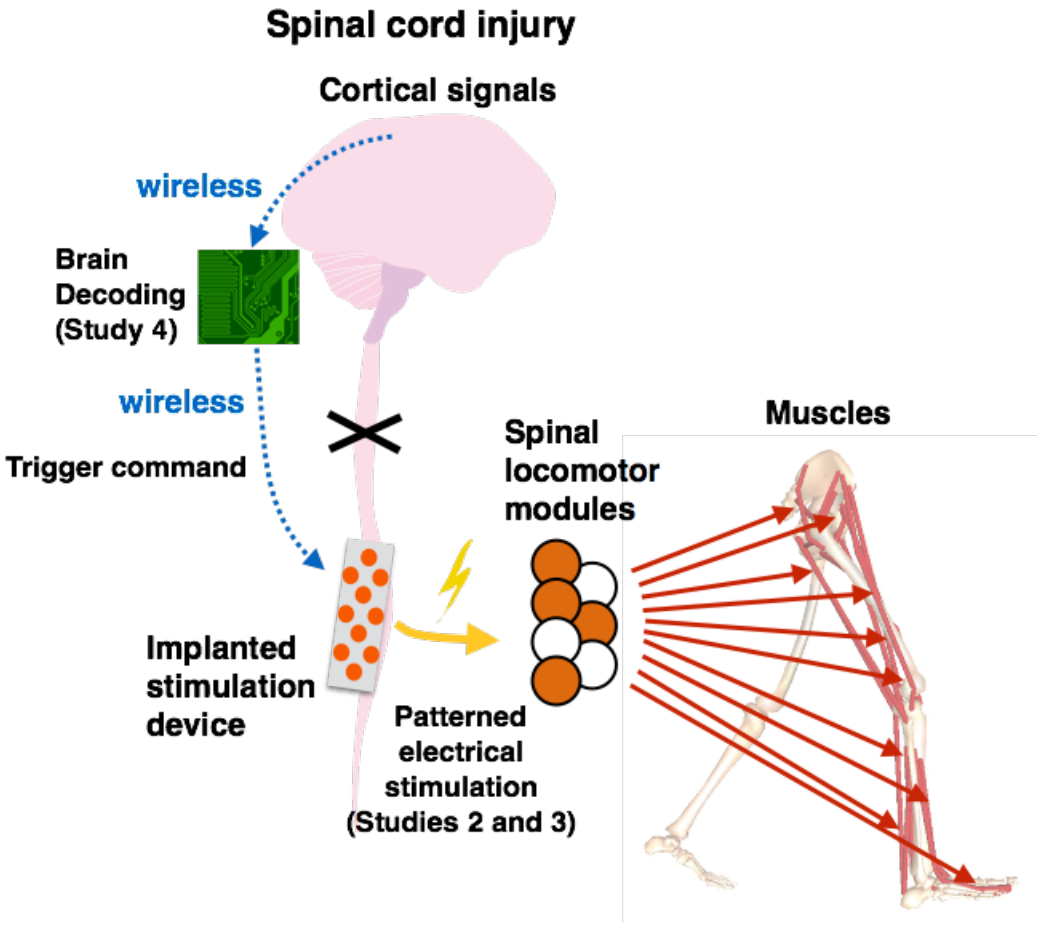

Figure 7-2. A conceptual scheme of a neural-interface system that enabled communication between the brain and spinal cord in humans. Locomotor related information is decoded from cortical neural activity. The decoded information is transmitted, as trigger signal, to an implanted stimulation device on the spinal cord via a wireless connection. The device sends patterned electrical stimulation that activated spinal locomotor modules in a proper sequence to generate locomotor muscle activity. In this system, the findings of Studies 2 and 4 would contributes development of a brain decoding technic and optimization of an electrical stimulation pattern, respectively.

7. 7. Concluding remarks

The purpose of the thesis was to explore and describe the roles of the spinal cord and the cortex in muscle control of human bipedal locomoton.

Based on the five studies, I conclude that human-specific upright biped locomotion is performed by cortically modifying the basic muscle activity pattern generated spinal locomotor circuits, which have high similarity to those for non-human vertebrates. The spinal cord simplifies the complex locomotor muscle activity through locomotor modules, and therefore would allow us to walk effortlessly. Cortical activity would be involved in activation of the locomotor modules for modifying muscle activity to adapt the biomechanical requirements of the upright bipedal gait. Additionally, the cortical involvement in muscle control is increased during walking under challenging environment, such as uneven terrain and slippery surface.

The novel findings should advance our understandings of neural control of human bipedal locomotion. Additionally, the commonality and differences in locomotor control between quadruped vertebrates and humans provide important insights into the evolution of vertebrate locomotion. Moreover, the brain decoding technics and detected locomotor related cortical activity could accelerate development of novel effective brain–machine interfaces for walking rehabilitation.

References

Alexander R (2004) Bipedal animals, and their differences from humans. J Anat. 204: 321-330.

Alibeji NA, Kirsch NA, Sharma N (2015) A muscle synergy-inspired adaptive control scheme for a hybrid walking neuroprosthesis. Front Bioeng Biotech 3:203.

Amos A, Armstrong D, Marple-Horvat D (1990) Changes in the discharge patterns of motor cortical neurones associated with volitional changes in stepping in the cat. Neurosci Lett 109:107-112.

Ampatzis K, Song J, Ausborn J, El Manira A (2013) Pattern of innervation and recruitment of different classes of motoneurons in adult zebrafish. J Neurosci 33:10875-10886.

Ampatzis K, Song J, Ausborn J, El Manira A (2014) Separate microcircuit modules of distinct v2a interneurons and motoneurons control the speed of locomotion. Neuron 83:934-943.

Andersson LS et al. (2012) Mutations in DMRT3 affect locomotion in horses and spinal circuit function in mice. Nature 488:642-646.

Andujar J-É, Lajoie K, Drew T (2010) A contribution of area 5 of the posterior parietal cortex to the planning of visually guided locomotion: limb-specific and limb-independent effects. J Neurophysiol 103:986-1006.

Arber S (2012) Motor circuits in action: specification, connectivity, and function. Neuron 74:975-989.

Armstrong D, Drew T (1984) Discharges of pyramidal tract and other motor cortical neurones during locomotion in the cat. J Physiol 346:471-495.

Armstrong D, Marple-Horvat D (1996) Role of the cerebellum and motor cortex in the regulation of visually controlled locomotion. Can J Physiol Pharmacol 74:443-455.

Armstrong DM (1988) The supraspinal control of mammalian locomotion. J Physiol 405:1-37.

Artoni F, Fanciullacci C, Bertolucci F, Panarese A, Makeig S, Micera S, Chisari C (2017)

Unidirectional brain to muscle connectivity reveals motor cortex control of leg muscles during stereotyped walking. NeuroImage 159:403-416.

Assaiante C, Thomachot B, Aurenty R (1993) Hip stabilization and lateral balance control in toddlers during the first four months of autonomous walking. Neuroreport 4:875-878.

Attal Y, Schwartz D (2013) Assessment of subcortical source localization using deep brain activity imaging model with minimum norm operators: a MEG study. PloS One 8:e59856.

Attal Y, Bhattacharjee M, Yelnik J, Cottereau B, Lefèvre J, Okada Y, Bardinet E, Chupin M, Baillet S (2007) Modeling and detecting deep brain activity with MEG & EEG. In: Engineering in Medicine and Biology Society, 2007. EMBS 2007. 29th Annual International Conference of the IEEE, 4937-4940.

Ausborn J, Mahmood R, El Manira A (2012) Decoding the rules of recruitment of excitatory interneurons in the adult zebrafish locomotor network. Proc Natl Acad Sci U S A 109:E3631-3639.

Babiloni C, Babiloni F, Carducci F, Cincotti F, Cocozza G, Del Percio C, Moretti DV, Rossini PM (2002) Human cortical electroencephalography (EEG) rhythms during the observation of simple aimless movements: a high-resolution EEG study. NeuroImage 17:559-572.

Bank PJ, Roerdink M, Peper C (2011) Comparing the efficacy of metronome beeps and stepping stones to adjust gait: steps to follow! Expe Brain Res 209:159-169.

Barzegaran E, Carmeli C, Rossetti AO, Frackowiak RS, Knyazeva MG (2016) Weakened functional connectivity in patients with psychogenic non-epileptic seizures (PNES) converges on basal ganglia. J Neurol Neurosurg Psychiatry 87:332-337.

Batschelet E, Batschelet E, Batschelet E, Batschelet E (1981) Circular statistics in biology: Academic press London.

Bauby CE, Kuo AD (2000) Active control of lateral balance in human walking. J Biomech

33:1433-1440.

Bell AJ, Sejnowski TJ (1995) An information-maximization approach to blind separation and blind deconvolution. Neural Comput 7:1129-1159.

Bellardita C, Kiehn O (2015) Phenotypic characterization of speed-associated gait changes in mice reveals modular organization of locomotor networks. Curr Biol 25:1426-1436.

Beloozerova I, Sirota M (1988) Role of motor cortex in control of locomotion. In: Stance and Motion, pp 163-176: Springer.

Beloozerova I, Sirota M (1993) The role of the motor cortex in the control of accuracy of locomotor movements in the cat. J Physiol 461:1-25.

Beloozerova IN, Sirota MG (2003) Integration of motor and visual information in the parietal area 5 during locomotion. J Neurophysiol 90:961-971.

Berens P (2009) CircStat: a MATLAB toolbox for circular statistics. J Stat Softw 31:1-21.

Berger DJ, Gentner R, Edmunds T, Pai DK, d'Avella A (2013) Differences in adaptation rates after virtual surgeries provide direct evidence for modularity. J Neurosci 33:12384-12394.

Berger W, Dietz V, Quintern J (1984) Corrective reactions to stumbling in man: neuronal co-ordination of bilateral leg muscle activity during gait. J Physiol 357:109.

Betley JN, Wright CV, Kawaguchi Y, Erdelyi F, Szabo G, Jessell TM, Kaltschmidt JA (2009) Stringent specificity in the construction of a GABAergic presynaptic inhibitory circuit. Cell 139:161-174.

Bikoff JB, Gabitto MI, Rivard AF, Drobac E, Machado TA, Miri A, Brenner-Morton S, Famojure E, Diaz C, Alvarez FJ (2016) Spinal inhibitory interneuron diversity delineates variant motor microcircuits. Cell 165:207-219.

Bonnot A, Whelan PJ, Mentis GZ, O'Donovan MJ (2002) Locomotor-like activity generated by the neonatal mouse spinal cord. Brain Res Rev 40:141-151.

Bouton CE, Shaikhouni A, Annetta NV, Bockbrader MA, Friedenberg DA, Nielson DM,

Sharma G, Sederberg PB, Glenn BC, Mysiw WJ (2016) Restoring cortical control of functional movement in a human with quadriplegia. Nature 533:247-250.

Bouvier J, Caggiano V, Leiras R, Caldeira V, Bellardita C, Balueva K, Fuchs A, Kiehn O (2015) Descending command neurons in the brainstem that halt locomotion. Cell 163:1191-1203.

Bradberry TJ, Gentili RJ, Contreras-Vidal JL (2010) Reconstructing three-dimensional hand movements from noninvasive electroencephalographic signals. J Neurosci 30:3432-3437.

Bradford JC, Lukos JR, Ferris DP (2016) Electrocortical activity distinguishes between uphill and level walking in humans. Journal of neurophysiology 115:958-966.

Bril B, Brenière Y (1993) Posture and independent locomotion in early childhood: Learning to walk or learning dynamic postural control? Advances in psychology 97:337-358.

Brown TG (1911) The intrinsic factors in the act of progression in the mammal. Proc Roy Soc Lond B 84:308-319.

Bruijn SM, Van Dieën JH, Daffertshofer A (2015) Beta activity in the premotor cortex is increased during stabilized as compared to normal walking. Front Hum Neurosci 9: 593.

Budick SA, O'Malley DM (2000) Locomotor repertoire of the larval zebrafish: swimming, turning and prey capture. J Exp Biol 203:2565-2579.

Bulea TC, Prasad S, Kilicarslan A, Contreras-Vidal JL (2014) Sitting and standing intention can be decoded from scalp EEG recorded prior to movement execution. Front Neurosci 8:376.

Bulea TC, Kim J, Damiano DL, Stanley CJ, Park H-S (2015) Prefrontal, posterior parietal and sensorimotor network activity underlying speed control during walking. Front Hum Neurosci 9:247.

Butt SJ, Kiehn O (2003) Functional identification of interneurons responsible for left-right

coordination of hindlimbs in mammals. Neuron 38:953-963.

Caggiano V, Cheung VC, Bizzi E (2016) An Optogenetic Demonstration of Motor Modularity in the Mammalian Spinal Cord. Sci Rep 6:35185.

Calancie B (2006) Spinal myoclonus after spinal cord injury. J Spinal Cord Med 29:413.

Calancie B, Needham-Shropshire B, Jacobs P, Willer K, Zych G, Green BA (1994) Involuntary stepping after chronic spinal cord injury evidence for a central rhythm generator for locomotion in man. Brain 117:1143-1159.

Capogrosso M, Milekovic T, Borton D, Wagner F, Moraud EM, Mignardot J-B, Buse N, Gandar J, Barraud Q, Xing D (2016) A brain–spine interface alleviating gait deficits after spinal cord injury in primates. Nature 539:284-288.

Cappellini G, Ivanenko YP, Poppele RE, Lacquaniti F (2006) Motor patterns in human walking and running. J Neurophysiol 95:3426-3437.

Carmena JM, Lebedev MA, Crist RE, O'Doherty JE, Santucci DM, Dimitrov DF, Patil PG, Henriquez CS, Nicolelis MA (2003) Learning to control a brain–machine interface for reaching and grasping by primates. PLoS Biol 1:e42.

Castermans T, Duvinage M, Cheron G, Dutoit T (2014) About the cortical origin of the low-delta and high-gamma rhythms observed in EEG signals during treadmill walking. Neurosci Lett 561:166-170.

Cazalets J-R, Bertrand S (2000) Ubiquity of motor networks in the spinal cord of vertebrates. Brain Res Bull 53:627-634.

Cazalets JR (2005) Metachronal propagation of motoneurone burst activation in isolated spinal cord of newborn rat. J Physiol 568:583-597.

Chao ZC, Nagasaka Y, Fujii N (2010) Long-term asynchronous decoding of arm motion using electrocorticographic signals in monkeys. Front Neuroeng 3:3.

Chatrian GE, Petersen MC, Lazarte JA (1959) The blocking of the rolandic wicket rhythm and some central changes related to movement. Electroencephalogr Clin Neurophysiol

11:497-510.

Chéron G, Duvinage M, De Saedeleer C, Castermans T, Bengoetxea A, Petieau M, Seetharaman K, Hoellinger T, Dan B, Dutoit T (2012) From spinal central pattern generators to cortical network: integrated BCI for walking rehabilitation. Neural Plasticity 2012.

Cheung VC, Piron L, Agostini M, Silvoni S, Turolla A, Bizzi E (2009) Stability of muscle synergies for voluntary actions after cortical stroke in humans. Proc Natl Acad Sci U S A 106:19563-19568.

Cheung VC, Turolla A, Agostini M, Silvoni S, Bennis C, Kasi P, Paganoni S, Bonato P, Bizzi E (2012) Muscle synergy patterns as physiological markers of motor cortical damage. Proc Natl Acad Sci U S A 109:14652-14656.

Choi JT, Bastian AJ (2007) Adaptation reveals independent control networks for human walking. Nat Neurosci 10:1055-1062.

Chvatal SA, Ting LH (2012) Voluntary and reactive recruitment of locomotor muscle synergies during perturbed walking. J Neurosci 32:12237-12250.

Chvatal SA, Macpherson JM, Torres-Oviedo G, Ting LH (2013) Absence of postural muscle synergies for balance after spinal cord transection. J Neurophysiol 110:1301-1310.

Clark DJ, Ting LH, Zajac FE, Neptune RR, Kautz SA (2010) Merging of healthy motor modules predicts reduced locomotor performance and muscle coordination complexity post-stroke. J Neurophysiol 103:844-857.

Corey DM, Dunlap WP, Burke MJ (1998) Averaging correlations: Expected values and bias in combined Pearson rs and Fisher's z transformations. J Gen Psychol 125:245-261.

Crone SA, Zhong G, Harris-Warrick R, Sharma K (2009) In mice lacking V2a interneurons, gait depends on speed of locomotion. J Neurosci 29:7098-7109.

Cuellar CA, Tapia JA, Juárez V, Quevedo J, Linares P, Martínez L, Manjarrez E (2009) Propagation of sinusoidal electrical waves along the spinal cord during a fictive motor

task. J Neurosci 29:798-810.

d'Avella A, Portone A, Fernandez L, Lacquaniti F (2006) Control of fast-reaching movements by muscle synergy combinations. J Neurosci 26:7791-7810.

Dalla Volta R, Fasano F, Cerasa A, Mangone G, Quattrone A, Buccino G (2015) Walking indoors, walking outdoors: an fMRI study. Frontiers in psychology 6:1502.

Danner SM, Hofstoetter US, Freundl B, Binder H, Mayr W, Rattay F, Minassian K (2015) Human spinal locomotor control is based on flexibly organized burst generators. Brain 138:577-588.

de Rugy A, Loeb GE, Carroll TJ (2013) Are muscle synergies useful for neural control. Front Comput Neurosci 7:10.3389.

Delorme A, Makeig S (2004) EEGLAB: an open source toolbox for analysis of single-trial EEG dynamics including independent component analysis. J Neurosci Metholds 134:9-21.

Delorme A, Palmer J, Onton J, Oostenveld R, Makeig S (2012) Independent EEG sources are dipolar. PloS One 7:e30135.

Delorme A, Mullen T, Kothe C, Acar ZA, Bigdely-Shamlo N, Vankov A, Makeig S (2011) EEGLAB, SIFT, NFT, BCILAB, and ERICA: new tools for advanced EEG processing. Comput Intell Neurosci 2011:10.

Den Otter A, Geurts A, Mulder T, Duysens J (2004a) Speed related changes in muscle activity from normal to very slow walking speeds. Gait Posture 19:270-278.

DiGiovanna J, Dominici N, Friedli L, Rigosa J, Duis S, Kreider J, Beauparlant J, Van Den Brand R, Schieppati M, Micera S (2016) Engagement of the Rat Hindlimb Motor Cortex across Natural Locomotor Behaviors. J Neurosci 36:10440-10455.

Dimitrijevic MR, Gerasimenko Y, Pinter MM (1998) Evidence for a spinal central pattern generator in humans. Ann N Y Acad Sci 860:360-376.

Dominici N, Ivanenko YP, Cappellini G, d'Avella A, Mondi V, Cicchese M, Fabiano A, Silei T, Di Paolo A, Giannini C, Poppele RE, Lacquaniti F (2011) Locomotor primitives in

newborn babies and their development. Science 334:997-999.

Donelan JM, Kram R (2001) Mechanical and metabolic determinants of the preferred step width in human walking. Proc Roy Soc Lond B 268:1985-1992.

Drew T (1988) Motor cortical cell discharge during voluntary gait modification. Brain Res 457:181-187.

Drew T (1993) Motor cortical activity during voluntary gait modifications in the cat. I. Cells related to the forelimbs. J Neurophysiol 70:179-199.

Drew T, Marigold DS (2015) Taking the next step: cortical contributions to the control of locomotion. Curr Opin Neurobiol 33:25-33.

Drew T, Jiang W, Widajewicz W (2002) Contributions of the motor cortex to the control of the hindlimbs during locomotion in the cat. Brain Res Rev 40:178-191.

Drew T, Prentice S, Schepens B (2004) Cortical and brainstem control of locomotion. Prog Brain Res 143:251-261.

Drew T, Kalaska J, Krouchev N (2008) Muscle synergies during locomotion in the cat: a model for motor cortex control. J Physiol 586:1239-1245.

Drew T, Jiang W, Kably B, Lavoie S (1996) Role of the motor cortex in the control of visually triggered gait modifications. Can J Physiol Pharmacol 74:426-442.

Dum RP, Strick PL (2002) Motor areas in the frontal lobe of the primate. Physiol Behav 77:677-682.

Duysens J (2002) Human gait as a step in evolution. Brain 125:2589-90

Duysens J, Pearson K (1980) Inhibition of flexor burst generation by loading ankle extensor muscles in walking cats. Brain Res 187:321-332.

Duysens J, Van de Crommert HW (1998) Neural control of locomotion; Part 1: The central pattern generator from cats to humans. Gait Posture 7:131-141.

Duysens J, De Groote F, Jonkers I (2013) The flexion synergy, mother of all synergies and father of new models of gait. Front Comput Neurosci 7:14.

Duysens J, Van Wezel B, Van de Crommert H, Faist M, Kooloos J (1998) The role of afferent feedback in the control of hamstrings activity during human gait. Eur J Morphol 36:293-299.

Dzeladini F, Van Den Kieboom J, Ijspeert A (2014) The contribution of a central pattern generator in a reflex-based neuromuscular model. Front Hum Neurosci 8:371.

El Manira A (2014) Dynamics and plasticity of spinal locomotor circuits. Curr Opin Neurobiol 29:133-141.

Enders H, Nigg BM (2016) Measuring human locomotor control using EMG and EEG: Current knowledge, limitations and future considerations. Eur J Sport Sci 16:416-426.

Engberg I (1964) Reflexes to foot muscles in the cat. Acta Physiol Scand Suppl 235:1-64.

Engel AK, Singer W (2001) Temporal binding and the neural correlates of sensory awareness. Trends Cogn Sci 5:16-25.

Engel AK, Fries P (2010) Beta-band oscillations—signalling the status quo? Curr Opin Neurobiol 20:156-165.

Fasano A, Aquino CC, Krauss JK, Honey CR, Bloem BR (2015) Axial disability and deep brain stimulation in patients with Parkinson disease. Nat Rev Neurol 11:98-110.

Feige B, Aertsen A, Kristeva-Feige R (2000) Dynamic synchronization between multiple cortical motor areas and muscle activity in phasic voluntary movements. J Neurophysiol 84:2622-2629.

Fitzsimmons NA, Lebedev MA, Peikon ID, Nicolelis MA (2009) Extracting kinematic parameters for monkey bipedal walking from cortical neuronal ensemble activity. Front Integr Neurosci 3:3.

Foster JD, Nuyujukian P, Freifeld O, Gao H, Walker R, Ryu SI, Meng TH, Murmann B, Black MJ, Shenoy KV (2014) A freely-moving monkey treadmill model. J Neural Eng 11:046020.

Frere J, Hug F (2012) Between-subject variability of muscle synergies during a complex motor

skill. Front Comput Neurosci 6:99.

Fukuyama H, Ouchi Y, Matsuzaki S, Nagahama Y, Yamauchi H, Ogawa M, Kimura J, Shibasaki H (1997) Brain functional activity during gait in normal subjects: a SPECT study. Neurosci Lett 228:183-186.

Garcia-Campmany L, Stam FJ, Goulding M (2010) From circuits to behaviour: motor networks in vertebrates. Curr Opin Neurobiol 20:116-125.

Garcia-Rill E (1986) The basal ganglia and the locomotor regions. Brain Res Rev 11:47-63.

Garcia-Rill E (1991) The pedunculopontine nucleus. Prog Neurobiol 36:363-389.

Garcia-Rill E (1997) Disorders of the reticular activating system. Med Hypotheses 49:379-387.

Gerasimenko Y, Gorodnichev R, Machueva E, Pivovarova E, Semyenov D, Savochin A, Roy RR, Edgerton VR (2010) Novel and direct access to the human locomotor spinal circuitry. J Neurosci 30:3700-3708.

Gerasimenko Y, Gad P, Sayenko D, McKinney Z, Gorodnichev R, Puhov A, Moshonkina T, Savochin A, Selionov V, Shigueva T (2016) Integration of sensory, spinal, and volitional descending inputs in regulation of human locomotion. J Neurophysiol 116:98-105.

Goetz L, Piallat B, Bhattacharjee M, Mathieu H, David O, Chabardès S (2016) On the role of the pedunculopontine nucleus and mesencephalic reticular formation in locomotion in nonhuman primates. J Neurosci 36:4917-4929.

Gorassini MA, Prochazka A, Hiebert GW, Gauthier M (1994) Corrective responses to loss of ground support during walking. I. Intact cats. J Neurophysiol 71:603-610.

Gosgnach S, Lanuza GM, Butt SJ, Saueressig H, Zhang Y, Velasquez T, Riethmacher D, Callaway EM, Kiehn O, Goulding M (2006) V1 spinal neurons regulate the speed of vertebrate locomotor outputs. Nature 440:215-219.

Gottschall JS, Okita N, Sheehan RC (2012) Muscle activity patterns of the tensor fascia latae and adductor longus for ramp and stair walking. J Electromyogr Kinesiol 22:67-73.

Goulding M (2009) Circuits controlling vertebrate locomotion: moving in a new direction. Nat Rev Neurosci 10:507-518.

Greiwe J, Kohrt W (2000) Energy expenditure during walking and jogging. J Sports Med Phys Fitness 40:297.

Grillner S (1974) On the generation of locomotion in the spinal dogfish. Expe Brain Res 20:459-470.

Grillner S (1981) Control of locomotion in bipeds, tetrapods, and fish. In: Handbook of physiology, Section 1, The nervous system, Motor control, Vol 2, Part 1 (Brookhart JM, Mountcastle VB, eds), pp 1179–1236. Bethesda, MD: American Physiological Society.

Grillner S, Rossignol S (1978) On the initiation of the swing phase of locomotion in chronic spinal cats. Brain Res 146:269-277.

Grillner S, Wallen P (1985) Central pattern generators for locomotion, with special reference to vertebrates. Ann Rev Neurosci 8:233-261.

Grillner S, Jessell TM (2009) Measured motion: searching for simplicity in spinal locomotor networks. Curr Opin Neurobiol 19:572-586.

Gwin JT, Gramann K, Makeig S, Ferris DP (2010) Removal of movement artifact from high-density EEG recorded during walking and running. J Neurophysiol 103:3526-3534.

Gwin JT, Gramann K, Makeig S, Ferris DP (2011) Electrocortical activity is coupled to gait cycle phase during treadmill walking. NeuroImage 54:1289-1296.

Haefeli J, Vögeli S, Michel J, Dietz V (2011) Preparation and performance of obstacle steps: interaction between brain and spinal neuronal activity. Eur J Neurosci 33:338-348.

Hägglund M, Dougherty K, Borgius L, Itohara S, Iwasato T, Kiehn O (2013) Optogenetic dissection reveals multiple rhythmogenic modules underlying locomotion. Proc Natl Acad Sci U S A 110:11589-11594.

Hagio S, Kouzaki M (2014) The flexible recruitment of muscle synergies depends on the

required force-generating capability. J Neurophysiol 112:316-327.

Hansen N, Nielsen J (2004) The effect of transcranial magnetic stimulation and peripheral nerve stimulation on corticomuscular coherence in humans. J Physiol 561:295-306.

Harada T, Miyai I, Suzuki M, Kubota K (2009) Gait capacity affects cortical activation patterns related to speed control in the elderly. Exp Brain Res 193:445-454.

Hart CB, Giszter SF (2010) A neural basis for motor primitives in the spinal cord. J Neurosci 30:1322-1336.

Hiebert GW, Whelan PJ, Prochazka A, Pearson KG (1996) Contribution of hind limb flexor muscle afferents to the timing of phase transitions in the cat step cycle. J Neurophysiol 75:1126-1137.

Hinckley CA, Alaynick WA, Gallarda BW, Hayashi M, Hilde KL, Driscoll SP, Dekker JD, Tucker HO, Sharpee TO, Pfaff SL (2015) Spinal locomotor circuits develop using hierarchical rules based on motorneuron position and identity. Neuron 87:1008-1021.

Hof A, Elzinga H, Grimmius W, Halbertsma J (2002) Speed dependence of averaged EMG profiles in walking. Gait Posture 16:78-86.

Hug F (2011) Can muscle coordination be precisely studied by surface electromyography? J Electromyogr Kinesiol 21:1-12.

Hug F, Turpin NA, Couturier A, Dorel S (2011) Consistency of muscle synergies during pedaling across different mechanical constraints. J Neurophysiol 106:91-103.

Ijspeert AJ, Crespi A, Ryczko D, Cabelguen J-M (2007) From swimming to walking with a salamander robot driven by a spinal cord model. Science 315:1416-1420.

Ivanenko Y, Grasso R, Macellari V, Lacquaniti F (2002) Control of foot trajectory in human locomotion: role of ground contact forces in simulated reduced gravity. J Neurophysiol 87:3070-3089.

Ivanenko YP, Poppele RE, Lacquaniti F (2004) Five basic muscle activation patterns account for muscle activity during human locomotion. J Physiol 556:267-282.

Ivanenko YP, Poppele RE, Lacquaniti F (2006) Spinal cord maps of spatiotemporal alpha-motoneuron activation in humans walking at different speeds. J Neurophysiol 95:602-618.

Ivanenko YP, Dominici N, Cappellini G, Lacquaniti F (2005a) Kinematics in newly walking toddlers does not depend upon postural stability. J Neurophysiol 94:754-763.

Ivanenko YP, Cappellini G, Poppele RE, Lacquaniti F (2008) Spatiotemporal organization of alpha-motoneuron activity in the human spinal cord during different gaits and gait transitions. Eur J Neurosci 27:3351-3368.

Ivanenko YP, Cappellini G, Dominici N, Poppele RE, Lacquaniti F (2005b) Coordination of locomotion with voluntary movements in humans. J Neurosci 25:7238-7253.

Ivanenko YP, Cappellini G, Dominici N, Poppele RE, Lacquaniti F (2007) Modular control of limb movements during human locomotion. J Neurosci 27(41):11149-11161.

Ivanenko YP, Dominici N, Cappellini G, Di Paolo A, Giannini C, Poppele RE, Lacquaniti F (2013) Changes in the spinal segmental motor output for stepping during development from infant to adult. J Neurosci 33:3025-3036a.

Jankowska E (2008) Spinal interneuronal networks in the cat: elementary components. Brain Res Rev 57:46-55.

Jasper H, Penfield W (1949) Electrocorticograms in man: effect of voluntary movement upon the electrical activity of the precentral gyrus. Eur Arch Psychiatry Clin Neurosci 183:163-174.

Jenkinson N, Nandi D, Muthusamy K, Ray NJ, Gregory R, Stein JF, Aziz TZ (2009) Anatomy, physiology, and pathophysiology of the pedunculopontine nucleus. Mov Disord 24:319-328.

Jessell TM, Surmeli G, Kelly JS (2011) Motor neurons and the sense of place. Neuron 72:419-424.

Jiang W, Drew T (1996) Effects of bilateral lesions of the dorsolateral funiculi and dorsal

columns at the level of the low thoracic spinal cord on the control of locomotion in the adult cat. I. Treadmill walking. J Neurophysiol 76:849-866.

Jiroumaru T, Kurihara T, Isaka T (2014) Establishment of a recording method for surface electromyography in the iliopsoas muscle. J Electromyogr Kinesiol 24:445-451.

Jordan LM (1998) Initiation of locomotion in mammals. Ann N Y Acad Sci 860:83-93.

Jung T-P, Makeig S, Humphries C, Lee T-W, Mckeown MJ, Iragui V, Sejnowski TJ (2000) Removing electroencephalographic artifacts by blind source separation. Psychophysiol 37:163-178.

Jurkiewicz MT, Gaetz WC, Bostan AC, Cheyne D (2006) Post-movement beta rebound is generated in motor cortex: evidence from neuromagnetic recordings. NeuroImage 32:1281-1289.

Kadaba MP, Ramakrishnan H, Wootten M (1990) Measurement of lower extremity kinematics during level walking. J Orthop Res 8:383-392.

Kaminski M, Blinowska KJ (1991) A new method of the description of the information flow in the brain structures. Biol Cybern 65:203-210.

Kaske A, Winberg G, Cöster J (2003) Emergence of coherent traveling waves controlling quadruped gaits in a two-dimensional spinal cord model. Biol Cybern 88:20-32.

Kato H, Cuellar CA, Delgado‐Lezama R, Rudomin P, Jimenez‐Estrada I, Manjarrez E, Mirasso CR (2013) Modeling zero‐lag synchronization of dorsal horn neurons during the traveling of electrical waves in the cat spinal cord. Physiol Rep 1:e00021.

Kehne J, Ketteler H, McCloskey T, Sullivan C, Dudley M, Schmidt C (1996) Effects of the selective 5-HT 2A receptor antagonist MDL 100,907 on MDMA-induced locomotor stimulation in rats. Neuropsychopharmacol 15:116-124.

Keller T, Weisberger A, Ray J, Hasan S, Shiavi R, Spengler D (1996) Relationship between vertical ground reaction force and speed during walking, slow jogging, and running. Clin Biomech 11:253-259.

Kendall FP, McCreary EK, Provance PG, Rodgers MM, Romani W (1993) Muscles, testing and function: with posture and pain.

Kiehn O (2011) Development and functional organization of spinal locomotor circuits. Curr Opin Neurobiol 21:100-109.

Kiehn O (2016) Decoding the organization of spinal circuits that control locomotion. Nat Rev Neurosci.

Kimura Y, Okamura Y, Higashijima S (2006) alx, a zebrafish homolog of Chx10, marks ipsilateral descending excitatory interneurons that participate in the regulation of spinal locomotor circuits. J Neurosci 26:5684-5697.

Kimura Y, Satou C, Higashijima S (2008) V2a and V2b neurons are generated by the final divisions of pair-producing progenitors in the zebrafish spinal cord. Development 135:3001-3005.

Kjaerulff O, Kiehn O (1996) Distribution of networks generating and coordinating locomotor activity in the neonatal rat spinal cord in vitro: a lesion study. J Neurosci 16:5777-5794.

Klarner T, Chan HK, Wakeling JM, Lam T (2010) Patterns of muscle coordination vary with stride frequency during weight assisted treadmill walking. Gait Posture 31:360-365.

Kline JE, Huang HJ, Snyder KL, Ferris DP (2015) Isolating gait-related movement artifacts in electroencephalography during human walking. J Neural Eng 12:046022.

Koenraadt, K. L., Roelofsen, E. G., Duysens, J., & Keijsers, N. L. (2014). Cortical control of normal gait and precision stepping: an fNIRS study. Neuroimage, 85, 415-422.

Korzeniewska A, Mańczak M, Kamiński M, Blinowska KJ, Kasicki S (2003) Determination of information flow direction among brain structures by a modified directed transfer function (dDTF) method. J Neurosci Methods 125:195-207.

Kriellaars D, Brownstone R, Noga B, Jordan L (1994) Mechanical entrainment of fictive locomotion in the decerebrate cat. J Neurophysiol 71:2074-2086.

Krouchev N, Drew T (2013) Motor cortical regulation of sparse synergies provides a framework

for the flexible control of precision walking. Frontiers in computational neuroscience 7:83.

Kuo AD (1999) Stabilization of lateral motion in passive dynamic walking. Int J Rob Res 18:917-930.

Kyriakatos A, Mahmood R, Ausborn J, Porres CP, Buschges A, El Manira A (2011) Initiation of locomotion in adult zebrafish. J Neurosci 31:8422-8431.

La Fougere C, Zwergal A, Rominger A, Förster S, Fesl G, Dieterich M, Brandt T, Strupp M, Bartenstein P, Jahn K (2010) Real versus imagined locomotion: a [18 F]-FDG PET-fMRI comparison. NeuroImage 50:1589-1598.

La Scaleia V, Ivanenko YP, Zelik KE, Lacquaniti F (2014) Spinal motor outputs during step-to-step transitions of diverse human gaits. Front Hum Neurosci 8:305.

Lanuza GM, Gosgnach S, Pierani A, Jessell TM, Goulding M (2004) Genetic identification of spinal interneurons that coordinate left-right locomotor activity necessary for walking movements. Neuron 42:375-386.

Lau B, Welter M-L, Belaid H, Fernandez Vidal S, Bardinet E, Grabli D, Karachi C (2015) The integrative role of the pedunculopontine nucleus in human gait. Brain 138:1284-1296.

Lebedev MA, Nicolelis MA (2006) Brain–machine interfaces: past, present and future. Trends Neurosci 29:536-546.

Lebedev MA, Nicolelis MA (2017) Brain-Machine Interfaces: From Basic Science to Neuroprostheses and Neurorehabilitation. Physiol Rev 97:767-837.

Lee DD, Seung HS (1999) Learning the parts of objects by non-negative matrix factorization. Nature 401:788-791.

Lee T-W, Lewicki MS, Girolami M, Sejnowski TJ (1999) Blind source separation of more sources than mixtures using overcomplete representations. IEEE Signal Process Lett 6:87-90.

Lemon R N, Griffiths J (2005) Comparing the function of the corticospinal system in different

species: organizational differences for motor specialization?. Muscle Nerve, 32(3), 261-279.

Lev‐Tov A, Etlin A, Blivis D (2010) Sensory‐induced activation of pattern generators in the absence of supraspinal control. Ann N Y Acad Sci 1198:54-62.

Lewicki MS, Sejnowski TJ (2006) Learning overcomplete representations. Learning 12.

Liddell E, Phillips C (1944) Pyramidal section in the cat. Brain 67:1-9.

Ljunggren EE, Haupt S, Ausborn J, Ampatzis K, El Manira A (2014) Optogenetic Activation of Excitatory Premotor Interneurons Is Sufficient to Generate Coordinated Locomotor Activity in Larval Zebrafish. J Neurosci 34:134-139.

Lovejoy CO (1988) Evolution of human walking. Scientific American 259:118-125.

Lundberg A (1979) Multisensory control of spinal reflex pathways. Prog Brain Res 50:11-28.

Maclellan M, Ivanenko Y, Massaad F, Bruijn S, Duysens J, Lacquaniti F (2014) Muscle Activation Patterns are Bilaterally Linked during Split-Belt Treadmill Walking in Humans. J Neurophysiol 111:1541-52

Makeig S, Bell AJ, Jung T-P, Sejnowski TJ (1996) Independent component analysis of electroencephalographic data. In: Advances in neural information processing systems, pp 145-151.

Marple‐Horvat D, Amos A, Armstrong D, Criado J (1993) Changes in the discharge patterns of cat motor cortex neurones during unexpected perturbations of on‐going locomotion. J Physiol 462:87-113.

Marsden J, Ashby P, Limousin-Dowsey P, Rothwell J, Brown P (2000) Coherence between cerebellar thalamus, cortex and muscle in man: cerebellar thalamus interactions. Brain 123:1459-1470.

Martínez M, Valencia M, Vidorreta M, Luis EO, Castellanos G, Villagra F, Fernández‐Seara MA, Pastor MA (2016) Trade‐off between frequency and precision during stepping movements: Kinematic and BOLD brain activation patterns. Hum Brain Mapp

37:1722-1737.

McCrea DA, Rybak IA (2008) Organization of mammalian locomotor rhythm and pattern generation. Brain Res Rev 57:134-146.

McHanwell S, Biscoe T (1981) The localization of motoneurons supplying the hindlimb muscles of the mouse. Philos Trans R Soc Lond B Biol Sci 293:477-508.

McLean DL, Dougherty KJ (2015) Peeling back the layers of locomotor control in the spinal cord. Curr Opin Neurobiol 33:63-70.

McLean DL, Fan J, Higashijima S, Hale ME, Fetcho JR (2007) A topographic map of recruitment in spinal cord. Nature 446:71-75.

McLean DL, Masino MA, Koh IY, Lindquist WB, Fetcho JR (2008) Continuous shifts in the active set of spinal interneurons during changes in locomotor speed. Nat Neurosci 11:1419-1429.

Mima T, Simpkins N, Oluwatimilehin T, Hallett M. (1999). Force level modulates human cortical oscillatory activities. Neurosci Lett, 275(2), 77-80.

Mima T, Steger J, Schulman AE, Gerloff C, Hallett M (2000) Electroencephalographic measurement of motor cortex control of muscle activity in humans. Clin Neurophysiol 111:326-337.

Miyai I, Tanabe HC, Sase I, Eda H, Oda I, Konishi I, Tsunazawa Y, Suzuki T, Yanagida T, Kubota K (2001) Cortical mapping of gait in humans: a near-infrared spectroscopic topography study. NeuroImage 14:1186-1192.

Monaco V, Ghionzoli A, Micera S (2010) Age-related modifications of muscle synergies and spinal cord activity during locomotion. J Neurophysiol 104:2092-2102.

Muceli S, Boye AT, d'Avella A, Farina D (2010) Identifying representative synergy matrices for describing muscular activation patterns during multidirectional reaching in the horizontal plane. J Neurophysiol 103:1532-1542.

Mullen T, Kothe C, Chi YM, Ojeda A, Kerth T, Makeig S, Cauwenberghs G, Jung T-P (2013)

Real-time modeling and 3D visualization of source dynamics and connectivity using wearable EEG. In: Engineering in Medicine and Biology Society (EMBC), 2013 35th Annual International Conference of the IEEE, pp 2184-2187: IEEE.

Mullen TR (2014) The dynamic brain: Modeling neural dynamics and interactions from human electrophysiological recordings: University of California, San Diego.

Murray M, Mollinger L, Gardner G, Sepic S (1984) Kinematic and EMG patterns during slow, free, and fast walking. J Orthop Res 2:272-280.

Muscolino JE (2008) The Muscle and Bone Palpation Manual with Trigger Points, Referral Patterns and Stretching: Elsevier Health Sciences.

Nathan K, Contreras-Vidal JL (2016) Negligible motion artifacts in scalp electroencephalography (EEG) during treadmill walking. Front Hum Neurosci 9:708.

Nathan P, Smith M, Deacon P (1996) Vestibulospinal, reticulospinal and descending propriospinal nerve fibres in man. Brain 119:1809-1833.

Neptune RR, Sasaki K, Kautz SA (2008) The effect of walking speed on muscle function and mechanical energetics. Gait Posture 28:135-143.

Neptune RR, Clark DJ, Kautz SA (2009) Modular control of human walking: a simulation study. J Biomech 42:1282-1287.

Neuper C, Pfurtscheller G (1996) Post-movement synchronization of beta rhythms in the EEG over the cortical foot area in man. Neurosci lett 216:17-20.

Nicolelis MA (2003) Brain–machine interfaces to restore motor function and probe neural circuits. Nat Rev Neurosci 4:417-422.

Nielsen J, Petersen N, Ballegaard M (1995) Latency of effects evoked by electrical and magnetic brain stimulation in lower limb motoneurones in man. J Physiol 484:791-802.

Nilsson J, Thorstensson A, HALBERTSMA J (1985) Changes in leg movements and muscle activity with speed of locomotion and mode of progression in humans. Acta Physiol Scand 123:457-475.

O'donovan MJ, Bonnot A, Mentis GZ, Arai Y, Chub N, Shneider NA, Wenner P (2008) Imaging the spatiotemporal organization of neural activity in the developing spinal cord. Dev Neurobiol 68:788-803.

Ogawa T, Kawashima N, Ogata T, Nakazawa K (2012) Limited transfer of newly acquired movement patterns across walking and running in humans. PloS One 7:e46349.

Ogawa T, Kawashima N, Obata H, Kanosue K, Nakazawa K (2015a) Distinct motor strategies underlying split-belt adaptation in human walking and running. PloS One 10:e0121951.

Ogawa T, Kawashima N, Obata H, Kanosue K, Nakazawa K (2015b) Mode-dependent control of human walking and running as revealed by split-belt locomotor adaptation. J Exp Biol 218:3192-3198.

Oliveira AS, Gizzi L, Farina D, Kersting UG (2014) Motor modules of human locomotion: influence of EMG averaging, concatenation, and number of step cycles. Front Hum Neurosci 8:335.

Oliveira AS, Schlink BR, Hairston WD, König P, Ferris DP (2017) Restricted vision increases sensorimotor cortex involvement in human walking. J Neurophysiol 118:1943-1951.

Omlor W, Patino L, Hepp-Reymond MC, Kristeva R. (2007). Gamma-range corticomuscular coherence during dynamic force output. Neuroimage, 34: 1191-1198.

Oostenveld R, Praamstra P (2001) The five percent electrode system for high-resolution EEG and ERP measurements. Clin Neurophysiol 112:713-719.

Oostenveld R, Oostendorp TF (2002) Validating the boundary element method for forward and inverse EEG computations in the presence of a hole in the skull. Hum Brain Mapp 17:179-192.

Orlovsky G (1972a) The effect of different descending systems on flexor and extensor activity during locomotion. Brain Res 40:359-372.

Orlovsky G (1972b) Activity of vestibulospinal neurons during locomotion. Brain Res 46:85-98.

Orlovsky GN, Deliagina T, Grillner S, Orlovskii G, Grillner S (1999) Neuronal control of locomotion: from mollusc to man: Oxford University Press New York:.

Palmer JA, Kreutz-Delgado K, Makeig S (2006) Super-Gaussian Mixture Source Model for ICA. In: Independent Component Analysis and Blind Signal Separation: 6th International Conference, ICA 2006, Charleston, SC, USA, March 5-8, 2006. Proceedings (Rosca J, Erdogmus D, Príncipe JC, Haykin S, eds), pp 854-861. Berlin, Heidelberg: Springer Berlin Heidelberg.

Palmer JA, Makeig S, Kreutz-Delgado K, Rao BD (2008) Newton method for the ICA mixture model. In: Acoustics, Speech and Signal Processing, 2008. ICASSP 2008. IEEE International Conference on, pp 1805-1808: IEEE.

Patil PG, Turner DA (2008) The development of brain-machine interface neuroprosthetic devices. Neurotherapeutics 5:137-146.

Pearson KG (2004) Generating the walking gait: role of sensory feedback. Prog Brain Res 143:123-129.

Peckham PH (1987) Functional electrical stimulation: current status and future prospects of applications to the neuromuscular system in spinal cord injury. Spinal cord 25:279-288.

Pérez T, Tapia JA, Mirasso CR, García-Ojalvo J, Quevedo J, Cuellar CA, Manjarrez E (2009) An intersegmental neuronal architecture for spinal wave propagation under deletions. J Neurosci 29:10254-10263.

Perry J, Garrett M, Gronley JK, Mulroy SJ (1995) Classification of walking handicap in the stroke population. Stroke 26:982-989.

Petersen TH, Willerslev‐Olsen M, Conway BA, Nielsen JB (2012) The motor cortex drives the muscles during walking in human subjects. J Physiol 590:2443-2452.

Pfurtscheller G, Aranibar A (1977) Event-related cortical desynchronization detected by power measurements of scalp EEG. Electroencephalogr Clin Neurophysiol 42:817-826.

Pfurtscheller G, Neuper C (1992) Simultaneous EEG 10 Hz desynchronization and 40 Hz

synchronization during finger movements. Neuroreport 3:1057-1060.

Pfurtscheller G, Neuper C (1994) Event-related synchronization of mu rhythm in the EEG over the cortical hand area in man. Neurosci Lett 174:93-96.

Pfurtscheller G, Da Silva FL (1999) Event-related EEG/MEG synchronization and desynchronization: basic principles. Clin Neurophysiol 110:1842-1857.

Pfurtscheller G, Neuper C, Kalcher J (1993) 40-Hz oscillations during motor behavior in man. Neurosci Lett 164:179-182.

Piallat B, Chabardès S, Torres N, Fraix V, Goetz L, Seigneuret E, Bardinet E, Ferraye M, Debû B, Krack P (2009) Gait is associated with an increase in tonic firing of the sub-cuneiform nucleus neurons. Neurosci 158:1201-1205.

Presacco A, Forrester LW, Contreras-Vidal JL (2012) Decoding intra-limb and inter-limb kinematics during treadmill walking from scalp electroencephalographic (EEG) signals. IEEE Trans Neural Syst Rehabil Eng 20:212-219.

Presacco A, Goodman R, Forrester L, Contreras-Vidal JL (2011) Neural decoding of treadmill walking from noninvasive electroencephalographic signals. J Neurophysiol 106:1875-1887.

Quinlan KA, Kiehn O (2007) Segmental, synaptic actions of commissural interneurons in the mouse spinal cord. The Journal of neuroscience 27:6521-6530.

Rabe Bernhardt N, Memic F, Gezelius H, Thiebes AL, Vallstedt A, Kullander K (2012) DCC mediated axon guidance of spinal interneurons is essential for normal locomotor central pattern generator function. Dev Biol 366:279-289.

Raethjen J, Govindan R, Binder S, Zeuner KE, Deuschl G, Stolze H (2008) Cortical representation of rhythmic foot movements. Brain Res 1236:79-84.

Reis PM, Hebenstreit F, Gabsteiger F, von Tscharner V, Lochmann M (2014) Methodological aspects of EEG and body dynamics measurements during motion. Front Hum Neurosci 8:156.

Reisman DS, Block HJ, Bastian AJ (2005) Interlimb coordination during locomotion: what can be adapted and stored? J Neurophysiol 94:2403-2415.

Reith ME (1990) 5-HT 3 receptor antagonists attenuate cocaine-induced locomotion in mice. Eur J Pharmacol 186:327-330.

Rigosa J, Panarese A, Dominici N, Friedli L, Van Den Brand R, Carpaneto J, DiGiovanna J, Courtine G, Micera S (2015) Decoding bipedal locomotion from the rat sensorimotor cortex. J Neural Eng 12:056014.

Roberts A, Soffe S, Wolf E, Yoshida M, Zhao FY (1998) Central circuits controlling locomotion in young frog tadpoles. Ann N Y Acad Sci 860:19-34.

Robilliard JJ, Pfau T, Wilson AM (2007) Gait characterisation and classification in horses. J Exp Biol 210:187-197.

Roemmich RT, Long AW, Bastian AJ (2016) Seeing the Errors You Feel Enhances Locomotor Performance but Not Learning. Curr Biol 26:2707-2716.

Roh J, Cheung VC, Bizzi E (2011) Modules in the brain stem and spinal cord underlying motor behaviors. J Neurophysiol 106:1363-1378.

Romanes G (1964) The motor pools of the spinal cord. Progress in brain research 11:93-119.

Rossignol S (2000) Locomotion and its recovery after spinal injury. Curr Opin Neurobiol 10:708-716.

Rybak I A, Dougherty K J, Shevtsova N A (2015). Organization of the mammalian locomotor CPG: review of computational model and circuit architectures based on genetically identified spinal interneurons. eNeuro, 2, 0069.

Salenius S, Schnitzler A, Salmelin R, Jousmäki V, Hari R (1997) Modulation of human cortical rolandic rhythms during natural sensorimotor tasks. NeuroImage 5:221-228.

Saltiel P, d'Avella A, Wyler-Duda K, Bizzi E (2015) Synergy temporal sequences and topography in the spinal cord: evidence for a traveling wave in frog locomotion. Brain Struct Funct 221:1-22.

Saltiel P, Wyler-Duda K, D'Avella A, Tresch MC, Bizzi E (2001) Muscle synergies encoded within the spinal cord: evidence from focal intraspinal NMDA iontophoresis in the frog. J Neurophysiol 85:605-619.

Saltiel P, Wyler-Duda K, d'Avella A, Ajemian RJ, Bizzi E (2005) Localization and connectivity in spinal interneuronal networks: the adduction-caudal extension-flexion rhythm in the frog. J Neurophysiol 94:2120-2138.

Satou C, Kimura Y, Higashijima S (2012) Generation of multiple classes of V0 neurons in zebrafish spinal cord: progenitor heterogeneity and temporal control of neuronal diversity. J Neurosci 32:1771-1783.

Schneider SP (1992) Functional properties and axon terminations of interneurons in laminae III-V of the mammalian spinal dorsal horn in vitro. J Neurophysiol 68:1746-1759.

Schultz W (1998) Predictive reward signal of dopamine neurons. J Neurophysiol 80:1-27.

Sébille SB, Belaid H, Philippe A-C, André A, Lau B, François C, Karachi C, Bardinet E (2017) Anatomical evidence for functional diversity in the mesencephalic locomotor region of primates. NeuroImage 147:66-78.

Selionov VA, Ivanenko YP, Solopova IA, Gurfinkel VS (2009) Tonic central and sensory stimuli facilitate involuntary air-stepping in humans. J Neurophysiol 101:2847-2858.

Sherrington CS (1910) Flexion-reflex of the limb, crossed extension-reflex, and reflex stepping and standing. J Physiol 40:28.

Shiavi R, Frigo C, Pedotti A (1998) Electromyographic signals during gait: criteria for envelope filtering and number of strides. Med Biol Eng Comput 36:171-178.

Shik M, Severin F, GN O (1966) Control of walking and running by means of electrical stimulation of mid-brain. Electroencephalogr Clin Neurophysiol 26:549.

Sinnamon HM (1993) Preoptic and hypothalamic neurons and the initiation of locomotion in the anesthetized rat. Prog Neurobiol 41:323-344.

Snyder KL, Kline JE, Huang HJ, Ferris DP (2015) Independent component analysis of

gait-related movement artifact recorded using EEG electrodes during treadmill walking. Front Hum Neurosci 9:639.

Suzuki M, Miyai I, Ono T, Kubota K (2008) Activities in the frontal cortex and gait performance are modulated by preparation. An fNIRS study. NeuroImage 39:600-607.

Suzuki M, Miyai I, Ono T, Oda I, Konishi I, Kochiyama T, Kubota K (2004) Prefrontal and premotor cortices are involved in adapting walking and running speed on the treadmill: an optical imaging study. NeuroImage 23:1020-1026.

Takakusaki K (2008) Forebrain control of locomotor behaviors. Brain Res Rev 57:192-198.

Takakusaki K, Okumura T (2008) Neurobiological Basis of Controlling Posture and Locomotion. Adv Rob 22:1629-1663.

Takakusaki K, Saitoh K, Nonaka S, Okumura T, Miyokawa N, Koyama Y (2006) Neurobiological basis of state‐dependent control of motor behaviors. Sleep Biol Rhythms 4:87-104.

Tallon-Baudry C, Bertrand O (1999) Oscillatory gamma activity in humans and its role in object representation. Trends Cognitive Sci 3:151-162.

Talpalar AE, Kiehn O (2010) Glutamatergic mechanisms for speed control and network operation in the rodent locomotor CPG. Front Neural Circuits 4:19.

Talpalar AE, Bouvier J, Borgius L, Fortin G, Pierani A, Kiehn O (2013) Dual-mode operation of neuronal networks involved in left-right alternation. Nature 500:85-88.

Talpalar AE, Endo T, Low P, Borgius L, Hagglund M, Dougherty KJ, Ryge J, Hnasko TS, Kiehn O (2011) Identification of minimal neuronal networks involved in flexor-extensor alternation in the mammalian spinal cord. Neuron 71:1071-1084.

Tashiro M, Itoh M, Fujimoto T, Fujiwara T (2001) 18 F-FDG PET mapping of regional brain activity in runners. J Sports Med Physical Fitness 41:11.

Tattersall TL, Stratton PG, Coyne TJ, Cook R, Silberstein P, Silburn PA, Windels F, Sah P (2014) Imagined gait modulates neuronal network dynamics in the human

pedunculopontine nucleus. Nat Neurosci 17:449-454.

Terao Y, Ugawa Y, Hanajima R, Machii K, Furubayashi T, Mochizuki H, Enomoto H, Shiio Y, Uesugi H, Iwata NK (2000) Predominant activation of I1-waves from the leg motor area by transcranial magnetic stimulation. Brain Res 859:137-146.

Thevathasan W, Pogosyan A, Hyam JA, Jenkinson N, Foltynie T, Limousin P, Bogdanovic M, Zrinzo L, Green AL, Aziz TZ (2012) Alpha oscillations in the pedunculopontine nucleus correlate with gait performance in parkinsonism. Brain 135:148-160.

Tibshirani R, Walther G, Hastie T (2001) Estimating the number of clusters in a data set via the gap statistic. J R Stat Soc Series B Stat Methodol 63:411-423.

Ting LH, Macpherson JM (2005) A limited set of muscle synergies for force control during a postural task. J Neurophysiol 93:609-613.

Ting LH, Chiel HJ, Trumbower RD, Allen JL, McKay JL, Hackney ME, Kesar TM (2015) Neuromechanical principles underlying movement modularity and their implications for rehabilitation. Neuron 86:38-54.

Tomlinson BE, Irving D (1977) The numbers of limb motor neurons in the human lumbosacral cord throughout life. J Neurol Sci 34:213-219.

Torres-Oviedo G, Macpherson JM, Ting LH (2006) Muscle synergy organization is robust across a variety of postural perturbations. J Neurophysiol 96:1530-1546.

Tresch MC, Saltiel P, Bizzi E (1999) The construction of movement by the spinal cord. Nat Neurosci 2:162-167.

Tresch MC, Cheung VC, d'Avella A (2006) Matrix factorization algorithms for the identification of muscle synergies: evaluation on simulated and experimental data sets. J Neurophysiol 95:2199-2212.

Udo M, Matsukawa K, Kamei H (1979) Effects of partial cooling of cerebellar cortex at lobules V and IV of the intermediate part in the decerebrate walking cats under monitoring vertical floor reaction forces. Brain Res 160:559-564.

Ushiyama J, Takahashi Y, Ushiba J (2010) Muscle dependency of corticomuscular coherence in upper and lower limb muscles and training-related alterations in ballet dancers and weightlifters. J Appl Physiol 109:1086-1095.

Van de Crommert HW, Mulder T, Duysens J (1998) Neural control of locomotion: sensory control of the central pattern generator and its relation to treadmill training. Gait Posture 7:251-263.

van den Brand R, Heutschi J, Barraud Q, DiGiovanna J, Bartholdi K, Huerlimann M, Friedli L, Vollenweider I, Moraud EM, Duis S, Dominici N, Micera S, Musienko P, Courtine G (2012) Restoring voluntary control of locomotion after paralyzing spinal cord injury. Science 336:1182-1185.

Vasudevan EV, Bastian AJ (2010) Split-belt treadmill adaptation shows different functional networks for fast and slow human walking. J Neurophysiol 103:183-191.

Vilensky JA (1987) Locomotor behavior and control in human and non-human primates: comparisons with cats and dogs. Neurosci Biobehav Rev 11:263-274.

Wagner J, Solis-Escalante T, Scherer R, Neuper C, Müller-Putz G (2014) It's how you get there: walking down a virtual alley activates premotor and parietal areas. Front Hum Neurosci 8:93.

Wagner J, Makeig S, Gola M, Neuper C, Müller-Putz G (2016) Distinct β band oscillatory networks subserving motor and cognitive control during gait adaptation. J Neurosci 36:2212-2226.

Wagner J, Solis-Escalante T, Grieshofer P, Neuper C, Müller-Putz G, Scherer R (2012) Level of participation in robotic-assisted treadmill walking modulates midline sensorimotor EEG rhythms in able-bodied subjects. NeuroImage 63:1203-1211.

Wainwright PC (2002) The evolution of feeding motor patterns in vertebrates. Curr Opin Neurobiol 12:691-695.

Wallén P, Williams T (1984) Fictive locomotion in the lamprey spinal cord in vitro compared

with swimming in the intact and spinal animal. J Physiol 347:225.

Walter JP, Kinney AL, Banks SA, D'Lima DD, Besier TF, Lloyd DG, Fregly BJ (2014) Muscle synergies may improve optimization prediction of knee contact forces during walking. J Biomech Eng 136:021031.

Ward JH (1963) Hierarchical grouping to optimize an objective function. J Am Stat Assoc 58.301 : 236-244.

Whelan PJ, Hiebert GW, Pearson KG (1995) Plasticity of the extensor group I pathway controlling the stance to swing transition in the cat. J Neurophysiol 74:2782-2787.

Widajewicz W, Kably B, Drew T (1994) Motor cortical activity during voluntary gait modifications in the cat. II. Cells related to the hindlimbs. J Neurophysiol 72:2070-2089.

Winter D, Yack H (1987) EMG profiles during normal human walking: stride-to-stride and inter-subject variability. Electroencephalogr Clin Neurophysiol 67:402-411.

Winter DA, Quanbury AO, Hobson DA, Sidwall HG, Reimer G, Trenholm BG, Steinke T, Shlosser H (1974) Kinematics of normal locomotion—a statistical study based on TV data. J Biomech 7:479-486.

Yang JF, Lam T, Pang MY, Lamont E, Musselman K, Seinen E (2004) Infant stepping: a window to the behaviour of the human pattern generator for walking. Canad J Physiol Pharmacol 82:662-674.

Yin M, Borton DA, Komar J, Agha N, Lu Y, Li H, Laurens J, Lang Y, Li Q, Bull C (2014) Wireless neurosensor for full-spectrum electrophysiology recordings during free behavior. Neuron 84:1170-1182.

Yokoyama H, Ogawa T, Kawashima N, Shinya M, Nakazawa K (2016) Distinct sets of locomotor modules control the speed and modes of human locomotion. Sci Rep 6.

Yokoyama H, Ogawa T, Shinya M, Kawashima N, Nakazawa K (2017) Speed dependency in α-motoneuron activity and locomotor modules in human locomotion: indirect evidence

for phylogenetically conserved spinal circuits. Proc R Soc Lond B 284:20170290.

Zar JH (1999) Biostatistical Analysis (2nd Ed.). Upper Saddle River, NJ: Prentice Hall.

Zelik KE, La Scaleia V, Ivanenko YP, Lacquaniti F (2014) Can modular strategies simplify neural control of multidirectional human locomotion? J Neurophysiol 111:1686-1702.

Zhang Y, Narayan S, Geiman E, Lanuza GM, Velasquez T, Shanks B, Akay T, Dyck J, Pearson K, Gosgnach S, Fan CM, Goulding M (2008) V3 spinal neurons establish a robust and balanced locomotor rhythm during walking. Neuron 60:84-96.

Zhong G, Sharma K, Harris-Warrick RM (2011) Frequency-dependent recruitment of V2a interneurons during fictive locomotion in the mouse spinal cord. Nat Commn 2:274.

Acknowledgments

First, I would like to express my sincere gratitude to my supervisor, Dr. Kimitaka Nakazawa for his endless encouragement, guidance, and support which have made me passionate about pursuing research and discovery, and taught me the pleasure of research. I especially would like to express my deepest appreciation to my co-supervisor, Dr. Tetsuya Ogawa for his detailed comments, suggestions, and constant support that make my studies of great achievement. I am also indebted to Dr. Noritaka Kawashima from the National Rehabilitation Center for Persons with Disabilities who provided guidance and inspiration which has allowed me to expend my research into the field of brain research. I express my deep appreciation to Dr. Dai Yanagihara, Dr. Kazutoshi Kudo, Dr. Hirofumi Sekiguchi, Dr. Shinsuke Yoshioka for their helpful comments on my study and my presentation from various perspectives. I express my deep appreciation to Dr. Masahiro Shinya, Dr. Hiroki Obata and Dr. Shun sasagawa for their helpful comments and suggestions from various perspectives. I also thank all the members of Nakazawa's laboratory and Kudo's laboratory at The University of Tokyo and Motor Control laboratory at Research Institute of National Rehabilitation Center for Persons with Disabilities. I'm really grateful to those who kindly volunteered to participate in my experiments. Lastly, I owe the greatest appreciation to my family for their enduring and endless support.